NOTICE

The quality of this microform is heavily dependent upon the quality of the original thesis submitted for microfilming. Every effort has been made to ensure the highest quality of reproduction possible.

If pages are missing, contact the university which granted the degree.

Some pages may have indistinct print especially if the original pages were typed with a poor typewriter ribbon or if the university sent us an inferior photocopy.

Reproduction in full or in part of this microform is governed by the Canadian Copyright Act, R.S.C. 1970, c. C-30, and subsequent amendments.

AVIS

La qualité de cette microforme dépend grandement de la qualité de la thèse soumise au microfilmage. Nous avons tout fait pour assurer une qualité supérieure de reproduction.

S'il manque des pages, veuillez communiquer avec l'université qui a conféré le grade.

La qualité d'impression de certaines pages peut laisser à désirer, surtout si les pages originales ont été dactylographiées à l'aide d'un ruban usé ou si l'université nous a fait parvenir une photocopie de qualité inférieure.

La reproduction, même partielle, de cette microforme est soumise à la Loi canadienne sur le droit d'auteur, SRC 1970, c. C-30, et ses amendements subséquents.

Hydrotreatment of Athabasca Bitumen Derived Heavy Gas Oil over Ni-W and Co-Mo Catalysts

By

Rafael Alfredo Díaz Real

Ottawa, Ontario. December 1987

A THESIS

PRESENTED TO THE UNIVERSITY OF OTTAWA

IN FULFILLMENT OF THE

THESIS REQUIREMENT FOR THE DEGREE OF

MASTER OF APPLIED SCIENCE

IN

CHEMICAL ENGINEERING

ISBN 0-315-53784-1

Abstract

Hydrotreatment of heavy gas oil derived from Athabasca tar sands was carried out in a trickle-bed reactor over Ni-W and Co-Mo catalysts supported on zeolite-alumina-silica, with the objective of testing these catalysts for their capability in hydrodesulfurization (HDS) and hydrodenitrogenation (HDN) at temperatures 350–425°C, a gas flow rate of 5000 scf/bbl (890 m^3 of hydrogen per m^3 of oil), a pressure of 6.9 MPa and LHSV of 1–4. Analyses for viscosity, density, aniline point, ASTM mid-boiling point distillation, C/H ratio and percentage of N and S in the final product were carried out to characterize the product oil. The amounts of N and S removed indicated the HDN and HDS activity of the catalysts.

The Ni–W catalyst gave better performance for hydrodesulfurization (HDS), whereas the Co–Mo catalyst gave better performance for hydrodenitrogenation (HDN). The data fitted a pseudo–first order model for both HDN and HDS.

Acknowledgement

I wish to express my gratitude to Dr. R. S. Mann for his guidance and encouragement throughout all stages of this work. I am also thankful to Dr. G. Neale, the former Graduate Student Coordinator and present Chairman, and to Dr. V. Hornof, the former Chairman, for departmental financial support and for the facilities used for this work. Dr. K. C. Khulbe and Dr. I. S. Sambi were always a great help whenever needed.

Thanks also to G. Gasperetti, A. Bonaldo and D. Lefebvre, whose technical assistance throughout the course of this work was invaluable. My deepest appreciation goes to all my professors and fellow classmates who have shown me the friendliness of the people of Canada.

To my father, Dr. Rafael Díaz Rico, to my mother, Dr. Irma Real de Díaz, and to my brother and sisters, Carlos, Rosana, Irma and Adriana, whose love and caring have taught me to love my neighbor as myself, and to strive for what I believe in. Finally to my grandfather Mr. Carlos Real Franyutti (RIP) for his faith in me.

Nomenclature

Symbols in the text, unless otherwise stated, have the following meaning:

a, b, c	General constants
A	Wetted area
A_{elf}	Ratio of wetted surface area to total surface area
bbl	Barrel (42 U. S. Gallons)
C	Concentration of reactant
C_i	Inlet reactant concentration
C_o	Outlet reactant concentration
COD	Coefficient of determination
d_p	Diameter of particle
d_s	Diameter of catalyst particle
d_t	Diameter of reactor tube
D_a	Effective axial dispersion
f	Wetting efficiency
$\mathcal{G}$	Gas flow rate (kg $m^{-2}s^{-1}$)
H	Liquid holdup
HDN	Hydrodenitrogenation (% by wt. of nitrogen removed)
HDS	Hydrodesulfurization (% by wt. of sulfur removed)
$\mathcal{I}$	Intercept for Equation 15 on page 92

k	Apparent kinetic constant
k'	Kinetic constant as defined on page 40
k'_m	m'th order reaction rate constant based on the total volume of catalyst
k'_1	First order rate constant
k_t	Mass transfer coefficient
K_H	Standard constant for hydrogen as defined on page 60
K_N	Standard constant for nitrogen as defined on page 60
L	Catalyst bed length
LHSV	Liquid-hourly-space-velocity (based on catalyst volume)
$\mathcal{L}$	Liquid flow rate (kg $m^{-2}s^{-1}$)
m, n	Orders of reaction
Pe	Peclet number ($\bar{u}d_p/D_a$)
Pe_d	Peclet number as defined on page 39
q	Parameter as defined on page 41
r	Reaction rate
R	Gas constant
Re	Reynolds number
$\bar{u}$	Mean fluid velocity
u_L	Superficial liquid velocity
z	Dimensionless length parameter

GREEK SYMBOLS

α, β, γ	General exponents
ε	Bed void fraction
η	Effectiveness factor
λ	Variable as defined on page 46
μ	Viscosity
ρ	Density
σ	Surface tension
ψ	Variable as defined on page 46

SUBSCRIPTS

A_i	Reactant A at the reactor inlet
A_o	Reactant A at the reactor outlet
f	For final
G	For gas
i	For initial, or at the inlet
L	For liquid
m	For reaction order
o	At the outlet
p	For particle
t	For reactor tube

Contents

List of Tables

List of Figures

Chapter 1

Introduction

Since World War II petroleum has played a key role in the world economy. Petroleum is a commodity that can make a country self-sufficient in energy resources, but it can cause a collapse in the economy if the country's external economy depends too heavily on it. Self-sufficiency in oil resources has been seen as one of the factors that has contributed to a steady social and economic growth.

Canadian reserves of heavy oil (about 250 billion bbl of heavy crude oil reserves as Tar Sands) are comparable in size to those of Saudi Arabia reserves of light oil. In the last, year political events have caused another "oil war" that has seen the oil price plummet below even $10.00 U.S. This has posed a major economic problem to oil companies that have seen their profits reduced to a minimum. Nonetheless, this surplus of light oil is only accelerating its depletion and in the future countries will have to rely more and more on heavy oil. Therefore, more efficient processes are continually sought and the research work in the field of catalysis used in the oil industry is an important part of this evolution.

Heavy oils are more difficult to process than light oils. The former ones have higher amounts of undesirable heteroatomic compounds that affect the stability of the final product. Therefore, it is desirable to further process these oils to remove the undesirable compounds. Some of the operations that attain such a goal are hydrocracking and hydrotreating, which are described in section 1.2.

An important part of these processes has been the use of catalysts. Around the year 1900 the German chemist Wilhelm Ostwald defined a catalyst as a substance which alters the rate of a chemical reaction without appearing in the end products. This insight provided a basis for scientific inquiry into the subject and paved the way for the widespread

investigation of catalytic phenomena. Since the time of Ostwald, the science of catalysis has progressed steadily. The scientific progress has been accompanied by enormous technological advances, ranging from the Haber process for ammonia synthesis to present-day processes for the catalytic cracking and reforming of petroleum fractions. More often than not, the technological advances have led to significant scientific advances [55].

1.1 Heavy Oil. Characteristics

Crude oils are classified for commercial purposes into light (API° gravity > 35), medium (20 ≤ API° gravity ≤ 35) and heavy oils (API° gravity < 20). For appropriate study the amounts of poisoning and contaminant materials also have to be considered. The term heavy oil applies to petroleum fractions boiling between 320°C and about 425°C. This upper limit is not a fixed one. Heavy oils contain objectionable heteroatomic compounds such as those containing sulfur (up to 10 % by weight) and nitrogen (up to 2 % by weight) which pose difficulties in further processing. There are also organometallic complexes (formed with V, Ni and Fe amongst others). These compounds not only cause problems in downstream processing, but make the final product unstable, and pose problems of environmental pollution and corrosion of machinery. On combustion, sulfur and nitrogen are discharged into air as SO_x and NO_x and thus are sources for air pollution [44]. Accounting for these last considerations, there is a more detailed specification for heavy oils [35]:

1. High Viscosities (> 330 SSU @ 37.8°C)
2. High Amounts of Contaminants :
   - Sulfur (> 2.5 wt. %)
   - Vanadium (> 150 ppm)
   - Nickel (> 40 ppm)
   - Ramsbottom Carbon (> 8 wt. %)
   - Insoluble in nC_5 (> 10 wt. %)
3. Low H/C ratio
4. High Production of Fuel Oil (> 50 % by crude volume)

1.1.1 Main Contaminants

As stated above, there are several objectionable elements that have to be removed from heavy oil before down-stream processing. The main ones are mentioned in this section.

Sulfur Compounds

Most of these compounds are thiophenes, but other forms like sulfides, sulfates, mercaptans, thiols and free sulfur can be found. The difficulty of sulfur removal increases with the complexity of the molecule. It increases in the order paraffins, naphthenes, aromatics. As the boiling point of the crude fraction increases so does the amount of sulfur, but if temperature is raised to such a level as to cause cracking, sulfur will eventually transfer to both light and heavy fractions [44].

Free sulfur and sulfides are highly corrosive. Thiophenes are detrimental to the octane number response to tetraethyl lead. Sulfur compounds lower resistance of lubricating oil to oxidation and increase deposition of solid material.

Nitrogen Compounds

There are two "types" of nitrogen in petroleum. They are 'basic' and 'non-basic' depending upon whether or not they can be titrated with perchloric acid in a 50/50 solution of glacial acetic acid and benzene. The basic nitrogen compounds are mainly pyridine and its homologues that exist in light and heavy fractions whereas the non–basic nitrogen compounds (e.g. pyrrole, indole and carbazole type compounds) occur mainly in the highest boiling fractions. Basic nitrogen is a temporary catalyst poison that causes a decrease in catalytic activity [60]. The major effect of a high basic nitrogen feed is depressed conversion. Also nitrogen compounds contribute to gum formation in such products as domestic fuel oil. The amount of nitrogen is generally associated with its carbon residue (or asphalthenes).

Oxygen Compounds

Oxygen in petroleum is significant when oil has been exposed to the atmosphere for a long period of time. The compounds it forms are alcohols, ethers, acids, anhydrides, acetates, ketones and furanes. Its presence is accentuated in heavier fractions. Although oxygen does not pose any major environmental problem its presence in finished products accelerates

their deterioration. Some acidic forms are the cause of corrosion. Oxygen compounds also generally promote gum formation in the finished product.

Metallic Impurities

Distillation process tends to concentrate metallic impurities in the heavier fractions. The presence of small amounts of these impurities, such as iron, copper, nickel, vanadium, sodium, etc., could be detrimental to the activity of the catalyst. Halogens, especially chlorine and fluorine, almost always occur as contaminants in the oil. They are quite serious catalyst poisons in that they cause high dry-gas makes, probably by formation of metal halides with the Ni, V, and other metals on the catalyst [60].

An important characteristic for assessing a residual oil as a cracking stock is the nickel and vanadium content. These metals occur naturally in the oil as metal porphyrines and as metallic salts. They are both excellent dehydrogenation and/or gas making catalysts when deposited on catalyst. When vanadium levels become too high on an equilibrium catalyst, the vanadium will form a low melting point eutectic with the aluminum silicate which will actually fuse into a dense, inactive particle. Most of V, Ni, Co and Fe can be precipitated along with the asphalthenes using n-pentane, reducing their concentrations up to 95 %, without damaging the catalyst. Davis and Rase [13] have studied the charateristics of nickel-contaminated cracking catalysts.

A common and severe poison for the cracking catalyst is sodium. It quantitatively poisons the zeolite catalyst by combining with the Si-Al in the catalyst and destroying the sieve structure. When sodium on equilibrium catalysts exceeds 1.0 % the catalyst will usually be so deactivated as to be useless. Sodium content of the catalyst may, in the long term, be the limiting factor in the refiner's ability to crack residua. So far no method can remove Na and retain the catalytic properties of the catalyst.

1.2 Oil Processing

The petroleum refining industry has undergone unexpected expansion and change since early 50's. Tremendous increases in the size of process units, new catalytic processes, shifting products demands, and new sources of petroleum from oil shales and tar sands have made present-day economics and technology of petroleum a very complex and sophisticated science.

Transforming crude oil into finished products requires several and sometimes complicated processes. Heavy oil, whose characteristics are given in section 1.1 above poses more serious difficulties for processing. A typical refinery flow diagram [19] is shown in Figure 1.

In this section the major refinery operations such as hydrotreating, reforming, cracking, hydrocracking, and hydroprocessing are treated in some detail. Their similarities, differences and interactions are addressed. Further details about them as well as information regarding other minor operations such as visbreaking are given by Gary et al. [19], Gruse [22], Speight [57], Little [33], Shaheen [54], and more recently by Meyers [43].

1.2.1 Catalytic Cracking

Catalytic Cracking is the refinery process used for converting heavy oils into more valuable gasoline and lighter products. Though in the beginning cracking was carried out thermally, it is now replaced by the catalytic process because it produces more higher octane gasoline and less heavy fuel oils and light gases.

During the cracking process coke is formed and remains on the catalyst particle lowering its activity. To overcome this, it is necessary to regenerate the catalyst by burning off the coke with air. This results in a continous movement of the catalyst from the reactor to the regenerator and back to the reactor. The cracking reaction is endothermic whereas the regeneration reaction is exothermic. The average reactor temperature ranges from 480 to 540°C with oil feed temperatures from 260 to 430°C and regenerator exit temperatures for catalyst from 650 to 790°C.

The process for accomplishing catalytic cracking can be classified as either moving-bed or fluidized-bed unit. An example of the former is the Thermafor catalytic-cracking process (TCC), and the Fluid catalytic-cracking process (FCC) is an example of the latter. The process flows for both processes are similar. The hot oil contacts the catalyst in either the feed riser line or the reactor. While the reaction goes on, coke is formed and deposited on the surface of the catalyst, deactivating it progressively. Hydrocarbon vapors and the catalyst are separated mechanically and oil remaining on the catalyst is removed by steam stripping before the catalyst enters the regenerator. The oil vapors are further separated in a fractionation tower into streams having the desired boiling ranges.

The products formed in catalytic cracking are the result of both primary and secondary reactions. Primary reactions are those involving the initial carbon–carbon scission and the immediate neutralization of the carbonium ion. Further details of this mechanism are given

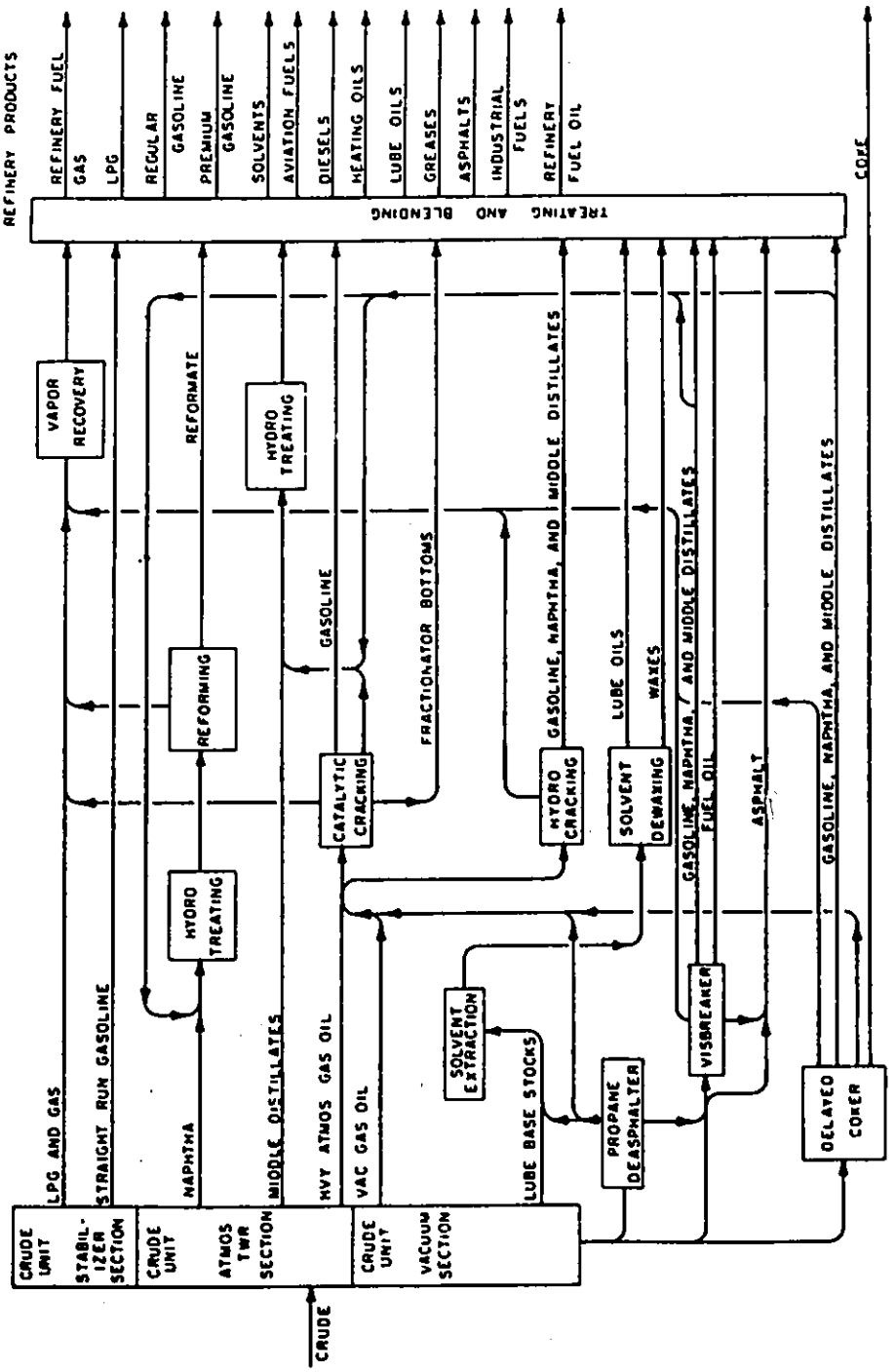

Figure 1: Refinery Flow Diagram

by Thomas [59] . The primary reactions can be represented as:

- Paraffin $\longrightarrow$ Paraffin + Olefin
- Alkyl – naphthene $\longrightarrow$ Naphthene + Olefin
- Alkyl – aromatic $\longrightarrow$ Aromatic + Olefin

Among the secondary reactions, one can consider olefine, naphthenic and aromatic cracking.

Cracking catalysts are similar in nature to those of hydrocracking. They consist of a crystalline mixture of silica-alumina and rare earths. Further explanation about the nature of catalysts is given on page 30. New zeolite cracking catalysts have helped improve the gasoline yield and octanes, reduce the recycle stock and gas formation. Cyclic oils that result from cracking operations with zeolite catalysts tend to be highly aromatic and therefore make excellent feedstock for hydrocracking.

In addition to the nature of the feed stock, the major operating variables that affect the conversion and product distribution are the recycle ratio, catalyst type and activity, space velocity, catalyst/oil ratio and cracking temperatures. Generally speaking, increasing reaction temperature, catalyst/oil ratio, catalyst activity and contact time results in an increase in conversion, whereas a decrease in space velocity increases conversion.

1.2.2 Hydrotreating

Hydrotreating is a process to "catalytically stabilize petroleum products and/or remove objectionable elements from products of feedstocks by reacting them with hydrogen". This can be considered a mild operation where stabilization involves converting unsaturated hydrocarbons like olefins and gum-forming unstable diolefins to paraffins. It is used with feedstocks that include naphtha to reduce crude. The objectionable elements to be removed include sulfur, nitrogen, oxygen, halides and trace metals. If the main purpose is sulfur removal the process is called hydrodesulfurization or HDS.

A typical industrial hydrotreating unit [19] is shown in Figure 2.

The oil feed is mixed with hydrogen-rich gas and enters the top of the fixed-bed reactor. The temperatures are between 260 and 425°C. When the process is carried out at higher temperature cracking is increased and mixture boiling point drops. In the presence of the metal-oxide catalyst, the hydrogen reacts with the oil to produce saturated hydrocarbons,

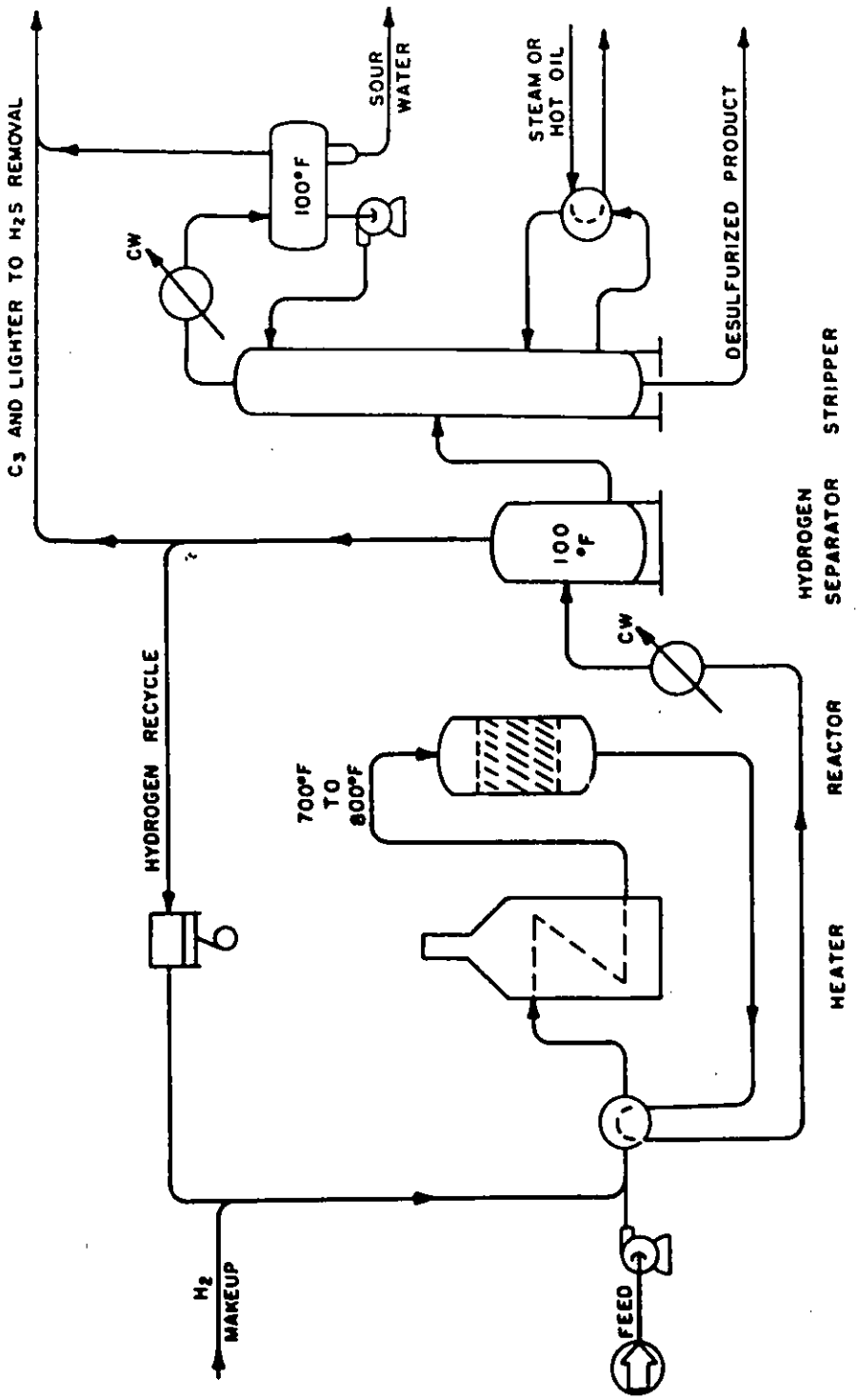

Figure 2: Catalytic Hydrodesulfurization Unit

ammonia, hydrogen sulfide and free metals. All the products but the metals leave the reactor with the oil-hydrogen stream. Metals remain on the surface of the catalyst. The reactor effluent is cooled and then the oil is separated from the hydrogen-rich gas. Remaining H_2S and light ends are stripped from the oil. The gas is treated to remove hydrogen sulfide and recycled to the reactor.

Several hydrotreating catalysts have been developed through the years. These include tungsten and nickel sulfides, vanadium oxide, nickel thiomolybdate, nickel oxide and cobalt and molybdenum on alumina [22]. The latter ones are most in use in present-day industry, because they have proven to be resistant to poisons, easy to regenerate and highly selective. For nitrogen removal (i.e. hydrodenitrogenation or HDN) catalysts composed of Ni-Co-Mo or Ni-Mo compounds supported on alumina are more efficient. HDN is usually more difficult to attain than HDS from hydrocarbon streams; thus any treatment which reduces nitrogen down to a satisfactory level will also achieve the same goal with sulfur. Some hydrotreating catalysts (particularly those containing nickel) need to be activated by presulfiding them. This has the objective of poisoning some acid sites making the process more selective. Further information about this subject is given in section 2.3.3. For HDS the most selective catalysts are those made with Co-Mo compounds and for HDN those made with Ni-Mo compunds [30]. Nickel-Molybdenum catalysts have higher hydrogenation activity than Cobalt-Molybdenum, which produces a greater amount of aromatic rings at the same operating conditions. This results in lighter products richer in naphthas. The sulfiding reaction is highly exothermic.

The main hydrotreating reaction is that of HDN, but many others take place. Typical reactions are :

1. Desulfurization :
   - Mercaptans : $RSH + H_2 \rightarrow RH + H_2S$
   - Sulfides : $R_2S + 2H_2 \rightarrow 2RH + H_2S$
   - Disulfides : $(RS)_2 + 3H_2 \rightarrow 2RH + 2H_2S$
   - Thiophenes : $C_4H_4S + 4H_2 \rightarrow C_4H_{10} + H_2S$
2. Denitrogenation :
   - Pyrrole : $C_7H_{13}OOH + 3H_2 \rightarrow C_7H_{16} + 2H_2O$
   - Pyridine : $C_4H_4NH + 4H_2 \rightarrow C_4H_{10} + NH_3$

3. Deoxidation :

   - Phenol : $C_6H_5OH + H_2 \rightarrow C_6H_6 + H_2O$
   - Peroxides : $C_7H_{13}OOH + 3H_2 \rightarrow C_7H_{16} + 2H_2O$

4. Dehalogenation :

   - Chlorides : $RCl + H_2 \rightarrow RH + HCl$

5. Hydrogenation :

   - Pentene : $C_5H_{10} + H_2 \rightarrow C_5H_{12}$

6. Hydrocracking : $C_{10}H_{22} \rightarrow C_4H_{18} + C_6H_{14}$

In hydrotreating reactions actual hydrogen makeup requirements are from two to ten times the amount of stoichiometric hydrogen required. The cause of this is the solubility loss in the oil leaving the reactor effluent separator. All reactions are exothermic and temperature rise through the reactor of 2 to 12°C is common.

Space velocity, hydrogen partial pressure and temperature are the main operating variables. Increasing temperature improves sulfur and nitrogen removal, although excessive increase can cause coke formation, and possibly affect the catalyst (e.g. sintering). Increasing space velocity reduces conversion, hydrogen consumption and coke formation. Higher pressures increase hydrogen saturation and lower coke formation. Raising both temperature and pressure produces better HDN and HDS but higher hydrogen consumption.

Typical conditions in hydrotreating operations are [19]

- Temperature, (°C) 315–425
- Pressure, MPa 0.7–20.97
- Hydrogen, m^3/m^3 (scf/bbl) charge
  1. Recycle 356 (2000)
  2. Consumption 35.6–142.4 (200-800)
- Space Velocity (LHSV) 1.5–8.0

A review of most of the commercial hydrotreatment processes is found in reference [23].

1.2.3 Hydrocracking

Increased demand for high octane gasoline and a decrease in demand for distillate fuels has prompted the conversion of higher boiling petroleum materials to gasoline and jet fuels. Hydrocracking refers to processes whose primary purpose is to reduce the boiling range and in which 100 % of the feed is converted to products with boiling ranges lower than that of the feed. It offers several advantages:

1. Better balance of gasoline and distillate production
2. Greater gasoline yield
3. Improved gasoline pool octane quality and sensitivity
4. Supplements catalytic cracking to upgrade several feedstocks

As stated above, catalytic cracking and hydrocracking complement each other. The latter uses more aromatic cycle oils and coke distillates as feed, whereas the former takes the more easily cracking paraffinic atmospheric and vacuum gas oil as charge stocks.

The mechanism of hydrocracking is that of catalytic cracking with hydrogenation superimposed. Catalytic cracking is the scission of a carbon–carbon single bond and hydrogenation is the addition of hydrogen to a carbon–carbon double bond. The reactions complement each other; cracking provides olefines for hydrogenation and hydrogenation gives heat for cracking. Cracking is endothermic and hydrogenation is exothermic.

Hydrocracking reactions usually take place at an average catalyst temperature between 280 and 400°C and at reactor pressures of 8.38 to 13.98 MPa. Circulating hydrogen in large quantities with the feedstock allows long runs without catalyst regeneration and helps to prevent catalyst fouling.

The feedstock is hydrotreated to saturate the olefins and to remove the sulfur, nitrogen and oxygen compounds. For some hydrocracking catalysts H_2S in low concentrations inhibits the saturation of aromatic rings, which produces a higher octane product. There are several hydrocracking processes available for license, e.g. GOFining from EXXON Research and Engineering and Isomex from Standard Oil Co.

Analysing cracking catalysts one can see that most of them consist of a crystalline mixture of silica-alumina with a small uniformly-distributed amount of rare earths contained within the crystalline lattice. The rare-earth metals promote hydrogenation while

the silica-alumina portion provides cracking activity. Catalyst selectivity changes with age. Therefore, in order to maintain activity, temperature has to be raised; however this produces more gas and less naphtha. Almost all hydrocracking catalysts use silica-alumina as the cracking base, but the rare-earth metals vary according to the manufacturers.

The process variables are reactor temperature, pressure, hydrogen consumption, nitrogen content of feed, H_2S content of the gases, and space velocity. An increase in temperature increases the reaction rate but does not change the conversion level as much because the reaction rate involves material that has already been converted. Increasing total pressure increases conversion. Decreasing space velocity augments conversion. An increase in organic nitrogen content of the feed causes a decrease in conversion. At low concentrations H_2S acts as a catalyst to inhibit the saturation of aromatic rings, whereas at high concentrations cracking is affected adversely.

1.2.4 Hydroprocessing

This refers to processes used to reduce the boiling range of the feedstock as well as to remove impurities such as metals, sulfur, nitrogen, and high carbon-forming compounds. Processes like H-Oil [23, page 214] fall into this category. Other names applied to this operation are resid HDS, hydrorefining, and hydroconversion.

Hydroprocessing units are used to prepare residual stream feedstocks for cracking and coking units. Typically the heavy naphtha fractions will be catalytically reformed to improve octanes, the atmospheric gas oil fraction hydrotreated to reduce aromatic content and improve cetane number, the vacuum gas oil fraction used as conventional FCC unit feed, and the vacuum tower bottoms sent to a heavy oil cracker. A typical process flow diagram is shown in Figure 3 [19].

All units operate at very high pressures, normally above 13.89 MPa, and low space velocities of 0.2 to 0.5. Typically each train will have a guard reactor to reduce metal contents and carbon-forming potential of the feed, followed by the three or four hydroprocessing reactors in series. The guard reactor's catalyst is a large pore-size (15–20 nm) silica-alumina catalyst with a low-level loading of hydrogenation metals (e.g. cobalt and molybdenum). The catalysts in the other reactors are tailor-made for the feedstock and conversion levels desired.

The process flow shown in Figure 3 is very similar to that of a conventional hydrocracking unit except for the guard reactor to protect the catalyst in the reactor train and for the amine

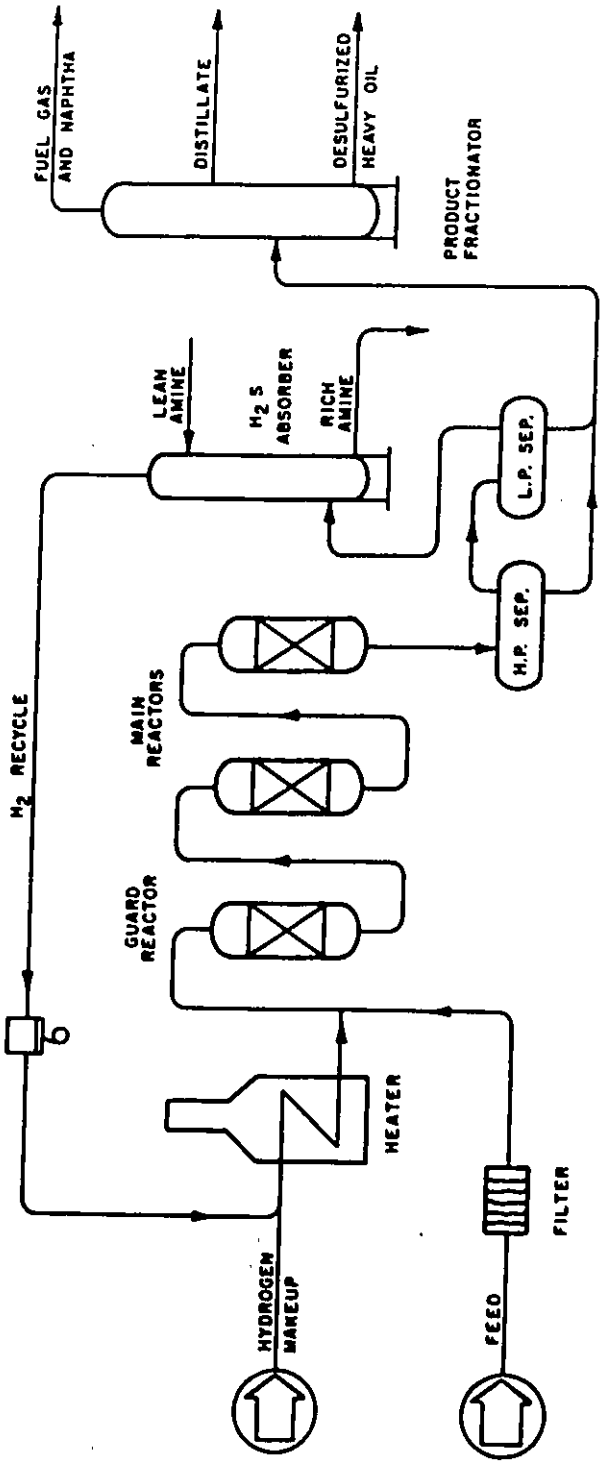

Figure 3: Exxon RESIDfining hydroprocessing unit

absorption unit to remove hydrogen sulfide from the recycle hydrogen stream. There is also a substantial reduction in the Conradson and Ramsbottom carbon in the guard reactor, and the feed to the following reactors is low in metals and carbon forming precursors. The three or four reactors following the guard reactor are operated to remove sulfur and nitrogen, and to crack the 560+°C material to lower boiling compounds. Recycled hydrogen is separated and the hydrocarbon liquid stream fractionated in atmospheric and vacuum distillation columns.

1.2.5 Catalytic Reforming

This refers to processes where the hydrocarbon molecules are not cracked, but where their structures are rearranged to form higher octane aromatics. Thus these processes primarily increase the octane of motor gasoline rather than increasing its yield.

The typical feedstocks are heavy straight-run gasolines and naphthas. These are composed of four major hydrocarbon groups: paraffins, olefins, naphthenes and aromatics. There are four major reactions that take place during reforming. They are: dehydrogenation of naphthenes to aromatics, dehydrocyclization of paraffins to aromatics, isomerization, and hydrocracking.

Aromatics have a higher liquid density than paraffins or naphthenes with the same number of carbons. Also, conversion to aromatics increases the gasoline end point because the boiling points of aromatics are higher than the boiling points of paraffins and naphthenes with the corresponding number of carbons.

The yield of aromatics is increased by:

1. High temperature
2. Low pressure
3. Low space velocity
4. Low hydrogen-to-hydrocarbon mole ratios

Isomerization of paraffins and cyclopentanes usually results in a lower octane product than does the conversion to aromatics. Nonetheless, this increase is substantially higher when compared with that of the unisomerized materials.

Isomerization yield is increased by:

1. High temperature

2. Low space velocity

3. Low pressure

The hydrocracking reactions are exothermic and result in the production of lighter liquid and gas products. The concentration of paraffins in the charge stock determines the extent of the hydrocracking reaction.

Hydrocracking yields are increased by:

1. High temperature

2. High pressure

3. Low space velocity

The active material in most reforming catalyst is platinum. Some metals, hydrogen sulfide, ammonia, and organic nitrogen and sulfur compounds deactivate the catalyst. Hydrotreating the feedstock is commonly employed to remove these materials. The hydrogen needed for the hydrotreater is obtained from the catalytic reformer.

Reforming processes are classified as continuous, cyclic, or semiregenerative depending upon the frequency of catalyst regeneration. A typical example of reforming operation is the Platforming semiregenerative process. A process flow diagram is shown in Figure 4.

The pretreated feed and recycle hydrogen are heated between 495 and 525°C before entering the first reactor. Here the major reaction is the dehydrogenation of naphthenes to aromatics. This causes a large drop in temperature, as the reaction is strongly endothermic. As the charge proceeds through the reactors, the reaction rates decrease and the reactors become larger, and the reheat needed becomes less. Under normal circumstances three reactors suffice to provide the desired degree of reaction. Heaters are needed before each reactor to bring the mixture up to reaction temperature. The reaction mixture from the last reactor is cooled and the liquid products condensed. The hydrogen-rich gases are separated from the liquid phase in a drum separator and the liquid from the separator is sent to a fractionator.

The normal operating conditions are: pressure 0.7 to 2.44 MPa, hydrogen charge ratios 712 to 1424 m^3/m^3 (4000 to 8000 scf/bbl) fresh feed and LHSV 2-3.

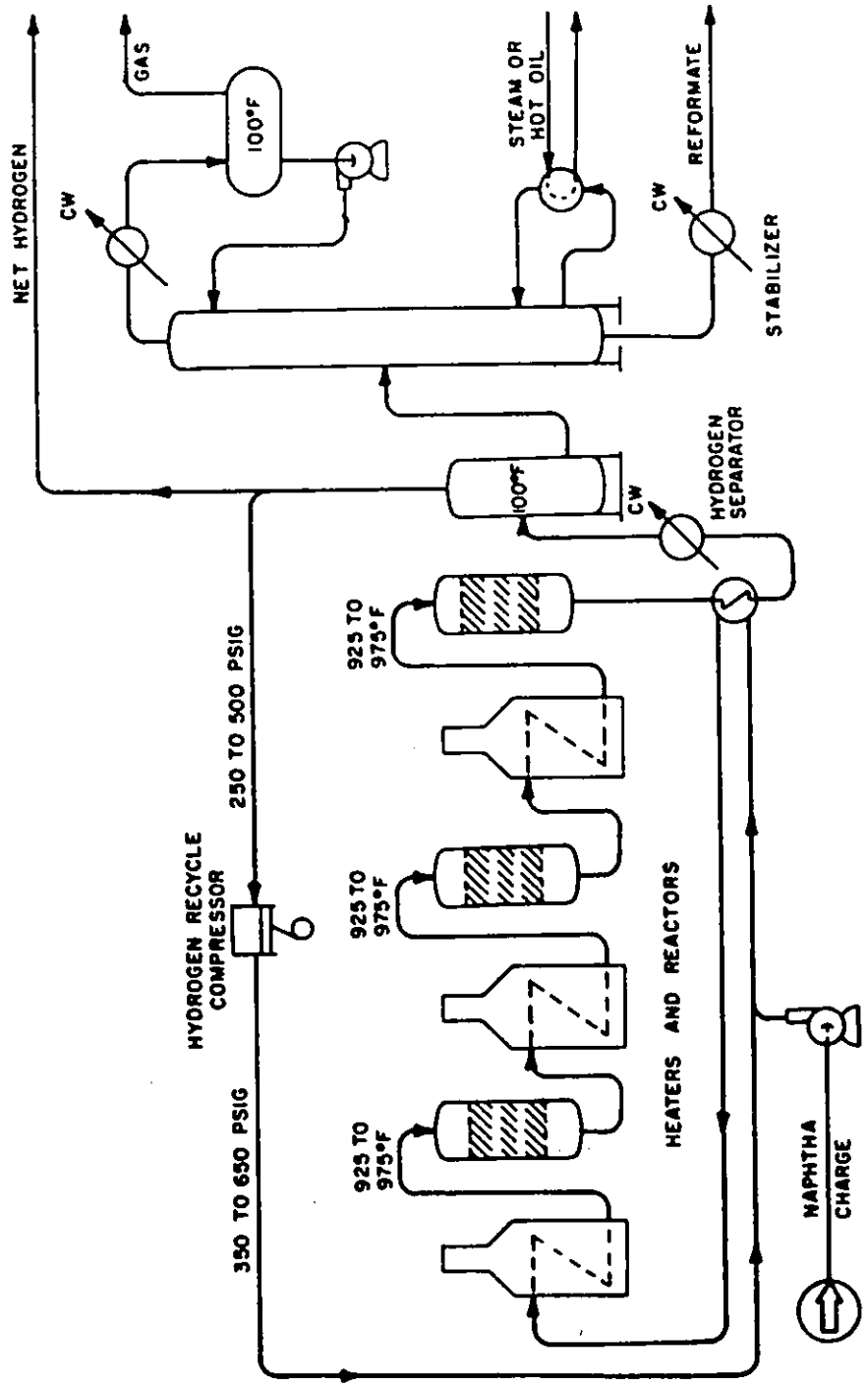

Figure 4: Catalytic Reforming, Semiregenerative

Table 1: Properties of Great Canadian Tar Sands Bitumen

Specific Gravity (16/16°C)	1.01
Sulfur (wt. %)	4.73
Ash (wt. %)	0.56
Viscosity (cst. at 99.2°C)	175.80
Conradson carbon residue (wt. %)	13.80
Benzene insoluble (wt. %)	15.60
Nickel (ppm)	68.00
Vanadium (ppm)	211.00

1.3 Heavy Oil Used during this Research

The heavy oil used during this research was a 345°C to 524°C heavy gas oil fraction derived from hydrocracking of Athabasca Tar Sands bitumen. The bitumen contains 51.5% wt. pitch (material that boils above 524°C) and about 0.6% wt. of ash. Bitumen properties copied from [51] are given in Table 1.

To obtain heavy oil, bitumen is hydrocracked at about 450°C with hydrogen pressure of around 13.89 MPa and liquid hourly space velocity (LHSV) of around 1. The reactor used is of the upward flow ebullated-bed type. During hydrocracking heteroatomic compounds are substantially reduced. The heavy gas oil derived from this process constitutes about 35% of the total liquid products. The oil used in this investigation was tested for its physical properties, ASTM D-2887 distillation and elemental analysis. Results are shown in Table 2. It should be noted that the properties of heavy oil shown here differ slightly from those given by Sambi [51], although the batch where the oil drums came from was assumed to be the same. This is due to experimental error and the oil changes in time. Considering that between his study and the one presented here there is a gap of one and a half years, few changes in the oil properties are expected, and should not affect the conclusions drawn from this study.

1.4 Previous Study

The basis for this research is taken from the investigations of Sambi and Mann [39,40,38]. In an initial study they upgraded heavy gas oil derived from Athabasca bitumen over commercially available, alumina supported Ni-W, Ni-Co and Co-Mo catalysts. Their activities

Table 2: Properties of Heavy Gas Oil

Specific Gravity, 16/16°C	0.9884
API gravity	11.7
Viscosity at 25°C, mPa·s	246.5
Asphaltene, wt. %	1
Aniline point, (°C)	47.8

Elemental Analysis, wt. %			
C = 87.20	H = 8.23	N = 0.49	S = 4.08

ASTM–2887 Distillation :					
Temperature (°C)	101.5	192.6	229.2	263.2	323.2
Volume %	10	20	30	40	50
	377.2	402.2	433.3	468.3	535.2
	60	70	80	90	100

were reported and compared. It was found that though Ni-W/Al_2O_3 catalyst was best for cracking hydrogenation and hydrodesulfurization (HDS), Ni-Mo/Al_2O_3 catalyst was best for hydrodenitrogenation (HDN) [50].

Recently, the hydrotreatment of Athabasca bitumen derived gas oil over zeolite supported Ni-Mo/Al_2O_3 catalyst in a trickle-bed reactor was also investigated. It was found that a zeolite catalyst containing 4.7 wt. % MoO_3, 1.65 wt. % NiO (with 14.5 % zeolite) was a very effective catalyst for removing S and N and in upgrading [51].

1.5 Aim of this Study

In the present work, the results obtained in the hydrotreatment of Athabasca bitumen derived gas oil over zeolite-alumina supported Ni-W and Co-Mo catalysts are reported. S and N removal is of particular interest.

Chapter 2

Literature Review

In this chapter three main aspects of hydrotreating are considered: the preparation of the catalyst; the zeolites and their effects on the process; the heart of the hydrotreatment system, the trickle-bed reactor.

2.1 Basis of Catalyst Preparation

Chemical composition is clearly the major factor in determining the catalyst properties. However, with a constant chemical composition, the catalytic characteristics may vary over a wide range depending on the conditions and methods of catalyst preparation, owing to the change in the nature of interaction of catalyst components, dispersion, pore structure, crystallochemical changes and other factors which may greately influence catalytic reactions.

The catalytic properties of a catalyst are measured by the following characteristics [6] :

1. Catalytic activity determined by the amount of a substance reacting per unit volume of the catalyst per unit time under given conditons.

2. Selectivity characterized by the ratio of the formation rate of the required product to the overall rate of conversion of the initial product at a certain temperature and reaction mixture composition.

3. Stability (thermal stability, resistance to poisoning, stable operation over a long period of time).

4. Mechanical strength.

5. Hydrodynamic characteristics determined by the size, shape and density of the catalyst grains.

The task of the theory of catalyst preparation is to find out:

1. What properties of a catalyst other than its chemical composition influence these basic characteristics?
2. What are the optimum values of these properties, or more exactly, what is the optimum combination of these values that will provide high quality of a catalyst for a particular reaction?
3. How can these properties be varied during the catalyst preparation in order to achieve their optimum value?

2.2 Supported Metal Catalysts

Selection of the proper hydrotreating catalyst has never been more important than now. The days of choosing the cheapest load available are gone. With escalating energy and hydrocarbon costs, performance has become the most significant basis for catalyst selection unless unusual specific unit circumstances exist.

The question of which catalyst type to choose has been a recurring one but the answers have not always been consistent. This is not surprising because hydrotreating catalysts are capable of handling a wide variety of feedstocks, process conditions and objectives. James Speight, in his book "The Desulfurization of Heavy Oils and Residua", describes ways of evaluating heavy oils [58] and residua for adequate selection of the desulfurization process.

2.2.1 Role of Catalyst

A great deal is required of industrial cracking catalyst, especially those devoted to HDS. Apart from the common requirements such as good activity, mechanical ruggedness, long life and the ability to sustain repeated regenerations, they must [14]:

1. effectively remove sulfur from the organo-sulfur molecule mostly through C–bond fission,
2. be able to operate in the presence of organosulfur compounds and H_2S (which excludes the use of the common metallic hydrogenation catalysts),

3. not be easily poisoned by other petroleum impurities such as nitrogen compounds, and metallic V and Ni,
4. they must not cause too much dehydrogenation and polymerization leading to "coking" and finally,
5. they should be able to hydrogenate selectively dienes and polyenes over mono-olefins, thereby reducing the tendency for coking, while maintaining desirable gasoline properties and minimizing the costly consumption of hydrogen.

2.2.2 Components of the Catalyst Formulation

In general, the metal catalyst formulation (be it a pellet, extrusion or grain) consists of: (a) the support, usually porous Al_2O_3, SiO_2, or SiO_2–Al_2O_3, upon which is deposited; (b) the catalytic agent; (c) promoters. Andrew [1], and Boreskov [6] give some guide about scientific steps to follow in heterogeneous catalyst preparation.

Supports

Since catalytic activity may be proportional to the concentration of active sites, supports of high area are commonly employed. Porous solids provide areas ranging from one to several hundred square meters per gram. In the silica-alumina cracking catalyst the active site is formed when one aluminum atom shares four oxygen atoms which in turn are shared by four silicon atoms. An acidic hydrogen ion is thought to be associated with the four oxygen atoms surrounding the aluminum atom. The catalytic activity is ascribed to this acidic hydrogen [59].

Thermal deactivation is a sintering process; i.e. the deposited crystallites grow in size, with the consequence that the number of surface atoms per unit mass of deposited metal decreases. This sintering is minimized with high dispersion, hence the advantages of high area supports. A high area support is characterized by pores of small diameter, which invites the diffusional intrusions. In general, a porous support is desirable, but the absolute magnitude of total area sought depends upon the particular reaction and operating conditions.

The support should not be assumed to be inert in the catalytic process for it may endow the deposited catalyst with certain properties (state of oxidation, valence) and

may exhibit the ability to adsorb reactants and/or atomic species dissociated by the deposited catalytic agents. Some of these effects are discussed by de Beer [14], and Lo Jacono and Schiavello [34]. Also, an overall review on this subject is given by Topsœet al. [61]. Nonetheless the higher-area supports are susceptible to sintering themselves.

Catalytic Agents

Deposited agents are metals and semiconductors, while insulator catalysts are unsupported. The supported catalytic ingredients are generally deposited upon the support from solution. It is to be noted that total impregnation of the support by the catalyst bearing solution is not readily realized, nor, in fact, is it always desirable [8]. Kotera et al. [32] found that, in the preparation of Co/Mo supported on alumina catalyst, impregnated catalysts exhibited higher catalytic activities than kneaded ones and that a different optimum Co/Mo ratio exists for both preparation methods.

Promoters

Promoters are classified as physical or chemical. Additives which serve to maintain the physical integrity of the support and/or deposited catalytic agent are termed physical promoters. Chemical promoters are those which increase the intrinsic activity of the crystallites, and are also those which inhibit undesirable products formation. Thus promoters can be added during catalyst preparation or during reaction.

2.2.3 Carbon Formation

Carbonaceous deposits (coke) can be formed on catalysts under a wide varity of conditions in a reducing environment. The factors involved in carbon formation on non-metallic catalysts, such as acid catalysts, are substantially different than those involved with metals. On non-metallic catalysts the deposit may contain considerable hydrogen, represented by an empirical formula CH_x in which x may vary between about 0.5 and 1. Carbon deposits on metals generally contain little or no hydrogen, depending in part on the reaction temperature. Many reactions can cause carbon deposits, but the process can be visualized in terms of the decomposition of CO (2CO

$\rightarrow C + CO_2$), of CH_4 ($CH_4 \rightarrow C + 2H_2$), or of other gaseous reactions (for example, $2H_2 + CO_2 \rightarrow C + 2H_2O$).

The thermodynamic equilibrium conditions under which solid carbon forms assume that the carbon is present as β-graphite. This has been questioned by Manning and coworkers [41] in a study of carbon deposition using nickel and cobalt catalysts where they postulate carbon deposits as a metastable metal-carbide intermediate.

Carbon is often formed as filaments that appear in some cases like hollow tubes, termed *filamentous carbon*. The carbon deposition mechanism causes attack on the metal and disperses it through a mass of finely divided carbon, which thus becomes very catalytically active because the metal is finely divided. With time the fibrous carbon structure may sinter and become more compact, whereupon it becomes less reactive. This phenomenon is a mechanism of attack on bulk metal and supported metal catalysts that can have serious consequences, such as rapid deactivation of the catalyst. Recently Chang and Crynes [9] have proposed a reaction-deactivation model, based on experimental observation, for predicting catalyst life for hydrotreating a solvent-refined coal oil. Klingman and Lee [31] have proposed a kinetic model of catalyst deactivation by multilayer coking.

2.2.4 Processing Objective

After the feed type is known, the remaining factor in choosing a catalyst is the processing objective. In general, cobalt-molybdenum catalysts are noted for desulfurization activity, while nickel-molybdenum catalyst are most suited for denitrogenation and hydrogen uptake. However, this does not mean that a cobalt-molybdenum catalyst is always the preferred choice for desulfurization. High-activity nickel-molybdenum catalysts do exhibit a substantial desulfurization activity over the entire range of feedstocks, and they can be superior in some circumstances involving unusual processing conditions or feedstock sources.

One common case where nickel-molybdenum catalysts are frequently the best choice occurs when feedstocks composed of more than about 20 % cracked stock are to be processed. In constrast to the flexibility of nickel-molybdenum catalysts, cobalt-molybdenum catalysts only exhibit reasonable denitrogenation activity with lighter

feedstocks. Hydrogen uptake involves a variety of processing objectives such as saturating aromatics, treating fluid catalytic cracking (FCC) feedstocks, improving color or thermal stability, and improving cetane number.

Experience is important in making the proper decision. The best experience is actual commercial operations with similar conditions and feedstocks. Combining this with catalyst comparisons normally obtained in the pilot plant, the rigid catalyst selection can be made with confidence. Where the feedstock and/or process conditions are unique to a particular operation, the experience and comparative data of a knowledgeable catalyst supplier can be very beneficial.

2.3 Zeolites

Zeolites are highly crystalline, hydrated aluminosilicates that upon dehydration develop into an ideal crystal having a uniform pore structure having minimum channel diameters (apertures) of from about 0.3 to 1.0 nm. The size depends primarily upon the type of zeolite and secondarily upon the cations present and the nature of treatments such as calcination and leaching. Zeolites have been of intense interest as catalysts for some two decades because of the high activity and unusual selectivity they provide in a variety of acid-catalysed types of reactions. In many cases, but not all, the unusual selectivity is associated with the extremely fine pore structure. This permits only certain molecules to penetrate into the interior of the catalyst particles, or only certain products to escape from the interior. Further descriptions of zeolites are given by Bolton [5], Scott [53], Gottardi [21] and Jacobs [28].

Zeolites are of practical interest for a variety of reasons. The fine pore structure permits adsorption separation to be carried out on the basis of molecular size and shape, so-called *molecular sieving*, as in the separation of n-paraffins from isoparaffins. The ability to alter zeolite properties by ion exchange permits the synthesis of adsorbents of unusual selectivity, even when all molecules have free access to the interior pores of the zeolite. The ion-exchange properties also allow a high degree of flexibility in synthesizing catalysts, for example the ability to produce a highly dispersed metal. From the catalytic point of view zeolites are of special interest in that they exhibit

unusual high activity for various acid-catalysed reactions such as cracking, the ability to combine a molecular sieving property with catalysis, and unusual selectivity behaviour.

2.3.1 Structure

The structure of a zeolite consists of a three-dimensional framework of SiO_4 and AlO_4 tetrahedra, each of which contains a silicon or aluminum atom in the center. The oxygen atoms are shared between adjoining tetrahedra, which can be present in various ratios and arranged in a variety of ways. Zeolites may be represented by the empirical formula

$$M_{2/n} \cdot Al_2O_3 \cdot xSiO_2 \cdot yH_2O$$

or by the structural formula

$$M_{x'/n}\{(AlO_2)_{x'}(SiO_2)_{y'}\} \cdot wH_2O$$

where M is the compensating cation for the net negative charge that is the result of isomorphic substitution of Si by Al, and the bracketed term is the crystallographic unit cell. The metal cation (of valence n) is present to produce electrical neutrality, since for each aluminum tetrahedron in the lattice there is an overall charge of -1. Access to the channels is limited by apertures consisting of a ring of oxygen atoms of connected tetrahedra. There may be 4, 5, 6, 8, 10, or 12 oxygen atoms in the ring. The largest apertures occur in the faujasite-type zeolites (types X and Y) and mordenite, which are of high current interests as catalysts. Zeolites are often prepared in the sodium form, which can then be replaced by various other cations or by hydrogen ions.

Pore Structure

During dehydration some movement of cation may occur; the cation may also move by interaction with adsorbed species and thus alter the structure. Hence the effective pore size of dehydrated zeolites cannot be directly inferred from that of the hydrated form. The effective pore diameter may also vary with the nature of the cation present, for example Na, Ca, H or the dehydroxylated form, and with other treatments. For

use in reactions, such as catalytic cracking, high temperature stability is important, and this is generally increased by minimum sodium content.

Zeolites Type X and Y

Types X and Y are structurally and topologically related to the mineral faujasite and frequently referred to as *faujasite-type* zeolites. They have three-dimensional intersecting channels in which the minimum free diameter is the same in each direction. They consist of an array of cavities having internal diameter of about 1.2 nm. Access to each cavity (also termed *supercage*) is through six equispaced necks having a diameter of about 0.74 nm. The X and Y zeolites have among the largest minimum aperture restrictions of any zeolite, and the highest void fractions. Their structure may be visualized by the line drawings of Figures 5, 6 and 7. In the foreground of Figure 5 is one of the necks, consisting of a ring of 12 oxygen atoms, through which may be seen slight portions of the three other necks. The rows of necks comprise an array of passageways perpendicular to one another in three dimensions.

2.3.2 Properties

In this section the properties of zeolites related to their use as catalysts are reviewed. Their ion-exchange capability, diffusion, thermal stability and molecular sieve effect are also described.

Ion-Exchange Capability

Owing to the isomorphic substitution of silicon by aluminum, the three-dimensional oxygen framework carries an excess negative charge, compensated by cations. The cations can be exchanged with other cations of different nature and valency, which permits the introduction of catalytically important elements. By changing the nature of the cation and the degree of exchange, a whole family of single cations can be exchanged, as well as complexes of cation such as $Cu(NH_3)_4^{2+}$ and $Pt(NH_3)_4^{2+}$. The only limitation to the nature of the cations that can be introduced by ion-exchange is the acid stability of the zeolite. Generally the zeolite is more stable in acidic solutions when the Si:Al ratio is higher. However, when the exchange solution is strongly acidic,

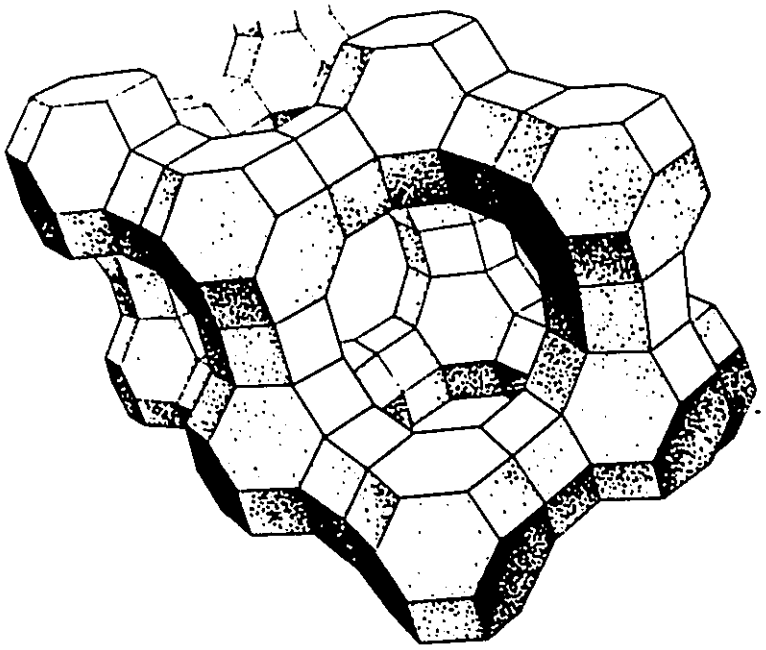

Figure 5: Zeolite X and Y (Faujasite) Structure

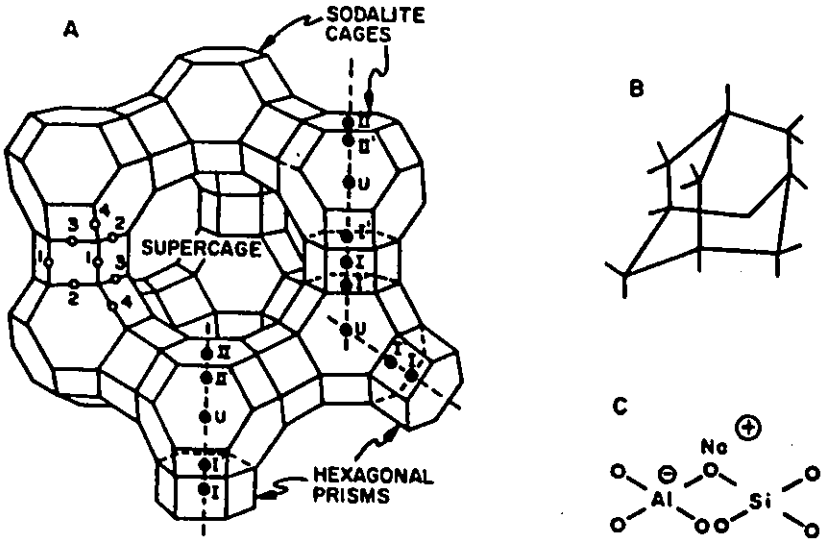

Figure 6: (A) Schematic of faujasite framework showing oxygen type (O) and nonframework (•) locations.
(B) Adamantanoid pore structure in faujasite.
(C) Basic unit of cation exchange/functionality

one should bear in mind that, in addition to a given cation, protons are also exchanged in the zeolite. In this way, a solid with strong acid sites in the pores is created.

Diffusion

Diffusion in zeolites is more complex than Knudsen diffusion or bulk diffusion, and the activation energy is usually substantially greater than that for Knudsen or bulk diffusion. Diffusion in zeolite pores of roughly 1 to 5 nm diameter, in which Knudsen diffusion merges with configurational diffusion, is essentially unexplored, but surface diffusion may well play a significant role under these circumstances.

In the configurational diffusion regime, the increase in diffusivity with change in zeolite generally parallels the increase in pore size, as determined by sorption measurements with different-sized molecules. For a specific zeolite, the activation energy generally increases with increasing molecular size of diffusing species, within a series of similar types of molecules. However, adsorption phenomena and the interaction energy between diffusing molecule and pore walls are also significant variables.

Unlike Knudsen diffusion, in which the fluxes of oppositely moving molecules are independent of one another, the diffusion in zeolites is such that the flux in one direction is markedly hindered by the opposing flux. Such counter diffusion is inevitable in catalytic reactions. Diffusivities can also be markedly affected by slight variation in zeolite structure, including the nature of the cations and the presence of impurities, and by the size and polarity of counter-diffusing molecules. The apparent activation energy for zeolite diffusion is greater than that for bulk or Knudsen diffusion. The few values that have been reported are relatively uncertain because of the limited temperature range covered and other difficulties such as deviations from Fick's law, sorption effects, and questions concerning the difference between unidirectional and counter-diffusion. Generally, the smaller the diffusion coefficient, the higher the activation energy.

In their commercial form zeolite catalysts are incorporated into a gel matrix, but diffusivities are much greater in the pores of the matrix than in the zeolite pores. Diffusion limitation inside the zeolite pores may not be significant in commercial catalytic cracking, but it depends on the feedstock, amount of carbon present on the catalyst, and other factors. Evidence is contradictory.

Haynes et al. [24] investigated the effects of hydrocracking mixtures of two-, three-, and four-ring structures over a nickel-tungsten sulfide ultrastable zeolite Y catalyst. They found that when diffusion is in the configurational zone, differences of the order of tenths of an Ångstrom unit in molecular size can have drastic influences on the zeolite diffusivity.

Thermal Stability

The structural stability of the less stable zeolites (X and Y) is increased after exchange with polyvalent ions such as Ca, Mg and La. The thermal stability of hydrogen zeolites, obtained by proton exchange or after decomposition of the ammonium-exchanged form, is several hundred degrees lower than that of the parent zeolite. For high-temperature reactions catalysed by these acidic forms of zeolite (e.g. cracking of hydrocarbons), it is necessary to stabilize the zeolite structure; one way is by prior exchange with polyvalent cations. In this way, rare earth-exchanged NH_4 Y-zeolites after dehydration are suitable cracking catalysts in terms of thermal stability and acidity of the solid. Thermal stability is also increased after gradually leaching out aluminum atoms from the lattice.

The practical use of zeolites as cracking and hydrocracking catalysts also requires a high hydrothermal stability. The structural resistance against steam treatment is also higher for zeolites with higher thermal stability and lower aluminum content.

Molecular Sieve Effect

Sieving of one type of molecule out of a feed containing a mixture of molecules with different shapes and/or sizes is possible as the free apertures of the zeolites have molecular dimensions. From the catalytic point of view, such a system contitutes a very selective catalyst if the sites responsible for the catalytic action are located inside the cavities or pores. The zeolite component is expected to be more selective than the matrix for the desired product. Similarly, the matrix may be considered more selective for other products [12].

2.3.3 Acid Sites

The discovery that silica-alumina catalysts were active for cracking reactions stimulated research to elucidate the nature of the active sites on the surface. It was found that acid sites were responsible for the cracking activity. The existence of those sites is readily demonstrated by the affinity of basic molecules such as ammonia, pyridine, or quinoline for the surface of silica-alumina. The amorphous silica-alumina (which is used as a matrix where the zeolite is dispersed in proportions from 10 to 20 wt. %) does not behave simply as mechanical mixture of silica and alumina. This is evident from the fact that silica alone is virtually inactive for cracking and that alumina alone is much less effective than silica-alumina. The catalyst actually behaves like a complex of the two substances. Typical silica-alumina cracking catalysts contain silica in excess, the amount of alumina being 10–25 wt. % . The structure in such materials is as described in section 2.2.2.

Both Brönsted and Lewis acid sites are found in zeolites. The former are protons attached to lattice oxygen atoms, while the latter can be the charge-compensating cations or trigonal aluminum atoms at oxygen-deficient sites or at cation positions. Protons can be introduced into the structure through ion exchange, thermal decomposition of the NH_4-exchanged form, hydrolysis of water of hydration of cations or reduction of cations to a lower valency state. If these structures are further dehydrated, this results in dehydroxylation and the formation of Lewis acid sites.

The ratio depends, then, on the temperature of pretreatment prior to the determination. As it is increased, the ratio of Lewis to Brönsted sites increases. The relative importance of the two types of acid sites in catalytic cracking has been debated extensively. However, the prevailing view is that Brönsted acidity is more important in the overall performance of a silica-alumina zeolite cracking catalyst [55]. A more in-depth study about zeolites as acidic catalysts is given by Barthomeuf [3].

2.3.4 Uses in Catalytic Processes

In the early 1960s, crystalline aluminosilicates or zeolites were introduced in catalytic cracking. Their use has been responsible for dramatic improvement in cracking processes. The industrial use of these solids as heterogeneous catalysts is nonetheless

limited. Their use in industrial processes implies that they exhibit higher activity and/or selectivity than existing catalysts. Their major applications as catalysts are found in the petroleum industry and are related to two important zeolite properties: the molecular sieve effect and the extremely high acidity of these solids [28]. Both characteristics have already been described above. More recently, wide-pore zeolites have been used as supports for highly dispersed metals. Commercial catalysts are of the faujasite type (X and Y) or are synthetic mordenites and zeolites T (erionite type).

The most important industrial applications of zeolites are in catalytic cracking, hydroisomerization, selective forming, hydrocracking and transformations of aromatic hydrocarbons [63]. A 100–10000 times improved activity [28] [16, page 34], for zeolite was claimed as compared to amorphous silica-alumina. This fact, coupled with an improved hydrogen transfer capability (presumably a consequence of hydrogen mobility between cracked molecules), was indicative of important potential of zeolitic materials for increasing conversions to gasolines with low coke yields [15]. The activity of modern zeolite cracking catalysts has improved to the point where for the most part only 1 to 4 seconds of contact time are required to effect substantially complete conversion of the non-aromatic portion of the feed.

The amount of gasoline produced from gas-oil fractions is much higher that can be obtained with amorphous silica-alumina catalysts. Gasolines produced by zeolite cracking generally have more isoparaffins and aromatics and less olefins than those obtained with silica-alumina. However, whether or not they show higher octane numbers depends upon which specific members of the groups paraffins, olefins, naphthenes and aromatics are present and in what ratio; this in turn is a function of feedstock composition and process variables. Zeolitic gasolines commonly are lower in sulfur and nitrogen content and have better storage stability and lead susceptibility.

Results obtained by a variety of methods indicated that the density of Brönsted acid sites was much higher for the Y-type zeolites in hydrocracking than for amorphous silica-aluminas. The higher selectivity to aromatics and isoparaffins indicates that hydrogen-transfer reactions occur more readily with zeolites as catalysts.

The tendency of metals to induce nonselective cracking in amorphous catalysts has

Table 3: Details of Zeolite Material

Description	:	Type Y, molecular sieve rare-earth exchanged	
Composition	:	SiO_2	- 65 %
		Al_2O_3	- 23 %
		Na_2O	- 2 %
		Rare-earth	- 11 %
Form	:	Powder	(38 to 53 μm)
Surface Area	:	Approx.	550 m^2/g
Catalogue no.	:	14–8910	
Manufacturer	:	Sterm Chemicals	U.S.A.

been extensively studied [52, page 143] [13,61]. Zeolite cracking catalysts have excellent resistance to contamination by vanadium, nickel, and other heavy metals, and appear to be superior to amorphous catalysts in this respect. This is evidenced by the lower carbon producing factor of a given metal loading for zeolites. The faujasite catalysts are also more resistant to poisoning by organic nitrogen compounds. These favorable attributes of zeolites are particularly valuable with the inevitable trend towards processing of increasingly heavy feedstocks.

The study of applications of zeolites to enhance the activity of the cracking catalysts continues. Examples of these are given by Goddard and Ruthven [20], who studied the adsorption of C_8 aromatics on Na Y-zeolites and by Kallo et al. [29] who studied the hydrosulfurization of the C=C bond on Me^{2+}-zeolites. Scott [53] updates until 1980 all the advances and developments of zeolite technology and its applications.

2.3.5 Zeolite Used in this Study

As seen above the rare-earth exchanged Y-type zeolite is the best option for hydroprocessing applications. This material was obtained from a commercial source. Some details of the zeolite material used in this study are listed in Table 3.

2.4 Reactors in Catalytic Processes

There are two types of industrial three-phase (gas–liquid–solid) reactors. In one case the bed of solids is fixed (e.g. trickle-bed reactor) and in the other the solids are in a suspended state (e.g. fluidized or ebullated-bed reactors). The fixed-bed reactors can operate co-currently (both gas and liquid in either upward or downward flow) or counter-currently, in which liquid flows downwards. As the prime concern of this review is related to the type of reactor used in this investigation, i.e. trickle-bed reactors, fluidized-bed reactors will not be described; however, some information on them can be found in the bibliography of this thesis [8,52,56].

2.4.1 Trickle-Bed Reactor

Evaluation of kinetic data obtained in single-phase continuous stirred tank reactors is comparatively simple task. When dealing with a single-phase catalytic flow reactor, back-mixing effects can be significant, and kinetic data analysis should account for such effects when important. Catalytic reactions which involve gas and liquid phases are often carried out in trickle-bed reactors, and kinetic data are usually obtained in laboratory-scale pilot plants units prior to commercial reactor design. In the analysis of data derived in a trickle-bed reactor, one is faced with an assessment of the relative importance of the various mass transfer resistances (gas-liquid, liquid-solid, back-mixing, etc.) and flow behaviour (e.g. holdup, incomplete catalyst wetting) effects, as well as the interaction of the effects with the conversion levels in the reactor.

The trickle-bed reactor is extensively employed in the hydroprocessing of petroleum fractions for the removal of impurities such as sulfur and nitrogen, for hydrocracking of lower boiling range materials, and for altering the quality of the feed for subsequent processing. At high conversion levels in a pilot plant trickle-bed reactor, mass transfer and flow effects are relatively more pronounced that at lower conversions, and can begin to have a substantial effect upon the design of commercial systems unless properly accounted for in the analysis of the pilot plant data.

Analysis of constant pressure, isothermal hydrotreating data for various petroleum derived feedstocks obtained in standard small-scale pilot plant trickle-bed units indicates that the following three effects may be of importance: internal diffusion within

the catalyst, reactor back-mixing, liquid holdup or incomplete catalyst wetting. Internal diffusion within the catalyst is characterized by the effectiveness factor, usually obtained experimentally by measuring kinetic rates using one or more catalyst particle size, under conditions where reactor holdup, incomplete catalyst wetting, and back-mixing effects are negligible.

Both back-mixing and liquid holdup or incomplete catalyst wetting reduce the efficiency of a trickle-bed reactor. Back-mixing is solely a mass transfer phenomenon, whereas liquid holdup is caused by poor distribution and by passing of liquid over the porous catalyst pellets. The poor distribution of the liquid within the catalyst bed causes an ineffective use of active catalyst sites. Although different in their basic nature, both backmixing (effectively characterized by the Peclet number) and liquid holdup or incomplete catalyst wetting have been correlated with the same system variables [46] by several researchers. Therefore, it is difficult to isolate the effect of back-mixing from that of liquid holdup or incomplete catalyst wetting in the analysis of kinetic data derived from a trickle-bed reactor. In general, both effects would be important in small scale pilot plant reactors.

Advantages of Trickle-Bed Reactors

Some of these advantages are as follows:

(a) Flow is close to plug-flow, which allows higher conversion in a single reactor.

(b) Liquid flows form a thin film on the solid packing, making the resistance of the gas diffusing to the solid surface almost negligible.

(c) Homogeneous side reactions are minimized by having a small liquid to solid ratio.

(d) Flooding is rarely a problem (especially with co-current flow) and pressure drop is very low. This results in essentially uniform partial pressure of reactants across the length of the reactor.

(e) A trickle-bed reactor sytem is easier to set up, to operate and to maintain than either a fluidized or ebullated bed reactor.

Disadvantages of Trickle-Bed Reactors

As mentioned in section 2.4.1 there are some inherent disadvantages in this kind of reactor systems. Poor distribution of liquid, such as channeling, bypassing and incomplete catalyst wetting can occur in a trickle-bed reactor when there are low liquid flow rates. Also, if the catalyst particle is too small, this could give rise to higher pressure drops and the possibility of bed plugging. It is necessary that catalyst particles in this system be large in size compared with fluidized bed systems and consequently intra-particle diffusional effects are more pronounced.

Poor radial mixing of heat could be a disadvantage for commercial scale trickle-bed reactors. It could cause excessive localized heating which would result in an increase of undesirable reactions and for rapid catalyst deactivation. This becomes important for reactions that involve high heat effects.

Applications in Hydrotreatment

As stated above, trickle-bed reactors are extensively employed in the hydroprocessing of the petroleum fractions because of the mentioned advantages. Undesirable homogeneous reactions are minimized by having low liquid holdups. A higher degree of conversion in a single reactor is attained thanks to the predominantly plug-flow behaviour inside the reactor.

Distributers are used at the top of the reactor to avoid channelling. In commercial applications, high liquid flow rates help to solve this problem. However, mass transfer effects at intra-particle level could still cause some problems. This makes the evolution and use of a high efficiency catalyst important. The special case of diffusivity in zeolites is discussed in section 2.3.2.

Hydrodynamics

In the case of co-current down-flow, the packed-bed reactor functions in two main regimes [11,45]:

(a) The trickle-flow regime in which initially, for zero gas rate, the liquid phase trickles over the packing in the discontinuous shape of films, rivulets and drops

in contact with a stagnant continuous gas phase; and

(b) the single-phase liquid regime in which initially, for zero gas rate, the liquid phase fills the voids of the packing.

When a gas flow rate $\mathcal{G}$ is introduced and increased, and the liquid flow rate $\mathcal{L}$ is kept constant, the following patterns are observed.

(1) For the trickle-bed reactor ($\mathcal{L} < 20$ kg $m^{-2}s^{-1}$) for spheres, beads and pellets there is :

- a trickling flow of the liquid phase and a continuous flow of the gas phase ("trickling flow");
- alternate gas-rich and liquid-rich parts passing through the column ("pulse flow");
- a poorly defined fluctuating flow that may be assumed to be continuous gas phase with a fraction of the liquid phase suspended as a mist in the gas stream and with the other fraction covering the packing surface in the shape of a film ("spray flow").

It must be noted that for small values of $\mathcal{L}$ ($\mathcal{L} < 2$–5 kg $m^{-2}s^{-1}$), there is not enough liquid to wet the whole packing surface, and the pulsing flow, which is due to liquid obstructing the flow of gas through the voids of the packing, is not encountered. When the liquid phase foams in the presence of gas flow, two new flow regimes exist (foaming flow and foaming pulsing flow) between trickling flow and pulsing flow.

The relative location of each gas of the flow patterns encountered is presented diagrammatically, in terms of the superficial mass velocities, in Figure 8 [10]. These diagrams were obtained for various gases and water, and different foaming and non-foaming hydrocarbons flowing through beds of 3 mm glass and alumina spheres and 1.8 mm × 6 mm and 1.5 mm × 5 mm alumina pellets. Other authors (e.g. Ng [45]) have studied similar systems for other shapes and sizes of packing, but unfortunately most of them are confined to water-air system.

The symbols in Figure 8 have the following meaning:

L = Superficial liquid mass velocity (kg/m^2s)

G = Superficial gas mass velocity (kg/m^2s)

The symbols ρ, μ, and σ represent, density, viscosity and the surface tension and their subscripts are G for gas, L for liquid, 'air' for air and 'wat' for water.

As can be observed from these flow regime charts, the values for viscosities, densities and surface tensions are necessary for making any prediction. Due to the complexity of a system such as that for hydrotreatment of heavy oil and the lack of data of this system, the best way of understanding the flow regimes in a hydrotreatment process is only through experimental studies.

For the present study the information obtained by Sambi [51] was extremely useful.

(2) For the reactor working initially with liquid phase alone ($\mathcal{L} > 20$ kg $m^{-2}s^{-1}$), either upward or downward, the following patterns are observed:

- after the introduction of gas, small unbroken bubbles appear in the continuous liquid phase ("bubble flow");
- the bubbles begin to coalesce and surround several packing elements ("distorted bubble flow"); with an increase in gas flow rate. This regime is followed by
- a pulse flow and a spray flow.

The relative location of each of these flow patterns may be found in the literature for various packing shapes, but again mainly for the air-water system [45], as previously mentioned.

A drawing illustrating the flow patterns in trickle-bed reactors is shown in Figure 9.

Gas and Liquid Distribution

In hydrotreatment processes, the limiting reactants are in the liquid phase. Therefore, liquid distribution is of primary importance. Generally, gas distribution is very good by itself and does not require special consideration. Depending upon the ratio of reactor tube diameter to particle diameter (d_t/d_p), it has been found that liquid has a tendency to channel toward the walls of the reactors. In the low interaction regimes, where superficial liquid velocity $u_L < 0.9\times10^{-3}$ m/s, liquid distribution has been found to be uniform (Herskowitz and Smith [?6]).

The same authors have reported [27] that for $d_t/d_p > 18$, the wall flow is negligible, and that granular particles cause less wall flow than cylindrical or spherical ones.

The d_t/d_p ratio is only one of the factors that affect liquid distribution (others are packing, fluid physical properties, etc.). Nonetheless, increasing the ratio (d_t/d_p) seems to have a positive effect on the uniformity of liquid distribution in trickle-bed reactors. Although there is not a single value good for all cases, these studies seem to indicate that at $d_t/d_p > 20$ the chances of a uniform liquid distribution are very good.

Herskowitz and Mosseri [25] studied the effects of gas and liquid flow rates on global rates of reaction in trickle-bed reactors. They found that increasing the gas and liquid rates enhances the rate of reaction. However, at relatively high gas rates, the rate of reaction may decrease with increasing gas rates due to the formation of dry zones in the catalyst bed. It must be noted that this investigation was carried out at very different conditions, with different reactants and catalysts, than those of hydrotreament. Therefore, the only reliable source of information about hydrotreatment systems such as the one studied here, is that from Sambi [51].

Catalyst Wetting

In hydrotreating, reactions occur in the liquid film on the catalyst particles as well as inside the pores of these particles. Therefore, catalyst particles must be wetted by liquid in order to use the active sites more efficiently. Increasing the liquid flow rate enhances both the rate of liquid-solid mass transfer and the wetting efficiency of the catalyst particles (defined as the fraction of the particle external surface covered by flowing liquid). The wetting efficiency f, is less than unity at liquid Reynolds numbers less than about 20.

If the particle is not completely covered by flowing liquid ($f < 1$), gaseous reactants may be transferred from the gas to the particle surface through a very thin layer of stagnant liquid (called the gas-covered surface or the dry surface). The resistance to mass transfer on the gas covered surface may be significantly lower than on the liquid-covered surface. This would enhance the global rate of reaction. As a result, the global rate of reaction may increase with decreasing liquid flow rate, even though the liquid-solid mass transfer rate decreases.

Liquid Holdup

Liquid holdup is the amount of liquid present in the packed bed at steady state conditions. This is further divided into two categories, dynamic and static holdup. The dynamic holdup is considered to be the amount of liquid that will drain out of the packed bed if the inflow of liquid is stopped at steady-state conditions. The difference between the total holdup and the dynamic holdup, i.e. what remains in the interior of the reactor, is considered as the static holdup.

Several kinetic models for hydrotreatment of different types of gas oil in trickle-bed reactors use the 'holdup' concept. For a first order reaction both Peclet number (sometimes referred to as Bodenstein number) and liquid holdup in a trickle-bed reactor are functions of liquid hourly space velocity (LHSV), catalyst size, catalyst bed length (L), liquid mass velocity, and the fluid properties, such as viscosity, density and surface tension. For a reactor packed with a certain size catalyst and operating at constant temperature and pressure, experimental data are usually obtained at various liquid hourly space velocities. The Peclet number (Pe) is related to LHSV, L and the feedstock viscosity by an empirical relation of the following type:

$$Pe_d = a(LHSV)^{\alpha}(L)^{\alpha} \tag{1}$$

Similarly, the holdup is correlated to LHSV and L by an expression of the type

$$H = b(LHSV)^{\beta}(L)^{\beta} \tag{2}$$

Equations 1 and 2 are derived for the undiluted catalyst beds and are developed assuming isothermal and isobaric conditions. Finally the effective catalyst wetting is also correlated as

$$A_{eff} = c(L)^{\gamma}(LHSV)^{\gamma} \tag{3}$$

The constants a, b, and c in the three previous equations are dependent upon the catalyst dimensions and fluid properties.

In a completely ideal situation, where back-mixing and holdup or incomplete catalyst wetting are negligible, the governing equation for the reactor performance may be expressed as (Mears [42])

$$\ln \frac{C_{Ai}}{C_{Ao}} = \frac{k}{LHSV} \tag{4}$$

where C_{Ai} and C_{Ao} are the concentrations of a reactant at the reactor inlet and the outlet respectively, and k is the apparent kinetic constant, which includes the catalyst effectiveness factor and the void fraction of undiluted catalyst. Equation 4 indicates that, in the absence of backmixing and holdup or incomplete catalyst wetting effects, a log–log plot of $\ln(C_{Ai}/C_{Ao})$ vs. 1/LHSV should be a straight line with a slope of unity. Furthermore, at constant LHSV, the conversion should be independent of catalyst bed length.

If the holdup effect is important but the back-mixing is insignificant, then combining Equations 2 and 4 gives

$$\ln \frac{C_{Ai}}{C_{Ao}} = \frac{k'(L)^{\beta}}{(LHSV)^{1-\beta}} \tag{5}$$

where $k' = kb$. An accepted value for β is $\frac{1}{3}$. Equation 5 implies that a plot of $\ln(C_{Ai}/C_{Ao})$ vs. 1/LHSV on a log–log scale should be a straight line with a slope $1-\beta$. Since β is most probably greater than zero and less than 1, the slope of the above line should be somewhere between 0 and 1. If the conversion data are taken at constant LHSV but varying catalyst length bed L, a log–log plot of $\ln(C_{Ai}/C_{Ao})$ vs. L should also be a straight line with the slope of the line equal to β.

Mears [42] reports that incomplete catalyst wetting has been observed at Reynolds number of 55. However, at large Reynolds numbers (of the order of 100) incomplete catalyst wetting does not appear to be feasible.

If back-mixing is important, then in the absence of holdup or catalyst wetting effects, a relation between C_{Ai} and C_{Ao} would be given by [46]

$$\frac{C_{Ao}}{C_{Ai}} = \frac{4q \exp\left(\frac{Pe}{2}\right)}{(1+q)^2 \exp\left(\frac{Peq}{2}\right) - (1-q)^2 \exp\left(-\frac{Peq}{2}\right)} \tag{6}$$

where $q = \sqrt{1 + 4k/Pe(LHSV)}$ and $Pe = Pe_d L/d_s$. Here d_s is the diameter of the catalyst. For a large Pe or a small deviation from plug flow, Equation 6 can be aproximated by

$$\frac{C_{Ao}}{C_{Ai}} = \exp\left(-\frac{k}{LHSV} + \frac{k^2}{(LHSV)^2} \cdot \frac{d_{s/L}}{Pe_d}\right) \tag{7}$$

Combining 1 and 7, one obtains

$$\ln \frac{C_{Ai}}{C_{Ao}} = \frac{k}{LHSV} - \frac{(k')^2}{(LHSV)^{2+\alpha}} \cdot \frac{1}{(L)^{1+\alpha}} \tag{8}$$

where $(k')^2 = k^2 d_s/a$.

It is clear from the above relationship that a log–log plot of $\ln(C_{Ai}/C_{Ao})$ vs. $1/LHSV$ obtained under a set of reaction conditions would not be a straight line for a first-order reaction. Similarly, a log–log plot of $\ln(C_{Ai}/C_{Ao})$ vs. L at constant LHSV and other reaction conditions would also be expected to show curvature.

Axial Dispersion

Deviations from plug flow may be caused by one or more of several effects. The void fraction of a packed bed next to the wall is higher than in the center. Because of the lower resistance at the wall, the linear velocity near the wall is greater. The contribution of wall flow to the total flow may be significant for low ratios of d_t/d_p, for example 10 or less, as previously discussed in section 2.4.1. The extent to which this may affect reactor performance, however, depends on several factors such as the value of Re, the bed length, and the conversion. At low Reynolds numbers, molecular diffusion may cause a significant axial dispersion. Regardless of the cause,

axial dispersion is usually represented by a Peclet number, $Pe = \bar{u}d_p/D_a$, where D_a is the effective axial dispersion and $\bar{u}$ the mean fluid velocity.

Usually, axial dispersion is of negligible importance, except for very short beds and high conversions at low flow rates. Since this can usually be overcome by lengthening the bed, the following criterion [52] is presented for the minimum reactor length necessary to avoid a significant dispersion effect.

$$\frac{L}{d_p} > \frac{20n}{Pe} \ln \frac{C_f}{C_i} \tag{9}$$

Here n is the order of reaction, and C_f/C_i is the fractional conversion. The Peclet number is about 2 for gases at Reynolds numbers above about 2 if the ratio d_t/d_p is sufficiently great that wall bypassing is not serious. According to this criterion, for axial dispersion effect on reactor performance to be less than 5 %, the reactor length to particle diameter ratio (L/d_p) should be more than 350.

Almost all the information on the effect of the Reynolds number on the Peclet number has been obtained from nonreacting, isothermal systems. At low values of Re, convection effects in laboratory reactors may be a far more important source of deviation from plug-flow than is generally recognized; for example, if an exothermic reaction is studied in a down-flow reactor, convection effects may be suspected, especially in short, squat types of configuration. It is difficult to predict such effects, but experimentally, if a fairly coarse catalyst is being studied and dispersion by convection is suspected, filling the void with an inert material may be an effective diagnostic procedure. If dispersion by convection is indeed significant, this would reduce convection and likely increase conversion.

Catalyst Dilutions

It is generally recognized that low space velocities in trickle-bed reactors may give rise to undesirable effects on the reactor performance. The downward flow of the liquid phase is largely established by gravity under normal trickle-flow conditions, consequently the liquid tends to drain from the reactor and the amount of liquid

adhering to the catalyst particles in the interstitial voids in the bed (dynamic holdup) is relatively small at low feed rates.

It thus appears very difficult to correct the non-ideal behaviour of laboratory trickle-bed reactors; however, catalytic dilution may help considerably to make this behaviour closer to ideal. Dilution of the catalyst bed with small inert particles is known to have a beneficial effect on catalyst contacting efficiency as well as reduces back-mixing [42].

A study of the effect of a diluted bed for deep denitrogenation reactions was carried out by van Klinken and van Dongen [62] They found that the number of transfer stages is tripled by diluting the catalyst bed. Since the diluted bed contained 35 % less catalysts, the rate of mass transfer per unit catalyst, k_tA, is even higher. This improvement must be attributed to a much larger wetted area A, assuming that the mass transfer coefficient k_t is primarly determined by pore diffusion and, therefore, not affected by the presence of a diluent in the catalyst bed.

They concluded that, by virtue of the small diluent particles, the amount of oil flowing in the reactor may be higher by a factor of four. A markedly positive effect on catalyst wetting may therefore be expected. As regards the trickling liquid, ideal plug flow can be assumed to occur in diluted beds in virtually all cases.

Mathematical Model for a Trickle-Bed Reactor

Some of the models have been presented in previous sections. In this section the only model considered is the ideal plug-flow model. This model can be assumed if the following conditions are satisfied:

(a) The catalyst is completely wetted by liquid.

(b) No significant axial dispersion.

(c) Negligible mass transfer resistance (gas-liquid and liquid–solid)

(d) Reaction occurs only at the liquid–solid interface.

(e) No vaporization of liquid or condensation of vapors occur.

(f) Heat effects are negligible and operation is isothermal.

For such a case, a differential mass balance of one of the reacting species will give a simple plug–flow equation of the following type

$$\frac{dC}{dz} = -\frac{k''_m(1-\varepsilon)\eta}{(LHSV)}[C]^m = -\frac{k'_m\eta}{(LHSV)}[C]^m, \qquad 0 < z \leq 1 \tag{10}$$

Where C is the concentration of the reactants, k''_m is the intrinsic rate of reaction and m is the order of reaction, z is the dimensionless length parameter, ε is the void fraction of the catalyst bed, LHSV is liquid hourly space velocity, which is generally taken as the volumetric hourly flow rate of liquid divided by the catalyst volume. η is the catalyst effectiveness factor and k'_m is the m'th order reaction rate constant based on the total volume of catalyst.

Integrating Equation 10 over the entire length of the reactor yields:

$$\ln\frac{C_i}{C_o} = \frac{k'_1\eta}{(LHSV)'} \tag{11}$$

where k'_1 is the first order rate constant for a first order reaction, and subscripts i and o indicate the inlet and outlet concentrations (in this investigation they are the concentration of sulfur or nitrogen).

The same Equation 10 can be integrated for a general case of m'th order reaction. The equation obtained is

$$[C_o]^{1-m} - [C_i]^{1-m} = (m-1)\frac{k_m}{(LHSV)} \tag{12}$$

According to the available literature the plug-flow model adequatedly fits the trickle-bed reactor used in this investigation. This was confirmed in a previous study [51].

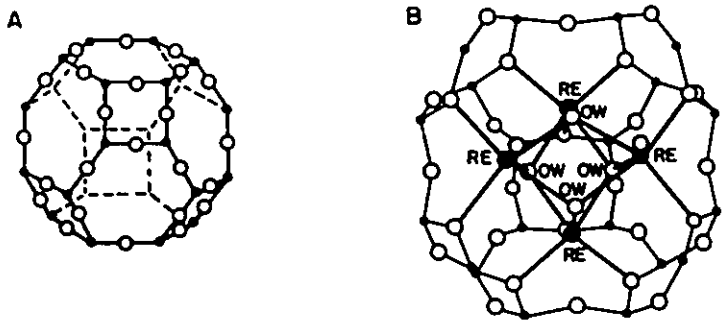

Figure 7: (A) Geometric representation of sodalite cage as a truncated octahedron. (B) Sodalite cage complex containing four rare earth cations. (·)=Si,Al; (O)=oxygen; (●)=rare earth

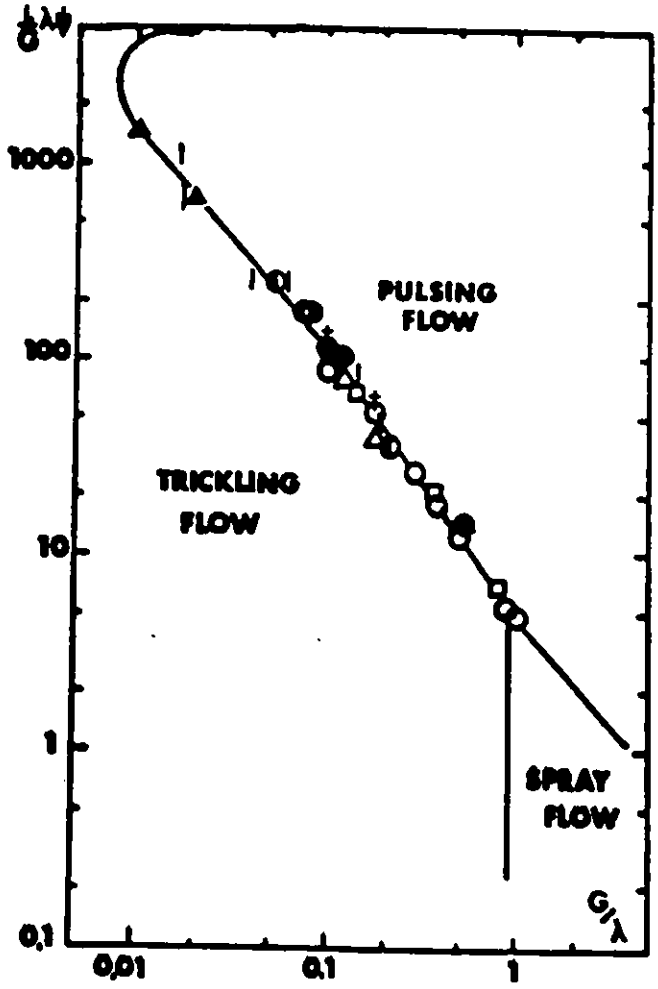

Flow Pattern Diagram for Nonfoaming Liquids.

$$\lambda = \left[\frac{\rho G}{\rho_{wat}} \cdot \frac{\rho L}{\rho_{air}}\right]^{0.5} \qquad \psi = \frac{\sigma_{wat}}{\sigma_L}\left[\frac{\rho_L}{\rho_{wat}}\left(\frac{\rho_{wat}}{\rho_L}\right)^2\right]^{0.33}$$

System	Packing	Key
Water-air	Spherical catalyst	○
Cyclohexane-air	Spherical catalyst	◐
Water-air	Cylindrical catalyst 1	□
Cyclohexane-nitrogen	Cylindrical catalyst 2	△
Gasoline-carbon dioxide	Cylindrical catalyst 2	●
Gasoline-nitrogen	Cylindrical catalyst 2	■
Gasoline-helium	Cylindrical catalyst 2	▲
Petroleum ether-nitrogen	Cylindrical catalyst 2	|
Petroleum ether carbon dioxide	Cylindrical catalyst 2	‡

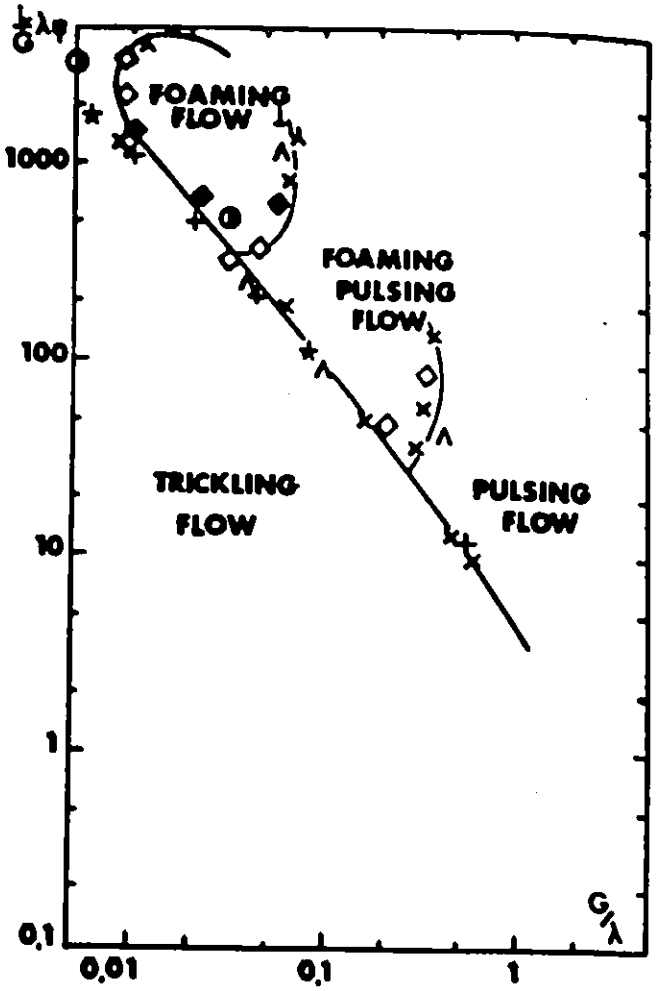

Flow Pattern Diagram for Foaming Liquids.

System	Packing	Key
Kerosene-air	Spherical catalyst	◑
Desulfurized gas oil-carbon dioxide	Cylindrical catalyst 2	+
Desulfurized gas oil-air	Cylindrical catalyst 2	×
Desulfurized gas oil-helium	Cylindrical catalyst 2	⋏
Nondesulfurized gas oil-carbon dioxide	Cylindrical catalyst 2	⋔
Nondesulfurized gas oil-air	Cylindrical catalyst 2	⋀
Nondesulfurized gas oil-helium	Cylindrical catalyst 2	⊥
Kerosene-air	Cylindrical catalyst 2	◇
Kerosene-nitrogen	Cylindrical catalyst 2	◆

Figure 8: Flow Pattern Diagrams for Nonfoaming and Foaming Liquids

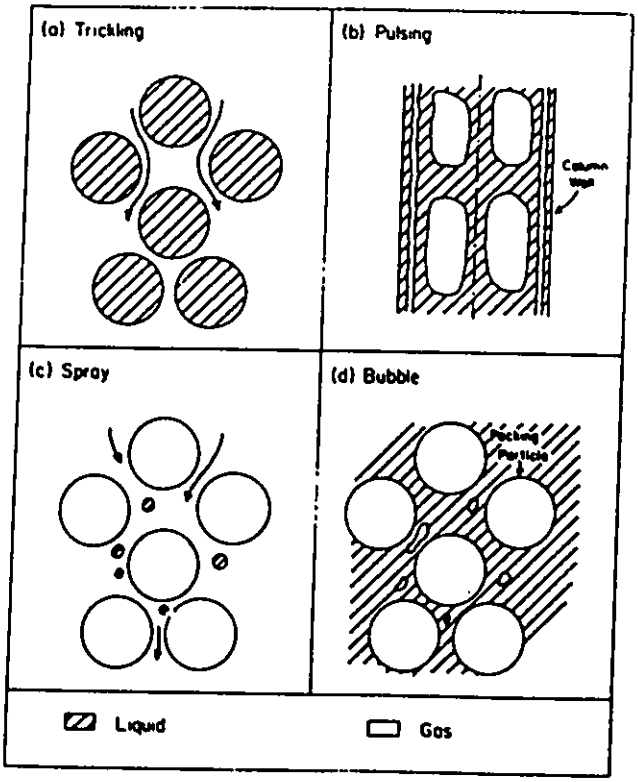

Figure 9: Flow Patterns in Trickle-Beds

Chapter 3

Experimental Section

3.1 Experimental Equipment

The equipment used for preparing the catalyst was mainly standard laboratory equipment (e.g. glassware, stirrers, mortars, ovens, muffle furnace, extruders, etc.). The equipment used for the hydrotreatment is described below. The process for preparing and testing the catalyst is virtually the same as that followed by Sambi [51]. He also gives a more extensive description of the equipment used.

3.1.1 Hydrotreatment System

This system has the main features given in section 1.2.2. It includes a trickle-bed reactor kept in a sand bath for isothermal operation. The heavy oil mixed with hydrogen was fed from the top, and the product oil removed from the bottom after passing a back pressure regulator. When a sample was to be taken, the product stream was connected to a weighed sample bottle; otherwise it was run through two one liter separators. The product gases were analysed with an on-line gas chromatograph. A scrubbing system was used to remove most of the H_2S before venting out the gases to the atmosphere. For safety reasons the entire set-up was installed inside a fume hood (except for the gas manifold). A schematic of the hydrotreatment system is shown in Figure 10.

A high pressure metering pump (Milton Roy Company, model no. 396-31) was used

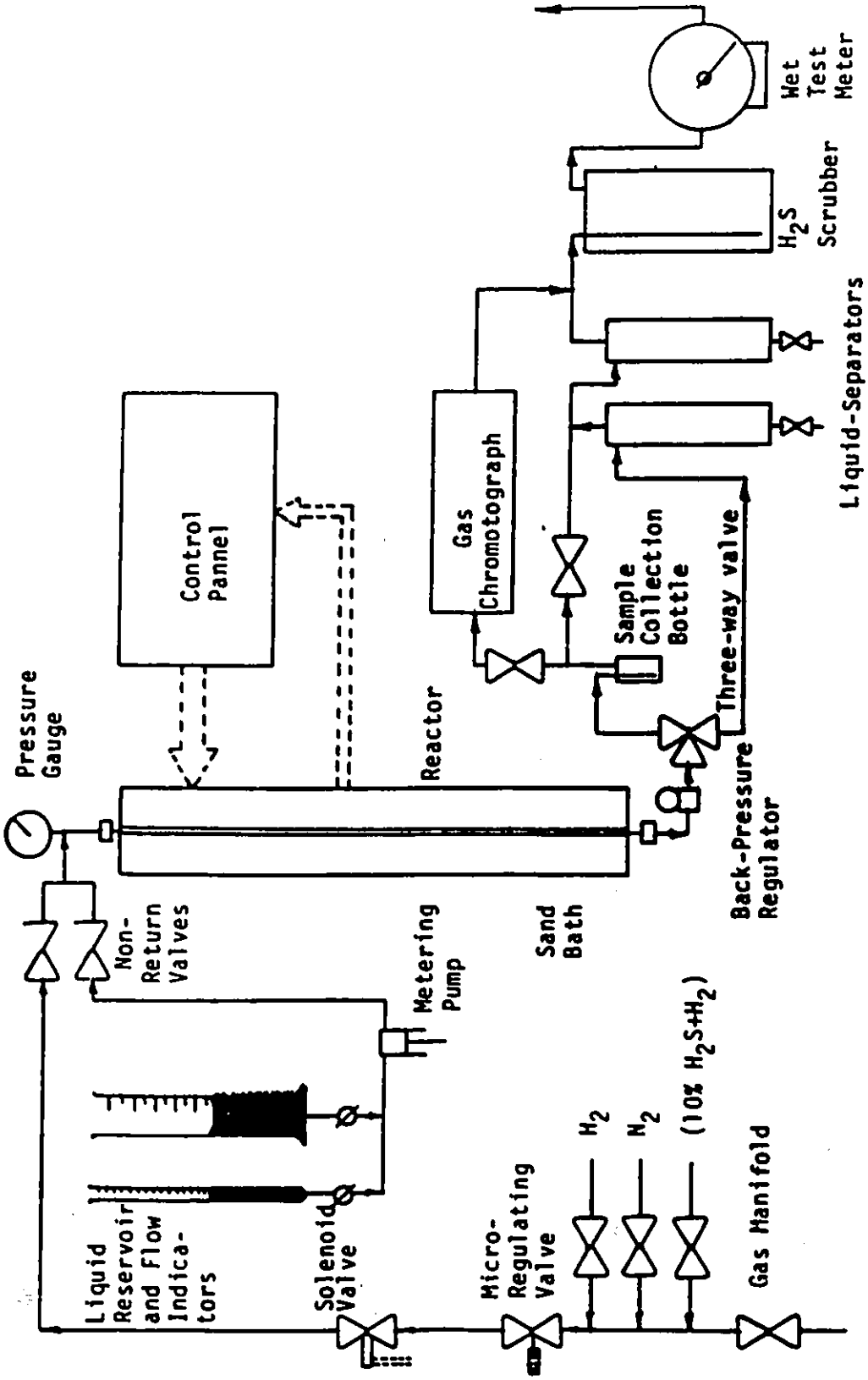

Figure 10: Schematic of the Hydrotreatment System

to pump the heavy gas oil into the reactor system. The pump was calibrated at an operating pressure of 6.9 MPa. The gas manifold held three gas cylinders, hydrogen, nitrogen and a 10 % by volume mixture of hydrogen sulfide in hydrogen. The gas flow was controlled with a set of valves which included a micro-regulating high pressure valve, a power-to-open solenoid valve, a pressure gauge and a non-return valve. All feed lines to the system were made of 3 mm O.D. 316 stainless steel tube. The reactor was a 316 stainless steel tube of 0.953 cm O.D. and 0.516 cm I.D. and 1 m in length. Both bottom and top ends had high pressure quick-connectors to simplify the frequent removal of the reactor. The sand bath was made out of a 50 mm nominal size pipe, with a conical hopper welded at the top to ease the filling and to prevent sand from being blown away with a sudden increase in the air flow. The bath and three separated heaters (at the top, middle and bottom of the system) were individually controlled with three Honeywell temperature controlers. It was insulated with ceramic and glass wool (layers of 40 and 25 mm respectively). The temperature inside the bath was checked several times at steady state with a digital thermometer, and it was always found to be within $\pm 1°C$ of the specified temperature.

The product oil and gas mixture was released through a back-pressure regulator into the oil separation and sampling system. The system included two one liter volume stainless steel separators connected in series. During sample withdrawal periods, the first separator was bypassed and the oil was separated from the outgoing gases in a 125 cm^3 glass bottle. The gases were analysed by passing part of the exit stream through a gas chromatograph. After being analysed, the gases were scrubbed in a H_2S scrubber. When samples were not withdrawn, the exit stream was passed through the separators to remove the oil from the outgoing gases.

For monitoring the exit gas flow continously, a Precision Scientific wet test meter (catalogue no. 63115) was used. This monitoring system included a modified Hewlett-Packard (HP) integrator (model no. 3373B) for timing each rotation of the wet test meter needle. A HP gas chromatograph (model no. 5700A) attached to a HP integrator (model no. 3380A) performed the analysis of the exit gases. A 0.5 cm^3 heated sample loop was used to inject the gas into the chromatograph. The column was a 23 % SP–1700 on 80/100 Chromosorb PAW packed in 0.3175 cm (1/8 in) O.D. 316 stainless steel tube 9.144 m (30 ft) long, from Supelco. For better separation of H_2S from n-butane, a 1.828 m (6 ft) long 0.3175 cm (1/8 in) O.D. Chromosil 310 column

was attached. The detector, as well as the auxiliary temperature control were kept at 100°C with a DC current of 200 mA. The carrier gas (helium) flow was maintained at 25 cm^3/min and the sample loop at 100°C. Columns were at 70°C all throughout the process. Attenuation was set at 1 for maximum resolution.

3.1.2 Analytical Equipment

Most of this equipment is of standard nature and was available in laboratory, therefore description of it is not made in much detail.

Catalyst Analysis

The chemical composition of the catalyst was determined with a Direct Current Argon Plasma Atomic Emission Spectrophotometer (Beckman Spectraspan–V). After grinding some catalyst particles to fine powder (less than 0.104 mm, equivalent to <150 mesh size), 0.1 g of it was fused with 0.5 g of lithium metaborate powder in a graphite crucible at 1000°C for 15 min. The melted extrusion was dissolved in 1 N nitric acid to a volume of 100 mL, forming the digestion to be analysed. For each catalyst three digestions were made and analysed for silicon, alumina and depending on the case, nickel and tungsten or cobalt and molybdenum.

The pore volume of the support material and that of the final catalyst were measured using the carbon tetrachloride adsorption method (Benesi et al. [4]). Surface area was measured using the standard BET method [7] with nitrogen as sorbate.

Oil Samples Analysis

Density of oil samples at 25°C was measured using a 2 cm^3 specific-gravity bottle. A calibrated Cannon–Fenske Routine viscometer (no. 400) was used for measuring the kinematic viscosity at 25°C. Aniline point of the samples was obtained following the standard procedure and equipment as per ASTM D–611. Elemental analysis for C, N, S and H was carried out with the Elemental Analyser model no. 240B from Perkin Elmer. Simulated distillation of the oil samples was carried out as per ASTM D–2887. The equipment used was a FID HP gas chromatograph (model no. 5730A) with a locally modified HP integrator (model no. 3373B) to give the area under the

chromatogram after every 2.5 min. The chromatogram was obtained with an HP chart recorder (model no. 7127A). The column used was a 1.5 % OV–101 on 100/120 mesh (clear opening between 0.147 and 0.074 mm) Chromosorb–GHP packed in 0.3175 cm (1/8 in) stainless steel 1.828 m (6 ft) plastic tube, from Supelco. The temperatures for the injection port and the detector were kept at 350°C. The oven temperature programming was set for 0°C (0 min)—16°C/min—350°C (16 min). The sample size was one microlitre (1 μL). A HP calibration sample (no. 5080-8716) was used for obtaining the retention times for different carbon numbers.

3.2 Experimental Procedure

This section includes the catalyst preparation and testing, and its utilization in the hytrotreatment trickle-bed reactor, as well as the methods for the analysis of product oil.

3.2.1 Catalyst Preparation

The catalysts for this study were prepared following the same scheme. First a silica-alumina gel was made. It was then mixed with zeolite material. The resulting gel was filtered, washed, extruded, dried, calcined, crushed, and screened to the proper size. The catalyst support particles were tested for pore volume. According to this result, the impregnation solution with the proper concentration of either nickel and tungsten or cobalt and molybdenum was prepared. Impregnation was carried out using the vacuum impregnation technique. Afterwards, particles were dried and calcined.

Once catalyst particles were ready, elemental analysis was performed, and pore volume and surface area were determined. After getting appropriate results from these test catalysts, particles were placed in the trickle-bed reactor for hydrotreatment testing.

Base Support Preparation

The gel was prepared in a 4 L beaker fitted with a pH meter and a stirrer. The appropriate amount of aluminum nitrate was dissolved in distilled water, and the required amount of sodium silicate was slowly added to the solution. The mixture was

stirred for 15 min. During that period of time, some ammonium hydroxide was added until the pH reached a neutral level. This caused silicon and aluminum to precipitate out as hydroxides, in the form of a white gel. The gel settled and aged for one day. Then, after decanting the clear liquid above the settled gel, the required amount of zeolite powder (Type-Y zeolite, according to characteristics given in Table 3) was added. The final composition of the gel that, once dehydrated, became the catalyst base support, was 10 % by weight silica, 65 % by weight alumina and 25 % by weight zeolite.

Two vacuum-filter funnels were used to filter the gel-powder mixture. The mixture was divided equally between the two funnels. After filtering, the resulting cakes were washed 3 times, each with 1.5 L of a 2 % by weight ammonium acetate solution. This was done to remove undesirable salts that might affect the base support properties. The cakes were not allowed to dry completely at any moment. After the washings, the cakes were left to dry, letting air run through the filtration funnels. Extrudates were made by passing the paste through a 0.95 cm (3/8 in) round hole dye of an extruder. These extrusions were dried for one day at room temperature and in an oven at 60°C for three to six hours depending on the water content of the extrusions. Calcination was carried out in a muffle furnace at 700°C for six hours. The calcined extrusions were crushed with a mortar and pestle. After being crushed, they were screened to a size of 0.21 to 0.17 mm in diameter (between 70 and 80 mesh).

Pore Volume Measurement

This measurement was performed using the carbon tetrachloride adsorption technique of Benesi et al. [4]. A mixture of 25.5 cm^3 of n-hexadecane and 182.5 cm^3 of carbon tetrachloride was placed in a 16 cm diameter glass desiccator. A 5 cm^3 narrow neck measuring bottle was used to contain about 1 to 2 g of dry catalyst support particles. The bottle with the sample was kept in the desiccator and the system was evacuated using a vacuum pump. A cold trap (with liquid nitrogen) was used for condensing about 10 cm^3 of carbon tetrachloride. This was an indication that all the air had been evacuated. Then the desiccator was isolated and left to reach equilibrium for a period of four hours. After this time the desiccator was opened, and the bottle with the sample closed immediately with a stopper. The bottle was weighed, and the

difference in weights gave the amount of carbon tetrachloride condensed on the bottle inner wall and in the catalyst pores.

This procedure was repeated with an empty bottle so as to obtain the amount of carbon tetrachloride adsorbed on the bottle inner wall. The mixture concentration was constantly checked by measuring its refractive index, and when necessary more carbon tetrachloride was added to keep the concentration constant. The amount of carbon tetrachloride adsorbed in the catalyst pores was then divided by its density and the dry sample weight to get the pore volume per unit weight of support particles.

Impregnation

The concentration of either nickel nitrate and ammonium metatungstate or cobaltous nitrate and ammonium molybdate required to get the desired amounts of the metals into the pores of a support material of known pore volume was estimated. About 60 cm^3 of the impregnation solution was used to soak about 30 g of support particles.

To drop the total amount of catalyst support particles into the impregnation solution, a specially designed twin flask was made from two 500 mL conical flasks. It was supported in such a way that its rotation would allow the evacuated catalyst particles to fall from one section of the flask to the other.

Before being placed in one of the impregnation flask sections, the catalyst support particles were dried at 110°C for five hours to remove any water that could have condensed in the pores during storage. The system was then connected to a vacuum pump and evacuated to a vacuum of 26.6 Pa (0.2 mm Hg) to remove all the gas from the pores. The flask was isolated from the vacuum pump. The impregnation solution was slowly introduced to the impregnation flask without splashing the catalyst support particles. The flask was rotated and the support particles fell into the impregnation solution. Once all the particles were immersed in the solution, atmospheric pressure was restored by letting air in slowly. The solution with the particles was left for 15 min to attain equilibrium. Afterwards, the slurry was put on to a coarse sintered glass filter funnel where the solution was separated from the impregnated particles. Finally, the particles were dried and calcined at 700°C for six hours in a muffle furnace.

Surface Area Determination (BET)

Surface area of catalyst particles was determined by using the laboratory BET apparatus constructed according to Technical Bulletin of Mellon Institute [17].

The equipment was verified several times for leaks, the glass burets recalibrated and bulb factors calculated. The values obtained turned out to be practically the same as the previous ones. A sample of 1 to 2 g of catalyst was put in the sample tube. The tube with the sample was plugged into the system and degassed for three hours at 200°C. Helium was used to calculate the empty space factors. Three to four points were obtained on the nitrogen adsorption isotherm up to a nitrogen pressure of about 35.45 kPa (0.35 atmospheres).

Sambi [51] wrote a computer program for fitting a straight line through the points of the adsorption data. This program was modified and used for determining surface area and is given in appendix A.

Chemical Composition

A Direct Current Argon Plasma Atomic Emission Spectrophotometer (Beckman Spectraspan-V) was used to determine the concentrations of silicon, aluminum, nickel, molybdenum, cobalt and tungsten. About 0.1 g of ground catalyst was placed in a graphite crucible and 0.5 g of lithium metaborate was added to it. The crucible was put in a muffle furnace for 15 min at 1000°C. A 400 mL beaker was placed on a magnetic stirrer and 75 mL of 1 N nitric acid was poured into it. The red hot crucible was taken out of the furnace and the melted bead (of the fused mass) was dropped into the beaker. The melt was dissolved using the magnetic stirrer, then the digestion was transferred to a 100 mL graduated cylinder and the volume was made up to the 100 mL mark. The digestion was stored in a plastic bottle while waiting for analysis.

The DCP Spectrophotometer was used to analyse the prepared digestion. Standard digestions for the 6 elements were made using the same procedure but using known standard element samples. Blank digestions were also prepared using only lithium metaborate. Blank digestions were used for zeroing the emission levels for each elements from where the average was obtained and used as value. The amount of each element was calculated from the weight of the catalyst powder used and the volume

of the digestion. Finally, the weight % of silica, alumina, nickel oxide, cobalt oxide, molybdenum oxide and tungsten oxide were determined.

3.2.2 Hydrotreatment

After obtaining satisfactory results with the prepared catalysts, their performances had to be tested in the trickle-bed reactor system. In this section the reactor filling with catalyst, catalyst activation, hydrotreatment, product oil sampling, system shut-down, and analyses of the products are described.

Loading the Reactor

As previously mentioned, catalyst particles were between 0.17 and 0.21 mm. The volume of catalyst used for each run was 8 cm^3. The catalyst was placed in a glass cylinder and weighed to obtain the bulk density. To achieve the maximum packing in every step of the process, a vibrator was used. For reasons indicated in section 2.4.1 catalyst was diluted with an equal volume of α-alumina of the same size. The reactor was filled with the catalyst–α-alumina mixture, but as the 1 m long reactor had a volume of 20.9 cm^3 the top part was filled with α-alumina only.

For preventing the catalyst particles from being carried away with the reactor effluent a 5 cm long 60 mesh stainless steel screen rod (clear opening 0.246 mm) was inserted at the bottom of the reactor tube. An approximately 1 cm long plug of quartz wool was placed at the top end of the reactor tube, and above this a small 60 mesh stainless steel screen was placed to prevent catalyst particles from clogging up the reactor entrance in case of flooding. Finally, the reactor was lowered into the sand bath and its high-pressure end fittings were set in position.

Catalyst Activation

After connecting the reactor, the complete system was checked for leaks. It was pressurized to 13.8 MPa (2000 psig) with nitrogen gas. Nitrogen was released and the activation of the catalyst started by sulfiding it. A flow of 10 % by volume mixture of hydrogen sulfide in hydrogen was passed through the reactor at a pressure of 380–415 kPa (~55–60 psig). As soon as this step was started, the sand bath was filled with

sand and heating started. Sulfiding was carried out for five hours at 350°C: one hour for reaching operating temperature and four hours for the sulfiding itself. Hydrogen was passed through the reactor for 30 min at the same conditions after the end of the sulfiding process.

Hydrotreatment Process

After activation and without cutting off the hydrogen flow through the reactor, reactor temperature was lowered below 150°C since it was not advisable to pass oil on hot dry catalyst because it can increase coke formation and accelerate deactivation of the catalyst. The pump was started and about 10 cm^3 of oil was passed through the reactor to wet all the catalyst particles before setting the actual operating conditions. The hydrogen cylinder and the back pressure regulators were accordingly adjusted to the operating pressure. The sand was put back into the sand bath and heating restored so as to reach the desired hydrotreating temperature.

Steady state was reached after about 90 min. In a normal run (without sampling), the reactor effluent was passed through the first one liter separator. Here the exit gases were separated from the liquid product that remained there. The gases were scrubbed and then passed through a wet-test meter connected to an integrator that gave a continuous record of the gas flowrates.

Sampling

For sampling the liquid oil product, a 125 cm^3 glass bottle was attached at the sample collection point. A three-way valve was used to shift the reactor effluent flow to the sample bottle. There the oil was separated from the gases. Part of the gas stream went to the gas chromatograph for analysis. The rest of it, along with the returning gas from the gas chromatograph, was scrubbed. The gas flow was monitored in the same way as when sampling was not carried out. At least 35 cm^3 of oil product were collected at each operating condition. This was considered a sufficient amount for further oil analyses.

The details of the gas chromatograph and accessories for analysing the exit gases have been described on page 50. Part of the reactor effluent gas going out of the sample

bottle was continuously passed through a heated 0.5 cm^3volume sample loop. The gas was injected into the gas chromatograph by flipping the sample valve. This was done every time the gas was to be analysed. Although the calibration process did not present any problem (when done with one gas sample), the column did not respond in the same way when reactor effluent gases were passed through. In some cases there was no response at all. For this reason the small amount of oil transformed into gas products could not be mesured. This was considered to be due to the failure of the column system. The amount not mesured is, however, not significant.

System Shut-Down

While in the start-up period an excess in coke build-up would have caused premature catalyst deactivation, during shut-down this would have given false data about the coking properties of the catalyst. To avoid this, the catalyst was never allowed to run dry under hot conditions. This means that the oil pump and the hydrogen flow through the reactor were not interrupted until the temperature inside the reactor was below the 100°C mark.

The heating was stopped and the sand withdrawn from the sand bath. For rapid cooling air was blown into the sand bath. When the system temperature dropped below 100°C, the pump was stopped and the system was slowly depressurized. While the hydrogen cylinder valve was closed, the nitrogen cylinder valve was opened to flush the remaining hydrogen from the system. A mixture of 25 % by volume of benzene in acetone was used as a cleaning solution to remove all the oil from inside the reactor. This cleaning procedure was repeated several times till clear solution started coming out of the reactor. Nitrogen was used to dry the catalyst. The reactor was removed from the sand bath and α-alumina and catalyst particles were collected.

Oil Sample Analyses

Several analyses were performed with the original heavy oil as well as with the product oil samples.

Density A 2 cm^3 Moore-Van Slyke specific gravity bottle was used for measuring the density. The bottle was previously calibrated using mercury. The measurements

were made at 25°C. The bottle was filled with the oil sample, covered with its stopper, wiped clean from outside and weighed. The density was determined from the bottle's volume and the weight of oil.

Viscosity The equipment for measuring viscosity was a Cannon-Fenske Routine calibrated viscometer no. 400. The viscometer with the sample in it was placed in a constant-temperature bath to keep the 7 cm^3 of oil sample at constant temperature. The oil was then sucked to just above the upper notch mark on the tube, and the time was taken until it passed the lower notch mark. This procedure was repeated four times, and the average value multiplied by the viscometer factor to get the kinematic viscosity. The normal viscosity was obtained by multiplying the kinematic viscosity by the oil sample density.

Aniline Point This analysis was performed following the procedures as per ASTM D-611. The aniline used for the analysis was first dried by contacting it with sodium hydroxide pellets in a glass bottle and stored overnight. Then it was distilled in a vacuum Rota-vapor equipment, discarding the first and last 10 %'s of the aniline volume. The distillate was stored in an opaque glass bottle under nitrogen atmosphere. The apparatus was assembled as per ASTM D-611 and a mixture of 10 cm^3 of oil and 10 cm^3 of distilled aniline was poured into the inner tube and kept well stirred. Heating was started at that moment and temperature noted when the mixture suddenly became cloudy throughout. This procedure was repeated three times and the average taken as the aniline point for that oil sample.

Mid-Boiling Point Distribution The Simulated Distillation as per ASTM D-2887 was utilized for determining the mid-boiling point distribution. The equipment used for this purpose is described on page 51. Before running any experiments the column was conditioned at 350°C overnight (16 h). The detector and the injection port temperatures were set at 350°C for starting the run. The oven programming, as mentioned before, was set at 0°C (0 min)–16°C/min–350°C (16 min). A blank run was made to verify satisfactory column performance (no noise and a constant baseline). After doing so, the retention times for various hydrocarbons were obtained. For this purpose 1 μL of standard sample (HP no. 5080-8716), containing C_5 to C_{40} normal

paraffins, was injected. One can observe a typical chromatogram obtained with the mentioned sample in Figure 11.

The boiling point distribution is shown in Figure 12. The same amount (1 μL) was injected for each one of the oil samples and the original oil. A typical chromatogram is shown in Figure 13. The area under the curve was measured every 2.5 min, and correlated with the boiling points at various retention times, generating a boiling point distribution curve. Three readings were taken for each sample and the average temperature was taken as the mid-boiling point. An example of the distribution curve is given in Figure 14. A computer program by Sambi [51] was modified and used for performing these calculations and is given in appendix A.

Elemental Analysis The analysis for determining the amounts of carbon, nitrogen, hydrogen and sulfur was carried out with a Perkin Elmer Elemental Analyser no. 240B. The equipment had to be calibrated with a sample of known composition. This would give the constants for each element for unknown samples. For hydrogen and nitrogen, acetanilide was uses as standard to obtaine the constants K_H and K_N. Although the amount of nitrogen was very small (<0.5% by weight) there were no problems with its determination. The standard used for sulfur determination was S-benzylthiuronium chloride. Carbon was obtained by difference, as the equipment range was not enough for such a large percentage. The only possible drawback is with respect to the accuracy of the results, because for such low percentages the analyser is taken to its limiting resolution capability.

After determining the K-factors the oil samples were analysed. About 2 μL of oil were weighed in an aluminum capsule. The capsule was sealed, put in a nickel shell and loaded in the combustion ladle. The ladle was introduced into the combustion tube and the machine program started. The machine performs almost all the process by itself, except for pushing in and pulling out the ladle from the combustion zone. The signals obtained for each element were recorded with a chart recorder. The values were read and the proper calculations were performed to obtain the weight percentage of every element of every sample.

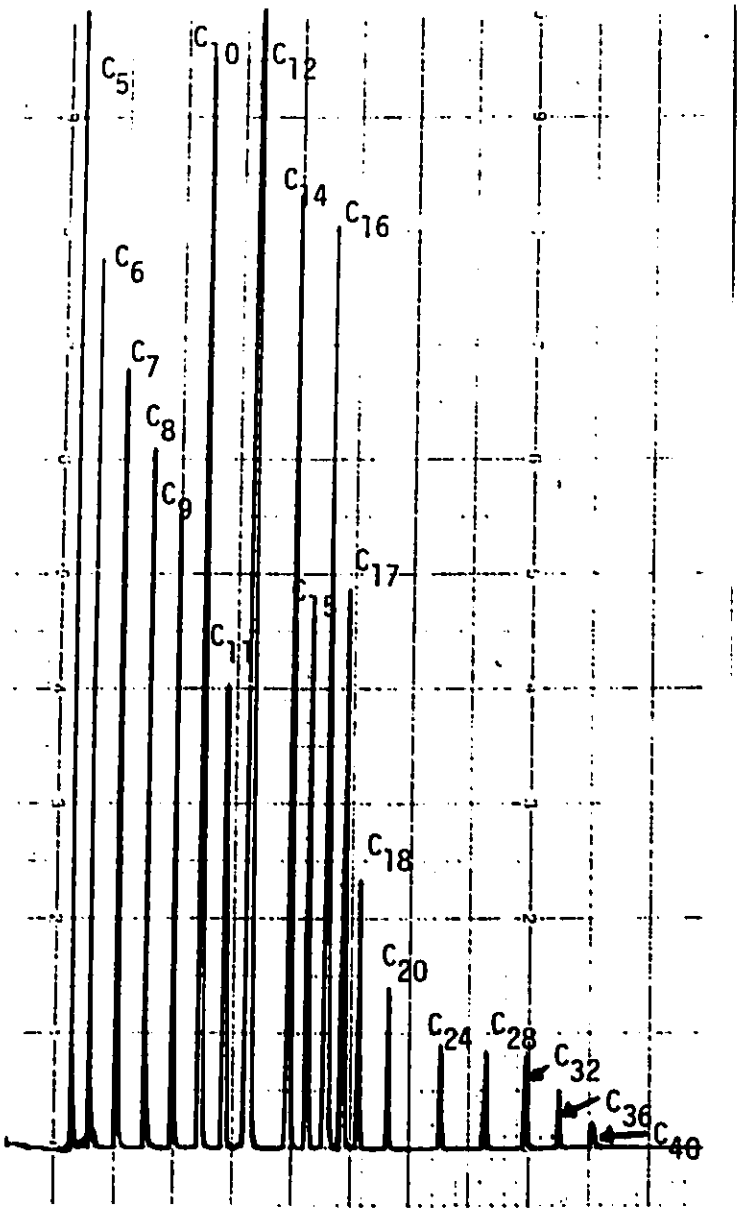

Hydrocarbon	Retention time (min)
C_5	0.703
C_6	1.405
C_7	2.468
C_8	3.655
C_9	4.823
C_{10}	6.005
C_{11}	6.958
C_{12}	8.135
C_{14}	9.808
C_{15}	10.555
C_{16}	11.405
C_{17}	12.063
C_{18}	12.668
C_{20}	13.890
C_{24}	16.088
C_{28}	17.983
C_{32}	19.623
C_{36}	21.053
C_{40}	22.383

Figure 11: Simulated Distillation (Standard Sample)

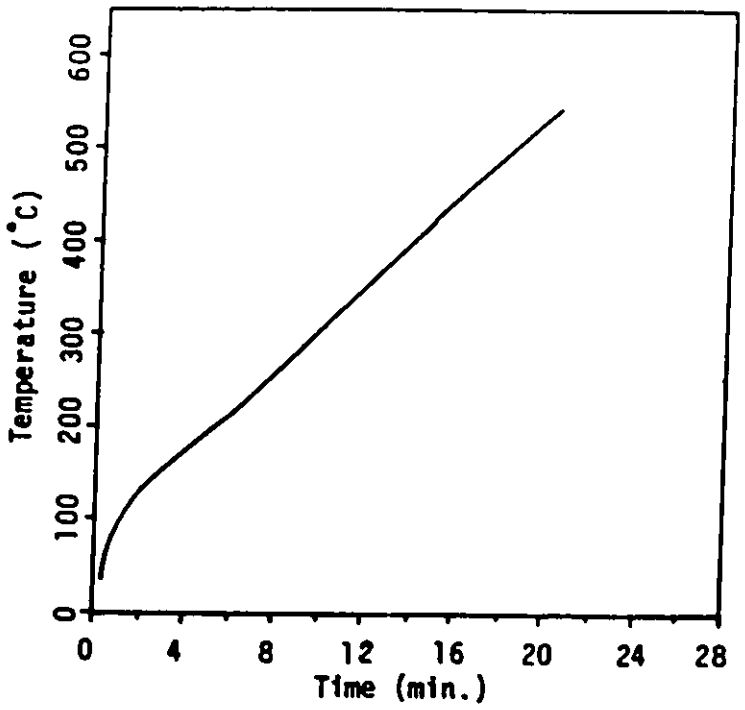

Figure 12: Boiling Point vs Retention Time for Standard Sample

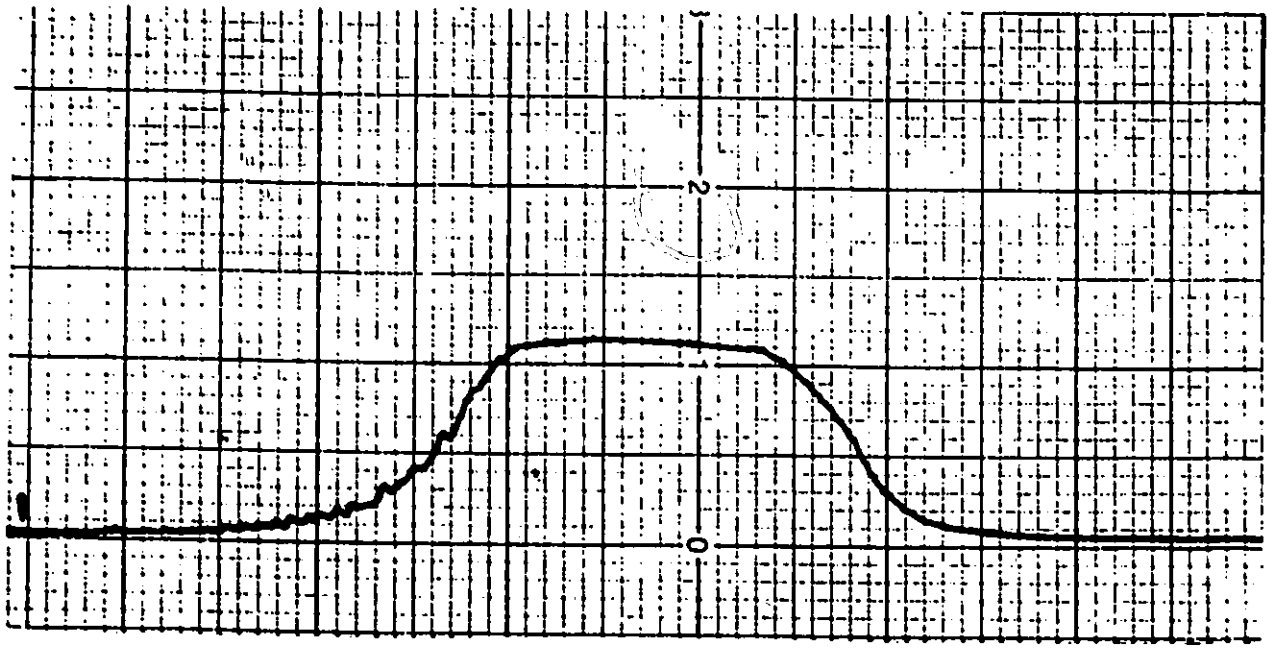

Figure 13: Simulated Distillation Chromatogram of a Typical Oil Sample

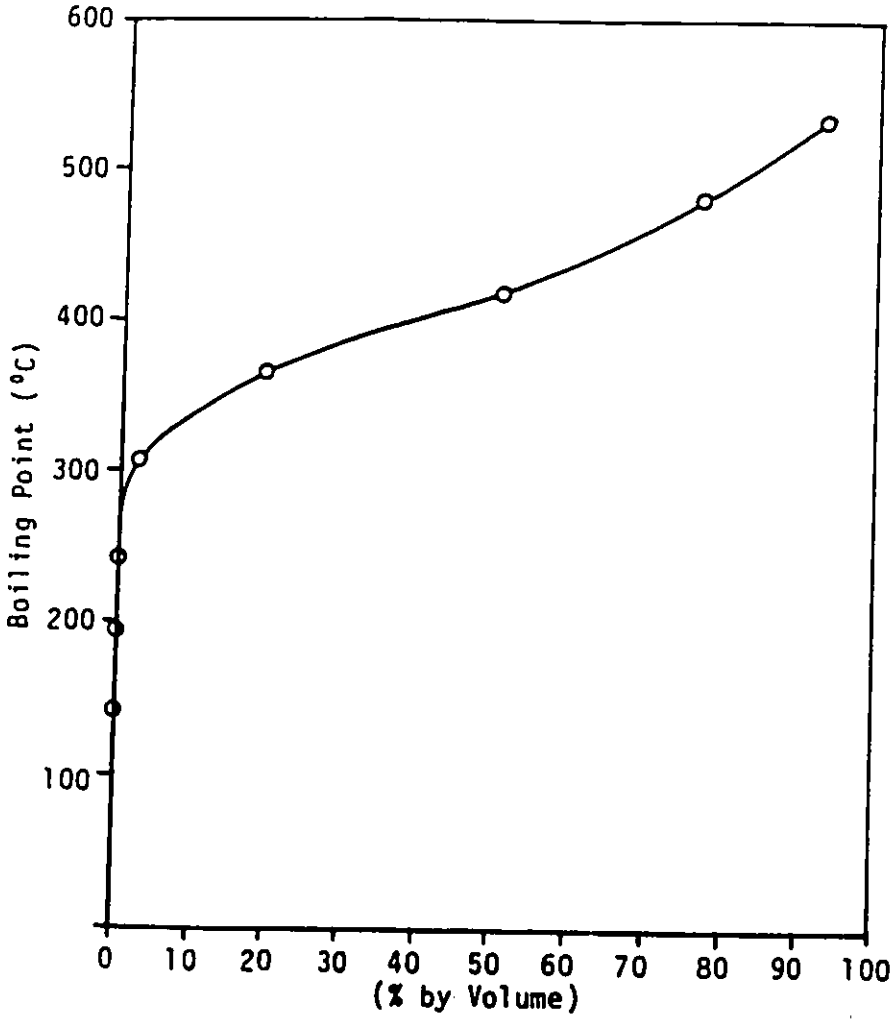

Figure 14: Boiling Point Distribution Curve

Chapter 4

Results and Discussion

The objectives of this work as well as the results and the analyses of these results are presented in this chapter.

4.1 Objectives

From the literature survey and especially from the work made by Sambi [51], the objective was to develop and test more efficient catalysts for hydrotreatment of heavy gas oil derived from Canadian Athabasca Bitumen. Some of the highlights of this work were:

(a) to try new metal catalysts (Ni-W and Co-Mo) on the same silica-alumina-zeolite based catalyst support used by Sambi,

(b) to test the reproducibility of the catalyst preparation scheme,

(c) to study the kinetics of the reactions over the two prepared catalysts by

- denoting the changes in physical properties of the final product as compared with the original oil (e.g. density, viscosity, etc.),
- testing their efficiency for HDN and HDS,
- evaluating rate constants and activation energies for both sulfur and nitrogen removal from the heavy oil.

4.2 Kinetic Study

This part deals with the results obtained, for both catalysts, from the hydrotreatment of heavy gas oil in the trickle-bed reactor. The data obtained for HDS and HDN were fitted to a first-order kinetic model and the resulting rate constants were evaluated. Data were obtained at different temperatures to obtain estimates of the activation energies for these reactions. The performance of the trickle-bed reactor, heat and mass transfer effects are also discussed.

4.2.1 Catalysts Used in this Study

The catalysts for this study were bimetallic catalysts supported on a silica-alumina-zeolite base. Further explanation of this kind of catalyst is given in section 2.3.4. The silica-alumina-zeolite base support was prepared so as to obtain the same optimum composition found by Sambi [51, page 129]. He found that a catalyst support material containing 25 % by wt. zeolite material, 10 % by wt. silica and 65 % by wt. alumina gave the best performance for sulfur and nitrogen removal. It also gave the product oil with lowest density, viscosity and mid-boiling point. The catalyst preparation and testing schemes are decribed in section 3.2. The properties of the prepared catalysts and the results of the analyses of their physical properties and chemical compositions are listed in Table 4.

4.2.2 Operating Conditions

The trickle-bed reactor was operated at a constant pressure of 6.9 MPa, and a gas flow rate equivalent to 890 m^3 of hydrogen per m^3 of oil (5000 scf/bbl) was maintained. The four temperatures selected were 350°C, 375°C, 400°C, and 425°C. The high temperature 425°C was only selected to see the catalysts performance at high temperature, although this high temperature is not recommended for hydrotreatment because it can crack the oil beyond the desired level. This high temperature can also lead to higher coke depositions that may cause catalyst deactivation, as explained in section 2.2.3. The liquid flow rates were varied to get liquid-hourly-space-velocities (LHSV) of 1.0, 1.333, 2.0., 4.0. The values of LHSV were chosen in order to obtain 1/LHSV factors of 1.0, 0.75, 0.5, 0.25. From previous experience [38] with the present

Table 4: Catalysts Used for the Kinetic Study

Catalyst	Bulk Density	Pore Volume	Surface Area (BET)	Pore Size (avg)
	g/cm^3	mL/g	m^2/g	nm
Ni-W	0.8224	0.3094	322.92	1.93
Co-Mo	0.6914	0.4196	272.58	3.09

Chemical Composition (wt. %)

Catalyst	SiO_2	Al_2O_3	NiO	WO_3	CoO	MoO_3
Ni–W	27.25	67.42	1.13	4.2		
Co–Mo	27.05	65.66			1.15	6.14

heavy oil, it is known that operating the trickle-bed reactor at LHSV of less than 1 leads to excessive coke formation on the catalysts that would deactivate them faster than expected.

4.2.3 Kinetic Study Results

The results obtained using the Co-Mo and Ni-W catalysts in the hydrotreatment of heavy gas oil are presented in this section. For each case, the respective volume of catalyst ($8cm^3$) was diluted with equal volume of inert material (α-alumina). The reason for this has been explained in section 2.4.1 and the procedure is described in section 3.2.2.

In each case the catalyst was first conditioned for a period of 20 h at the standard operating conditions, i.e. temperature of 350°C, pressure of 6.9 MPa, LHSV of 1.5 and gas flow rate of 890 m^3/m^3. This was done with the purpose of reaching a steady-state activity period for the catalyst. As stated by Sambi [51, page 111], the inital high activity of the catalyst drops to lower levels within the first 5 to 20 h of run. Further decrease in activity takes place at a much smaller rate. It was shown that in a period of 100 h after the first drop in activity, it did not change by more that 5 %. This was

the period where product samples were taken.

The sampling scheme is the same as the one followed by Sambi. The runs were started at the lowest temperature of 350°C, followed by the higher temperatures in increasing order. Liquid flow rates were changed from the maximum flow of 32 mL/h (LHSV = 4.0) to the lowest selected flow of 8 mL/h (LHSV = 1.0) for each temperature. The operating conditions were changed to the standard operating conditions, and samples were drawn in the beginning and at the end as well as in between various temperatures. This was done to check the catalyst activity during the kinetic study runs. Further details of the sampling and analysing procedure are given in chapter 3.

The results of the analyses of the samples obtained from this study are given in Tables 9 and 10 for the Ni-W catalyst and in Tables 11 and 12 for the Co-Mo catalyst, in appendix B.

Effects of Temperature

The effect of temperature on catalytic hydrotreatment of heavy oil was studied at 350–425°C, 6.9 MPa and at flow rates corresponding to LHSV of 1–4 for the catalysts.

Figures 15 to 18 show the effect of temperature on density. It is shown that the density of the product decreased with temperature increase for both catalysts. They showed similar densities at all temperatures except at 425°C. This phenomenon will be explained later.

The viscosity decreased with increase in temperature for both catalysts in a similar way. In this case it can also be said that both catalysts showed similar viscosities at all temperatures except at 425°C. Figures 19 to 22 show the effect of temperature on viscosity at all studied flow rates.

The aniline point analysis tells us about the amount of paraffinicity in the product oil. The higher the aniline point temperature the higher the amount of aromatics and the lower the amount of paraffins with respect to the other samples. In the present case for both catalysts the aniline point started low at 350°C, increased to a maximum between 375 and 400°C, and reached a minimum at 425°C. This behaviour is more pronounced at lower liquid flow rates. It indicates that the highest production of aromatics is found somewhere between 375 and 400°C. Figures 23 to 26 show the

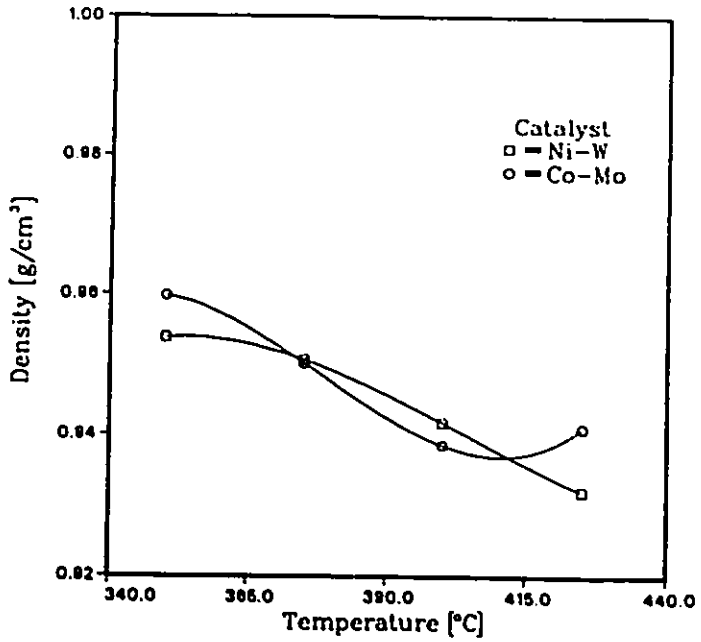

Figure 15: Effect of Temperature on Density. LHSV = 1

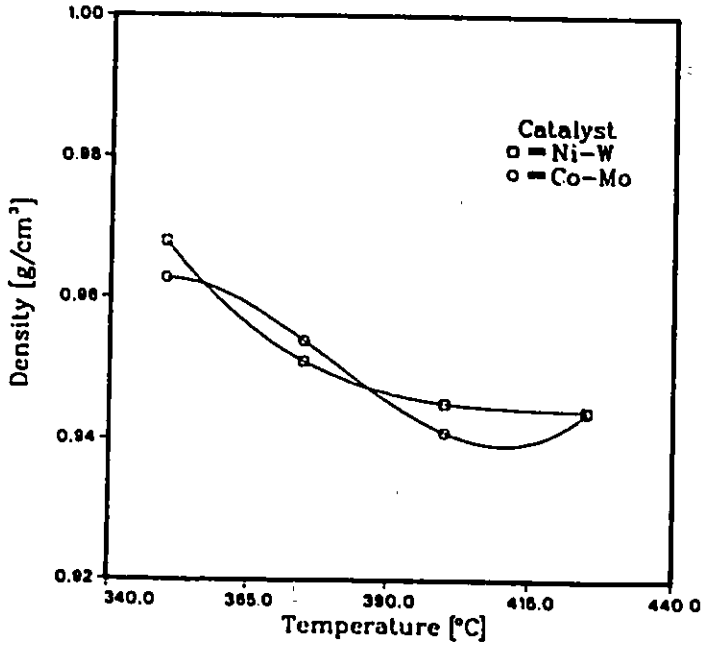

Figure 16: Effect of Temperature on Density. LHSV = 4/3

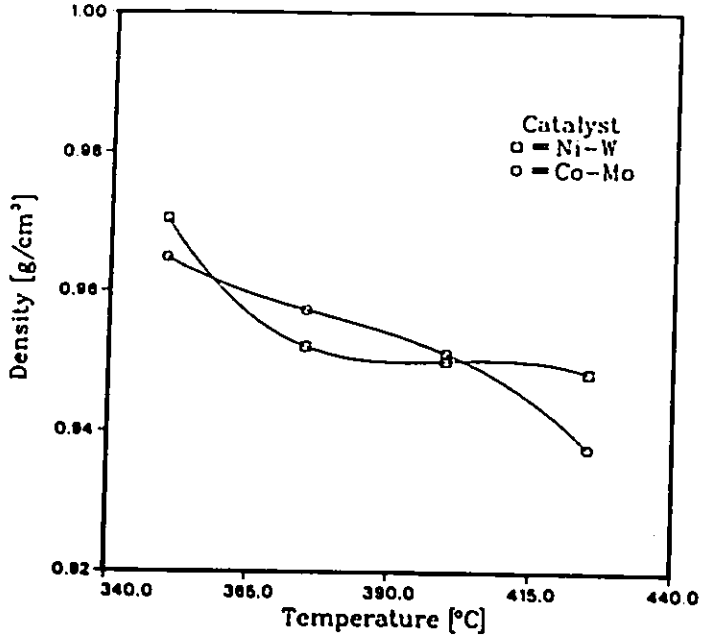

Figure 17: Effect of Temperature on Density. LHSV = 2

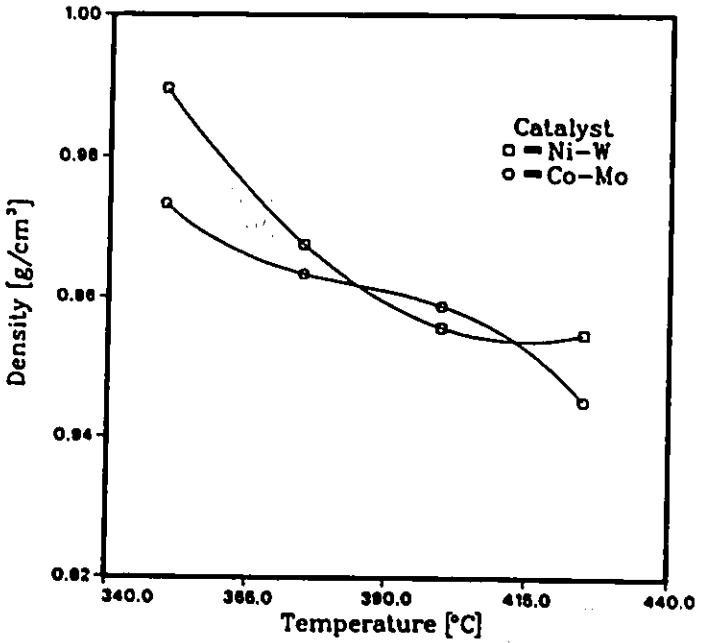

Figure 18: Effect of Temperature on Density. LHSV = 4

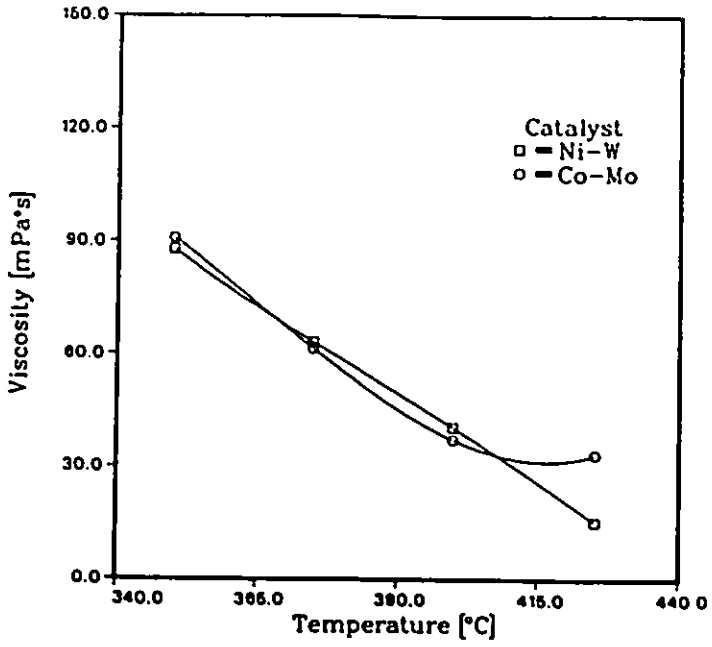

Figure 19: Effect of Temperature on Viscosity. LHSV = 1

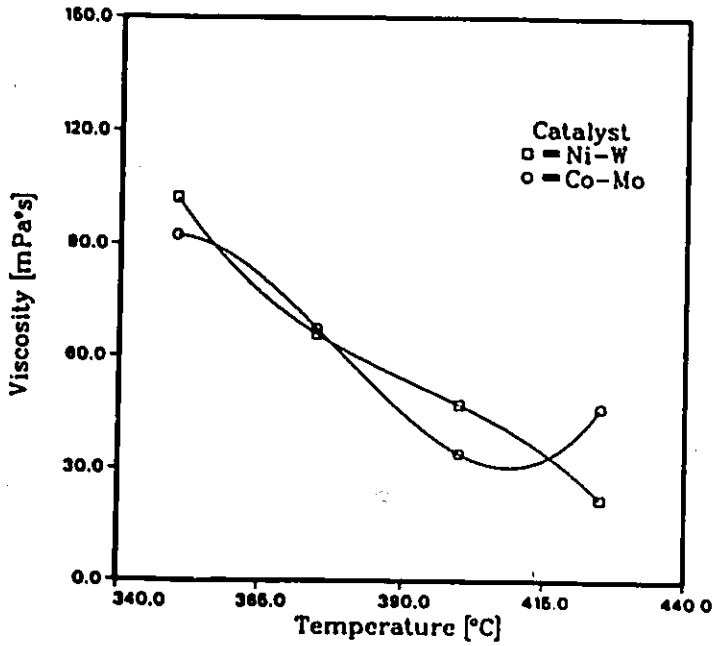

Figure 20: Effect of Temperature on Viscosity. LHSV = 4/3

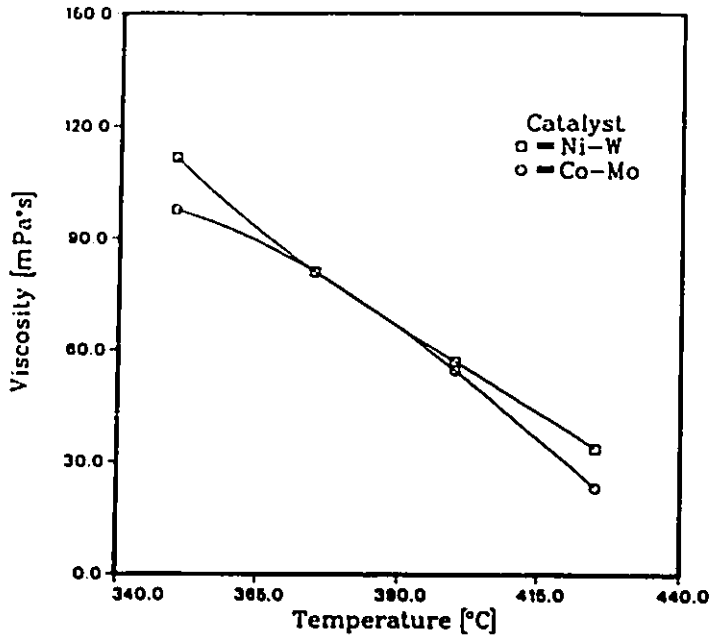

Figure 21: Effect of Temperature on Viscosity. LHSV = 2

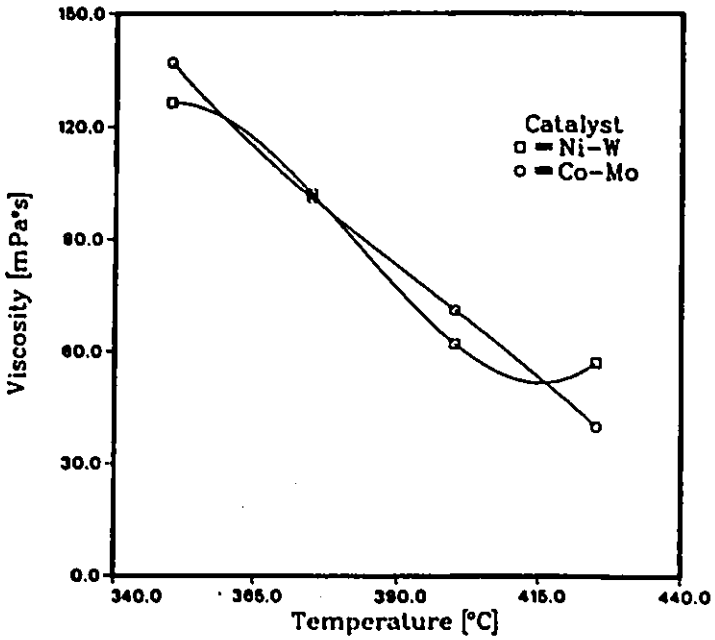

Figure 22: Effect of Temperature on Viscosity. LHSV = 4

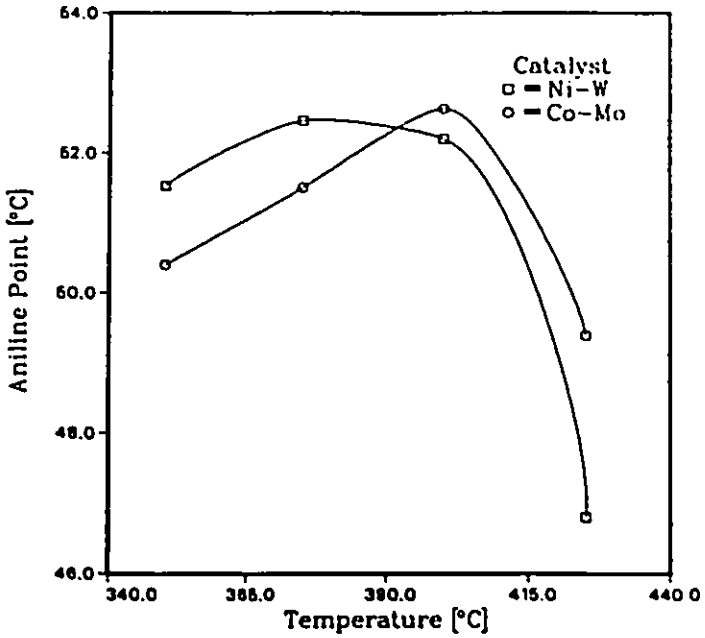

Figure 23: Effect of Temperature on Aniline Point. LHSV = 1

effect of temperature on aniline point.

The mid-boiling point of the products for all catalysts did not show a well defined behaviour with temperature change. For the Ni-W catalyst in general, it is at its lowest point at 375°C, but for the Co-Mo catalyst no trend could be observed. Also, at 425°C, some unexpected effects occurred. These are explained below. Figure 27 shows the effect of temperature on mid-boiling point of the product oil at LHSV equal to 1.

The C/H ratio was not severely affected by the temperature. But as expected it increased slightly with increase in temperature due to the lower amount of N and S. Figure 28 shows the effect of temperature on C/H ratio at LHSV of 1.

The hydrodenitrogenation activities of the catalysts are shown in Figures 29 to 32. HDN activity increased with increasing temperatures. While Co-Mo showed higher HDN activity at most temperatures, both catalysts were equally active at 425°C.

The hydrodesulfurization activities of the catalysts are shown in Figures 33 to 36. HDS activity increased with increasing temperatures. In all cases Ni-W showed better HDS activity. Close to 100 % desulfurization of the product was observed.

Some comments must be made about the product oil obtained at 425°C. As already

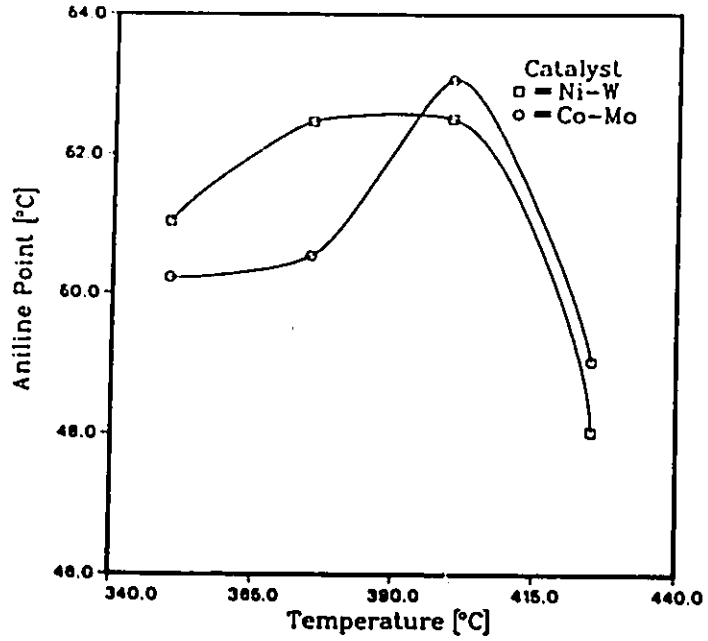

Figure 24: Effect of Temperature on Aniline Point. LHSV = 4/3

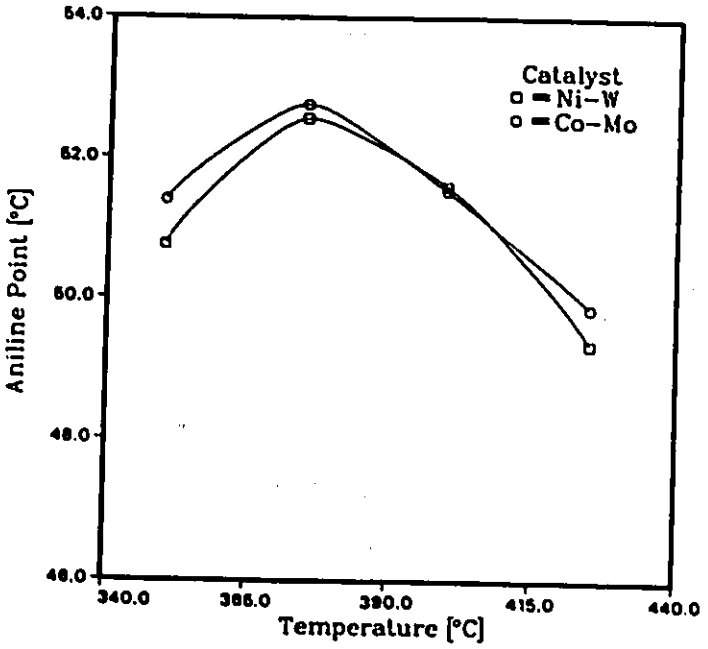

Figure 25: Effect of Temperature on Aniline Point. LHSV = 2

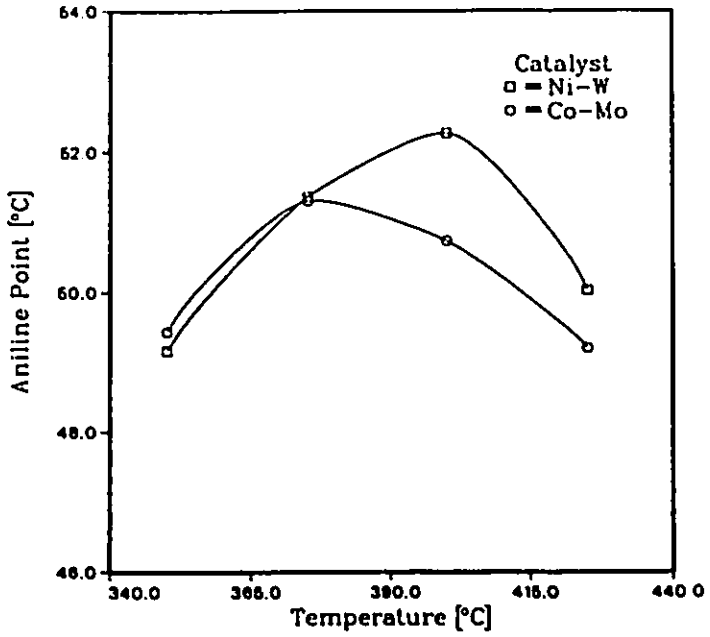

Figure 26: Effect of Temperature on Aniline Point. LHSV = 4

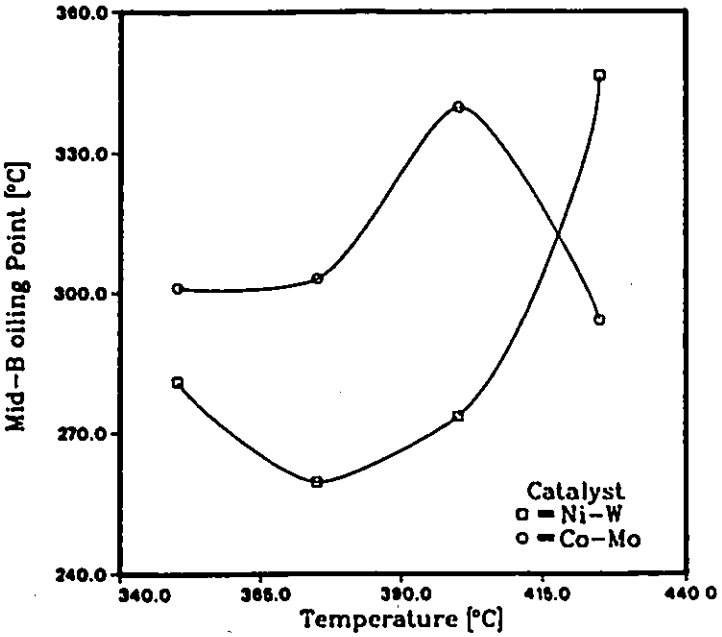

Figure 27: Effect of Temperature on Mid-Boiling Point. LHSV = 1

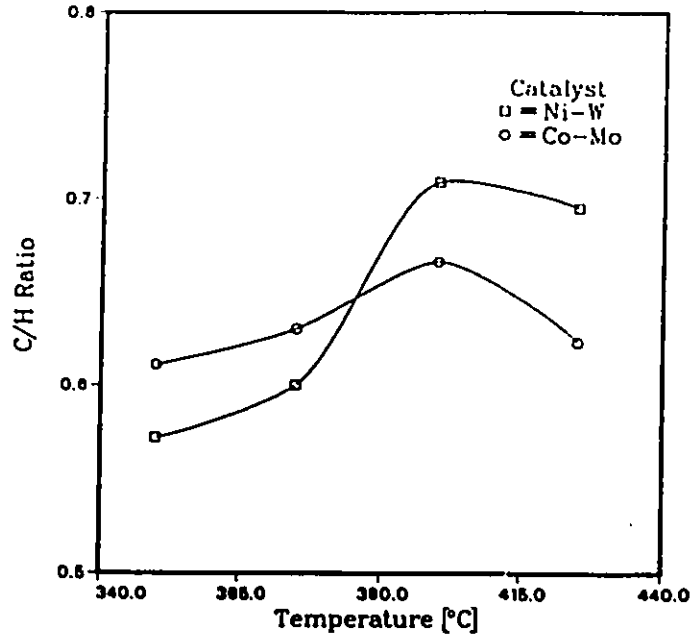

Figure 28: Effect of Temperature on C/H Ratio. LHSV = 1

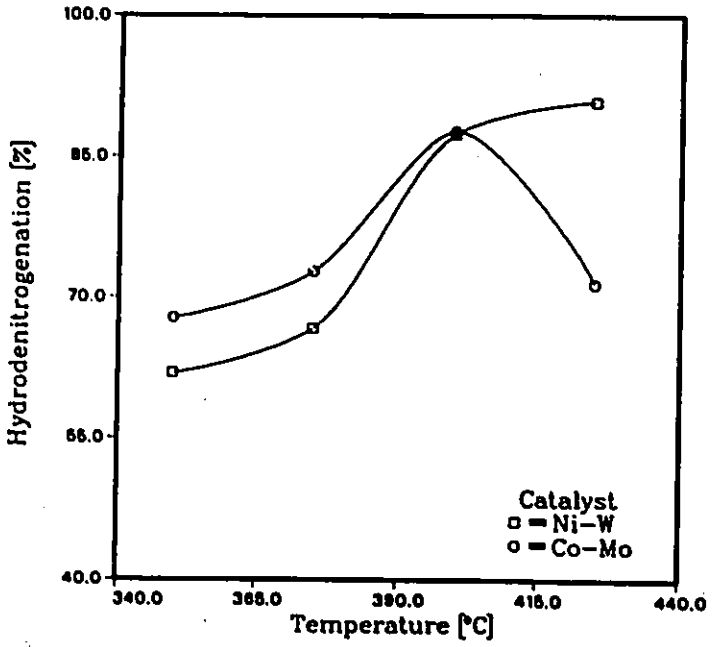

Figure 29: Effect of Temperature on Hydrodenitrogenation. LHSV = 1

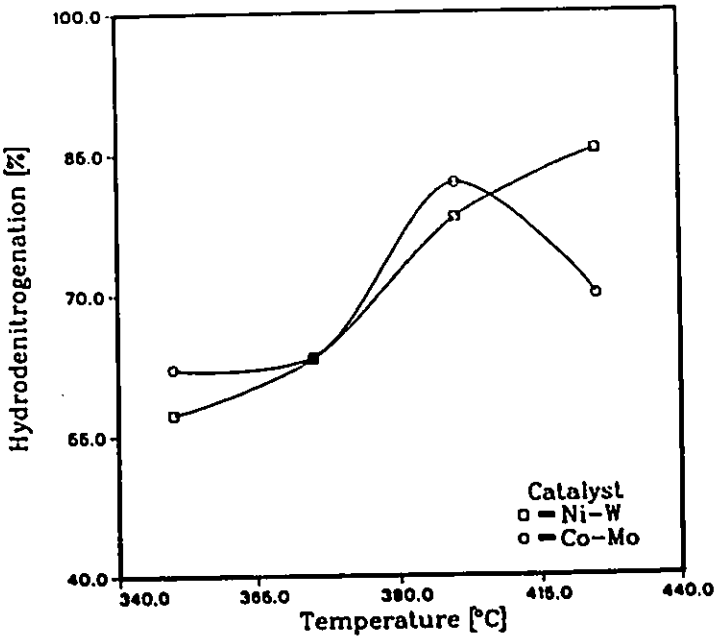

Figure 30: Effect of Temperature on Hydrodenitrogenation. LHSV = 4/ 3

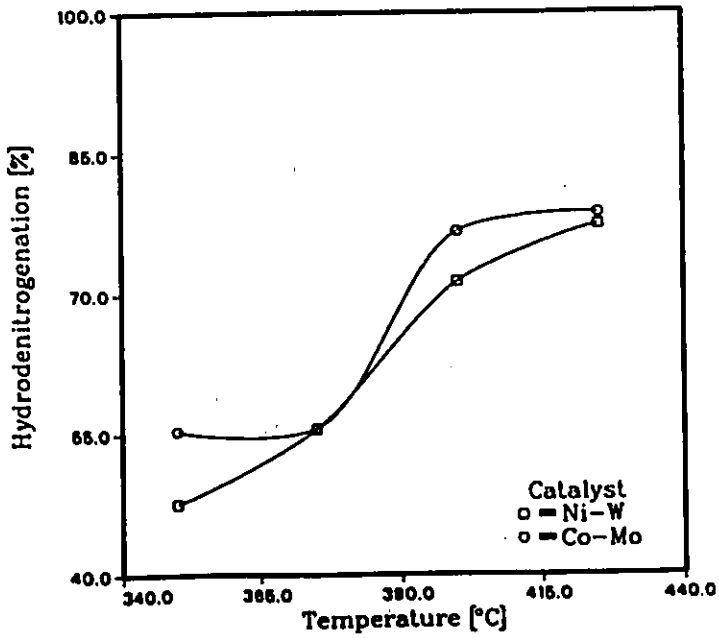

Figure 31: Effect of Temperature on Hydrodenitrogenation. LHSV = 2

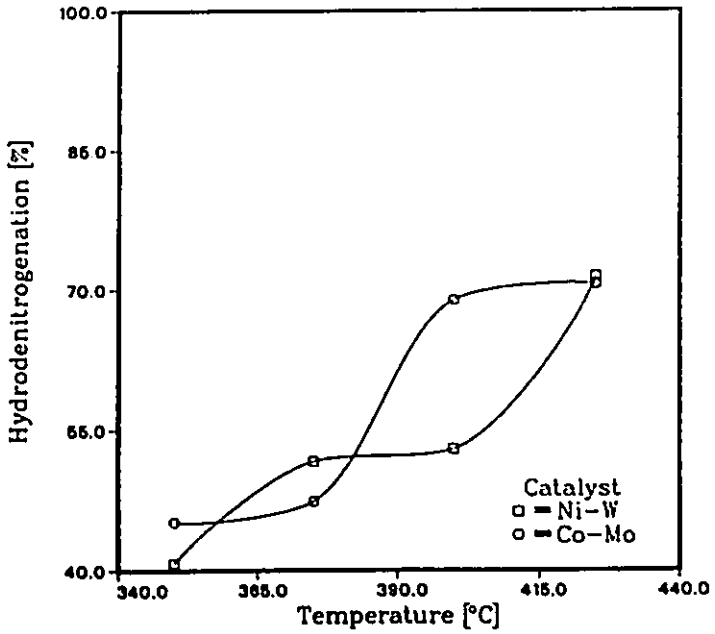

Figure 32: Effect of Temperature on Hydrodenitrogenation. LHSV = 4

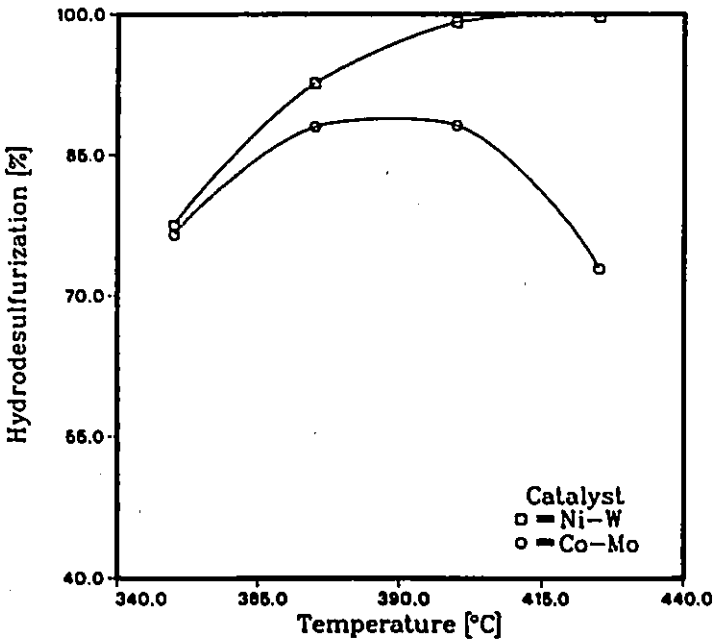

Figure 33: Effect of Temperature on Hydrodesulfurization. LHSV = 1

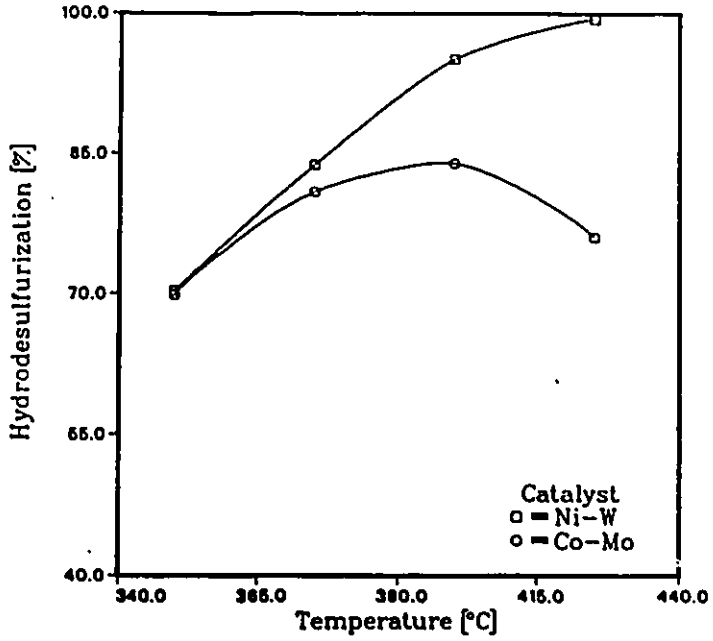

Figure 34: Effect of Temperature on Hydrodesulfurization. LHSV = 4/ 3

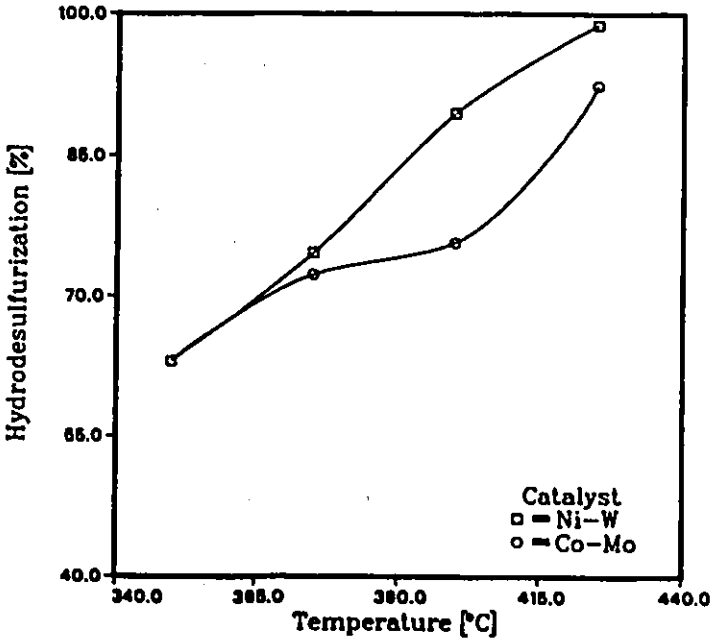

Figure 35: Effect of Temperature on Hydrodesulfurization. LHSV = 2

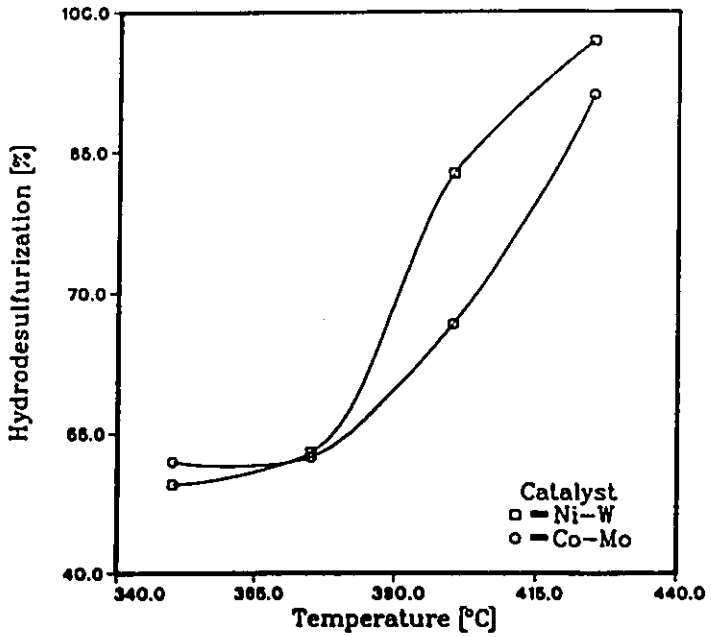

Figure 36: Effect of Temperature on Hydrodesulfurization. LHSV = 4

mentioned in section 1.2.2, this is the maximum recommended temperature for hydrotreatment. Therefore, some unusual behaviour must be expected when one operates at this extreme condition. It is possible that somehow the increase in temperature has affected the catalyst so as it does not conform to the expected behaviour. Unfortunately the equipment required for such verification was not available.

This last remark may apply to some unusual readings obtained for the aniline point and the mid-boiling point analyses. These analyses are more qualitative than quantitative. The product oil had a large number of components, and without equipment capable of identifying them it is not possible to explain properly the unusual behaviour of some data points.

Finally the two samples taken at 425°C at LHSV of $\frac{4}{3}$ and 1 for the Co-Mo catalyst could not be considered very reliable. The reason is that the reactor became unstable and for some time it was clogged. This was evident from a greater deposit of coke on this catalyst (see appendix D), compared with the Ni-W catalyst. This may have affected the catalyst activity.

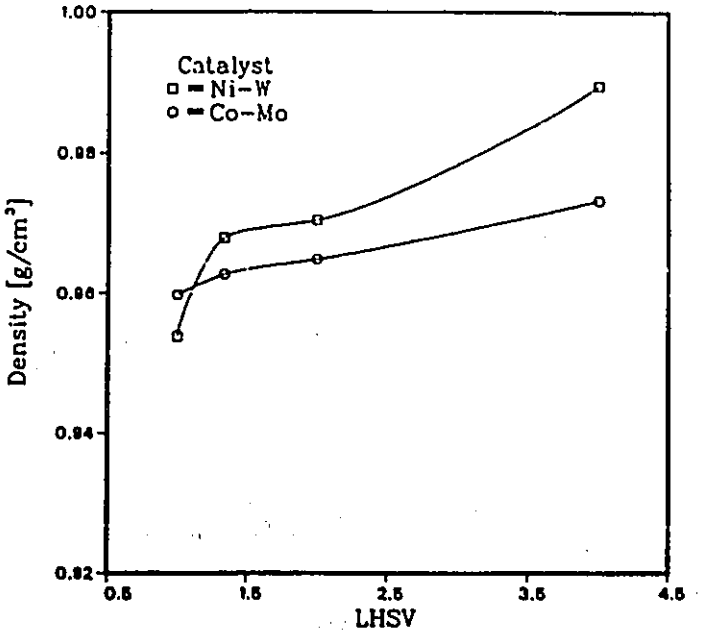

Figure 37: Effect of LHSV on Density. T = 350°C

Effects of Liquid Feed Rates

The effect of the change of feed rates of heavy oil on the products was studied at 6.9 MPa and at temperature of 350 to 425°C. The flow rate of the gas oil was varied between 8 and 32 mL/h (LHSV = 1.0–4.0).

Figures 37 to 40 show the effect of LHSV on density. It is observed for all cases that the density of the product oil decreased with a decrease in LHSV. The Ni-W catalyst gave rise to products of higher densities at most flow rates.

The viscosity of the products also decreased with decrease in LHSV. Although at some LHSV values there are differences in the viscosities for both catalysts, viscosity for LHSV of 1 is practically the same in all cases. The phenomenon at 425°C has been explained in the previous section. Figures 41 to 44 show the effect of LHSV on viscosity.

The aniline point increased slightly with decrease in flow rate for the temperatures between 350 and 400°C. At 425°C no defined behaviour could be observed, probably due to the reasons already given in the previous section. A specific trend for both catalysts with only this information could not be found. Figure 45 shows the effect of LHSV on aniline point at 350°C.

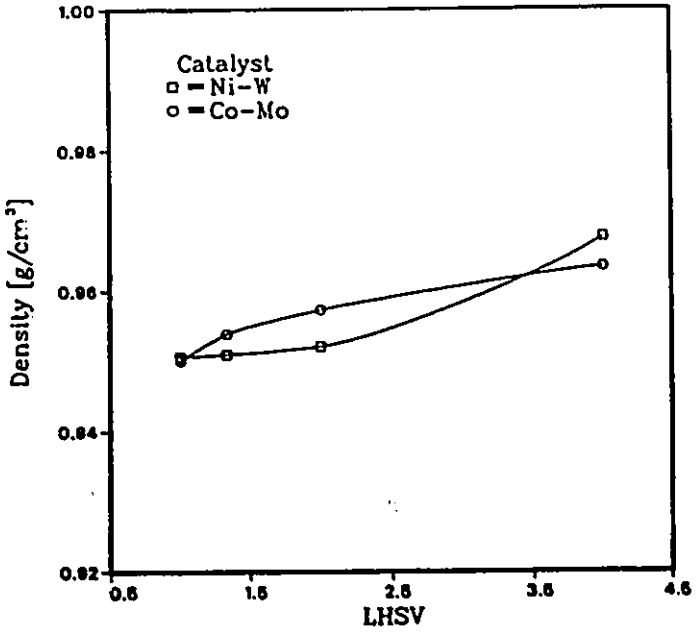

Figure 38: Effect of LHSV on Density. T = 375°C

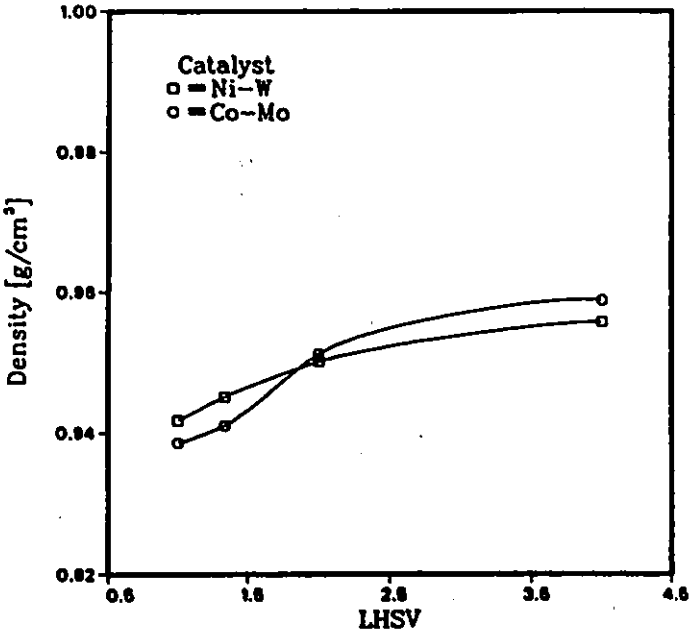

Figure 39: Effect of LHSV on Density. T = 400°C

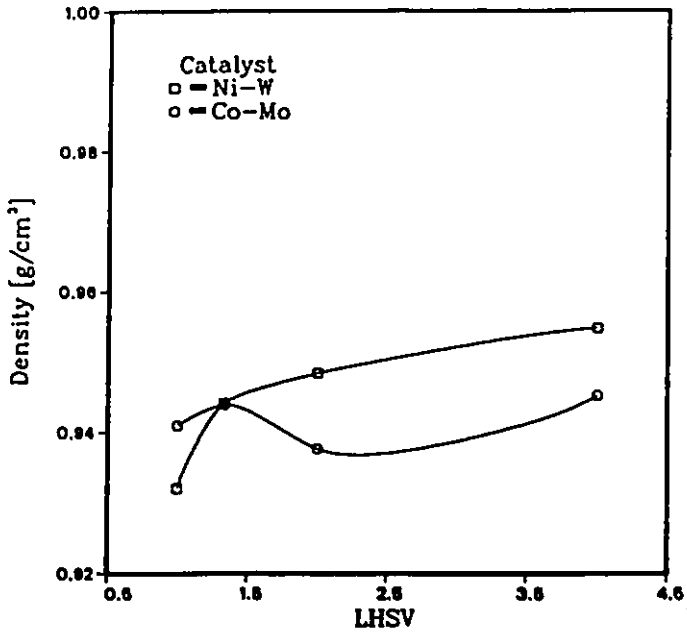

Figure 40: Effect of LHSV on Density. T = 425°C

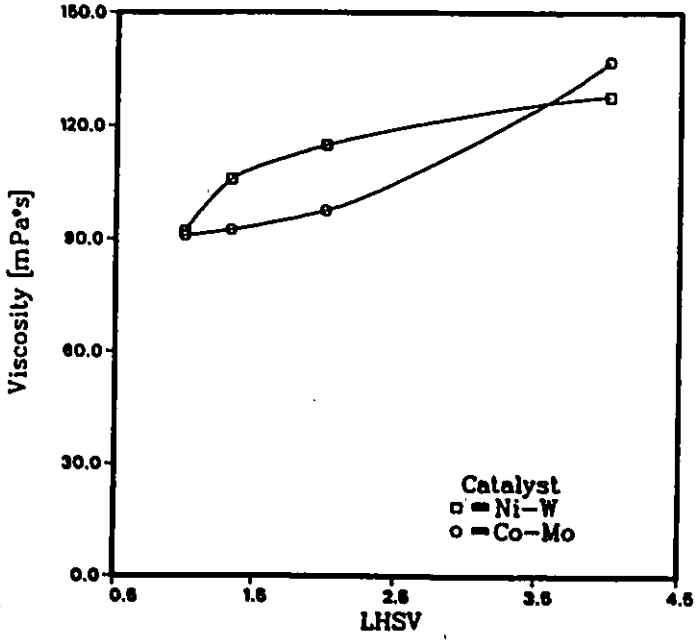

Figure 41: Effect of LHSV on Viscosity. T = 350°C

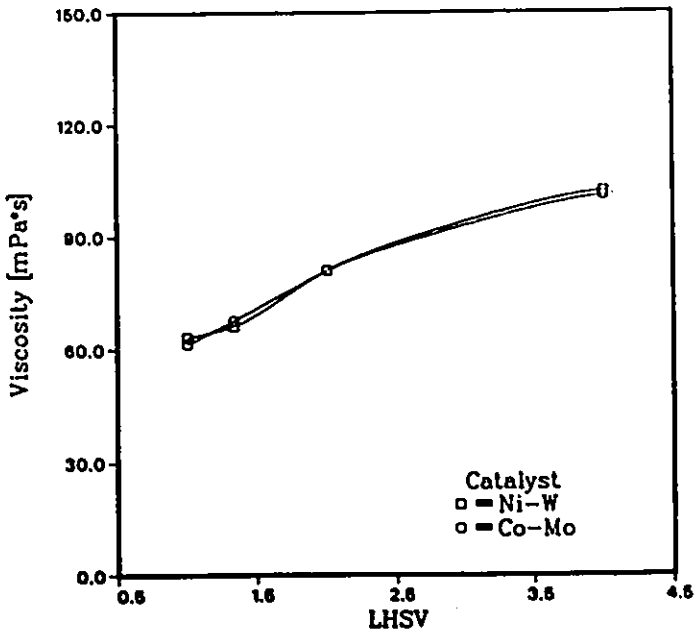

Figure 42: Effect of LHSV on Viscosity. T = 375°C

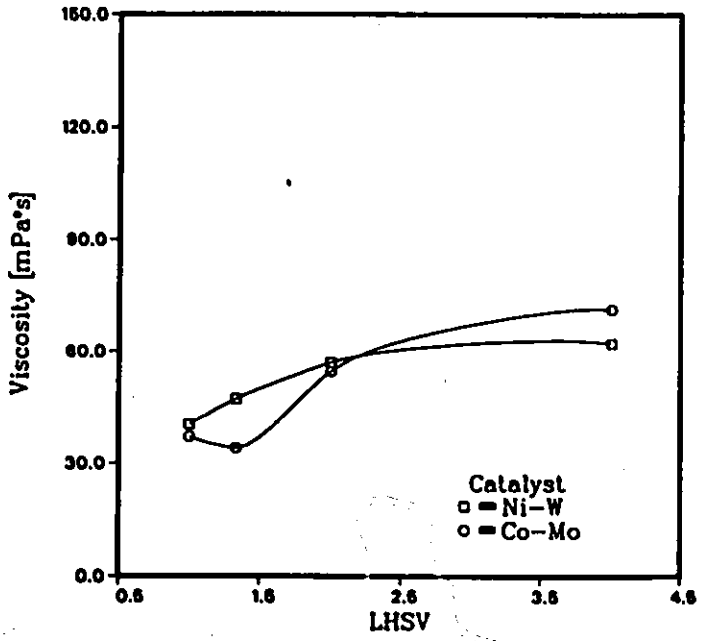

Figure 43: Effect of LHSV on Viscosity. T = 400°C

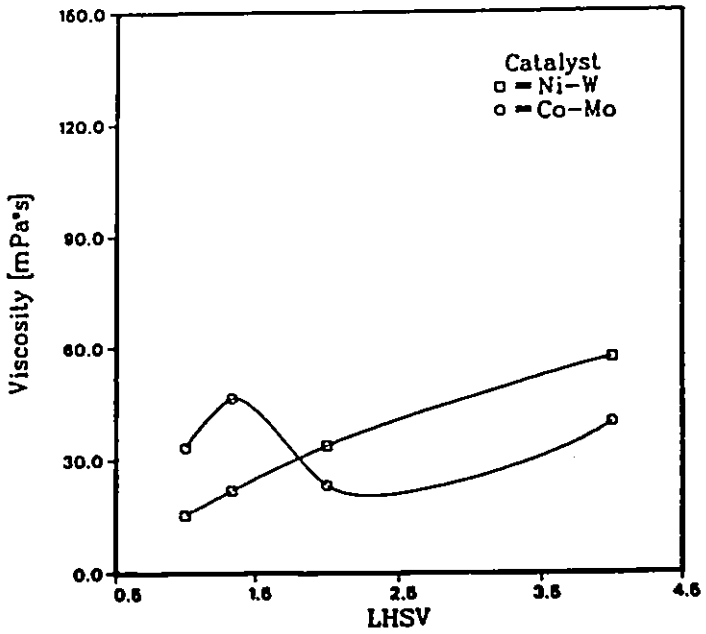

Figure 44: Effect of LHSV on Viscosity. T = 425°C

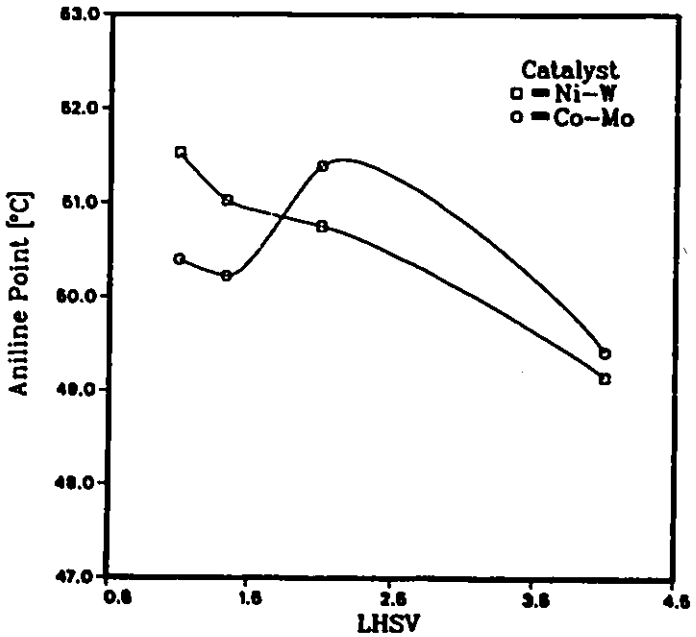

Figure 45: Effect of LHSV on Aniline Point. T = 350°C

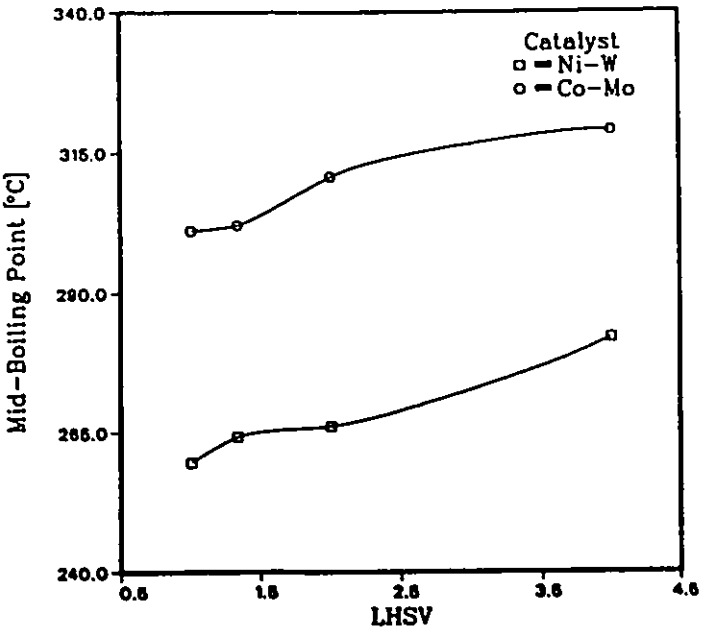

Figure 46: Effect of LHSV on Mid-Boiling Point. T = 375°C

In general mid-boiling point slightly decreased with decrease in flow rate. However the same comments made about the aniline point analysis can be applied here. Figure 46 shows the effect of LHSV on mid-boiling point at 375°C.

The C/H ratio did not vary much. However, it can be observed that at higher temperatures the value of C/H ratio is higher than at lower temperatures. Figures 47 and 48 show the effect of LHSV on C/H ratio.

The hydrogenation activities of the catalysts are shown in Figures 49 to 52. HDN increased with a decrease in flow rate. The Co-Mo catalyst was more effective for HDN than the Ni-W catalyst at almost all conditions.

The hydrodesulfurization activities of the catalysts are shown in Figures 53 to 56. HDS activity increased with decreasing flow rates. The Ni-W catalysts showed superior HDS activity at all conditions compared with the Co-Mo catalyst. This superiority is better shown at higher temperatures.

Catalyst Activity

To test the deactivation of the catalyst five replicates were taken at the standard conditions (i.e. 350°C, 6.9 MPa, LHSV of 1.5 and a gas flow rate of 890 m^3/m^3).

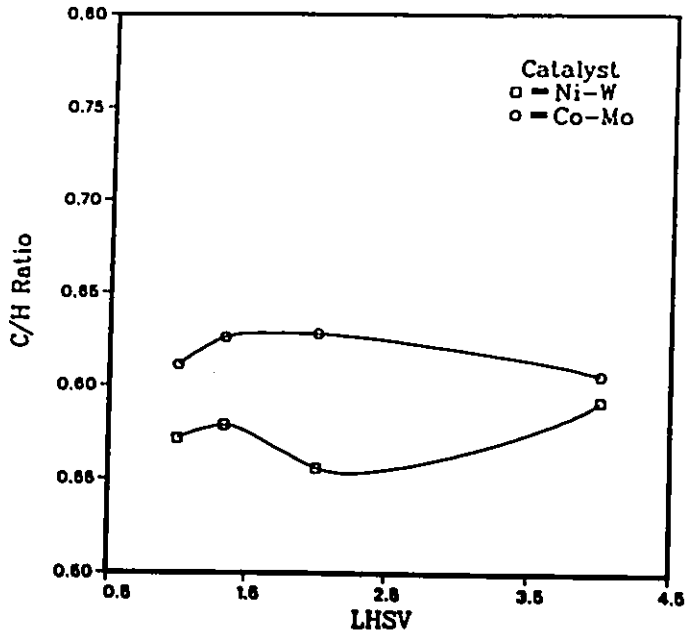

Figure 47: Effect of LHSV on C/H Ratio. T = 350°C

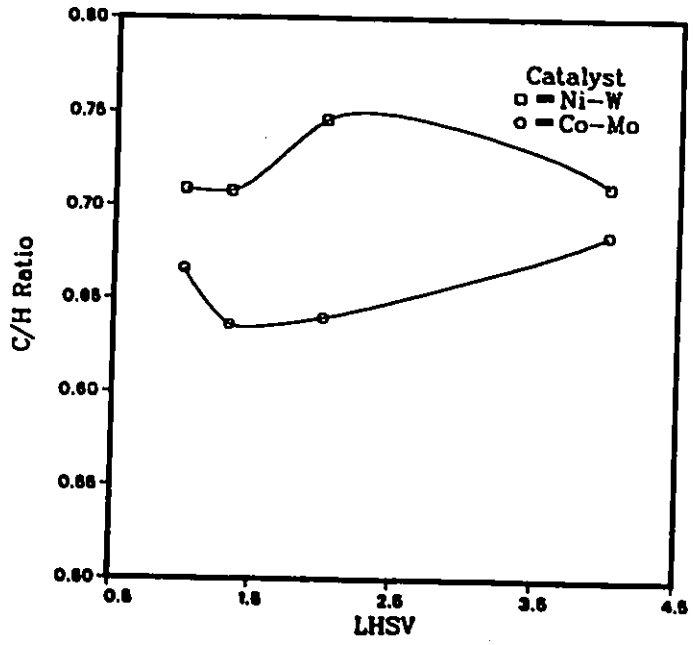

Figure 48: Effect of LHSV on C/H Ratio. T = 400°C

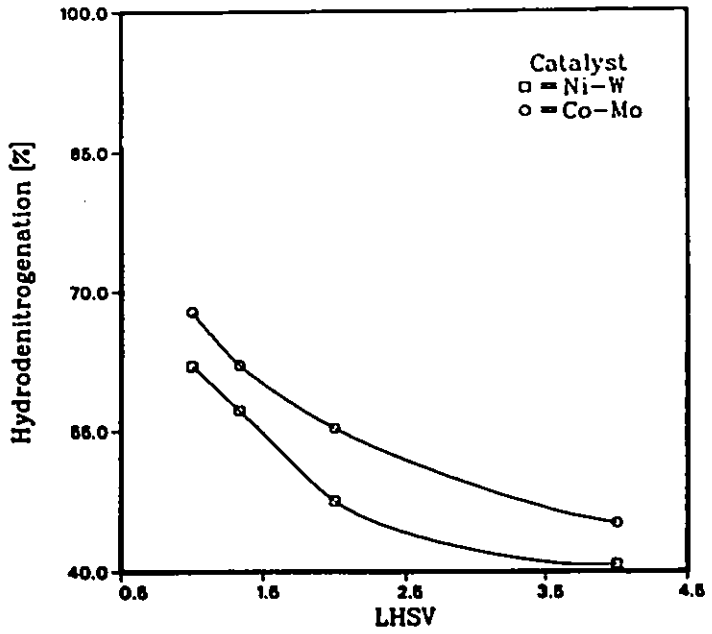

Figure 49: Effect of LHSV on Hydrodenitrogenation. T = 350°C

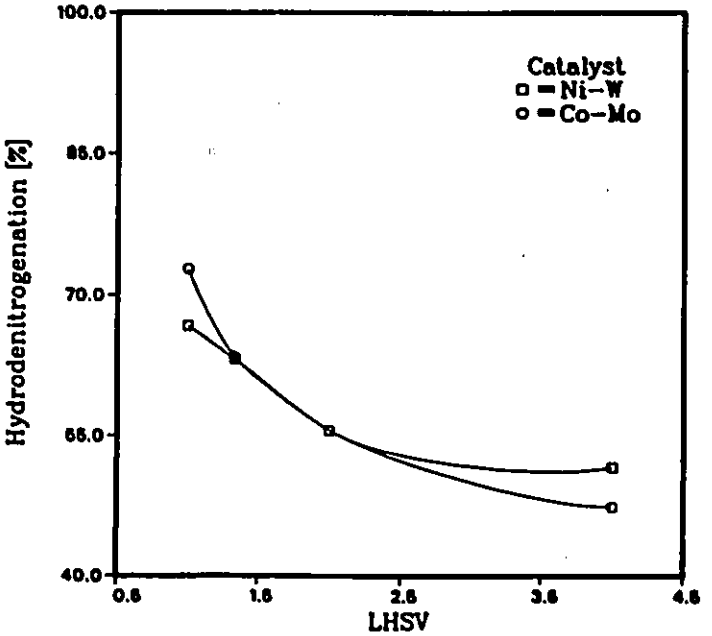

Figure 50: Effect of LHSV on Hydrodenitrogenation. T = 375°C

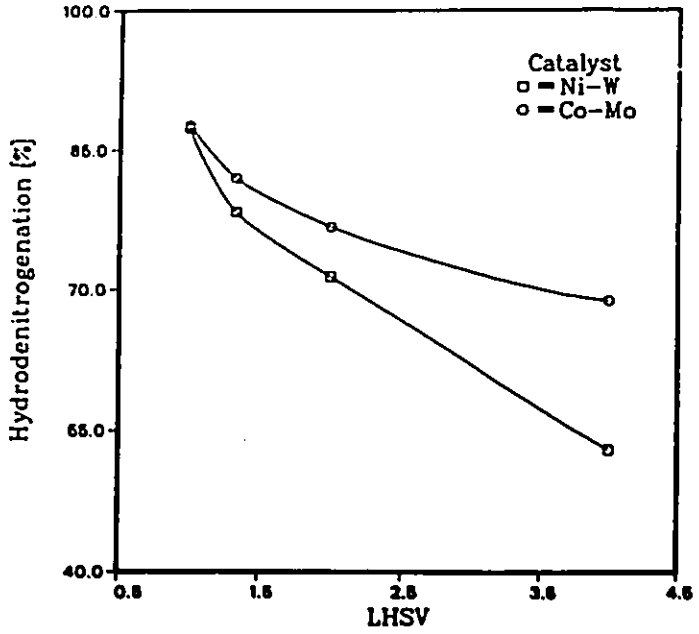

Figure 51: Effect of LHSV on Hydrodenitrogenation. T = 400°C

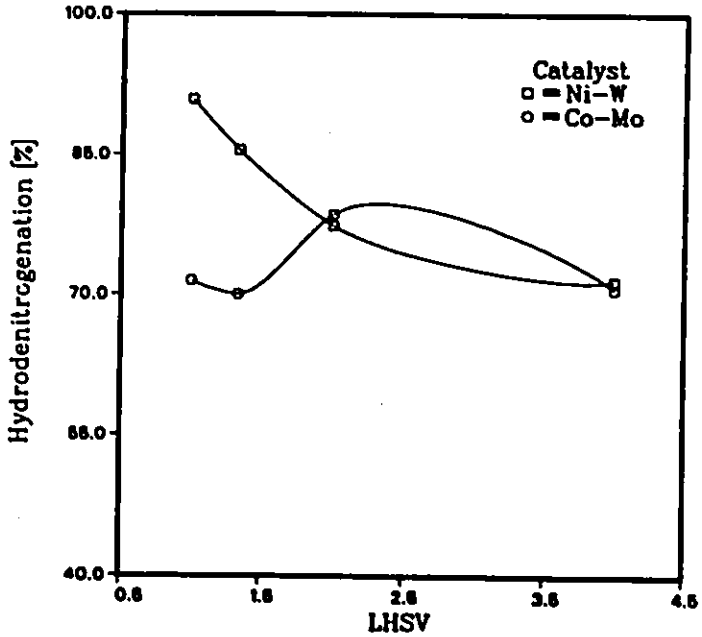

Figure 52: Effect of LHSV on Hydrodenitrogenation. T = 425°C

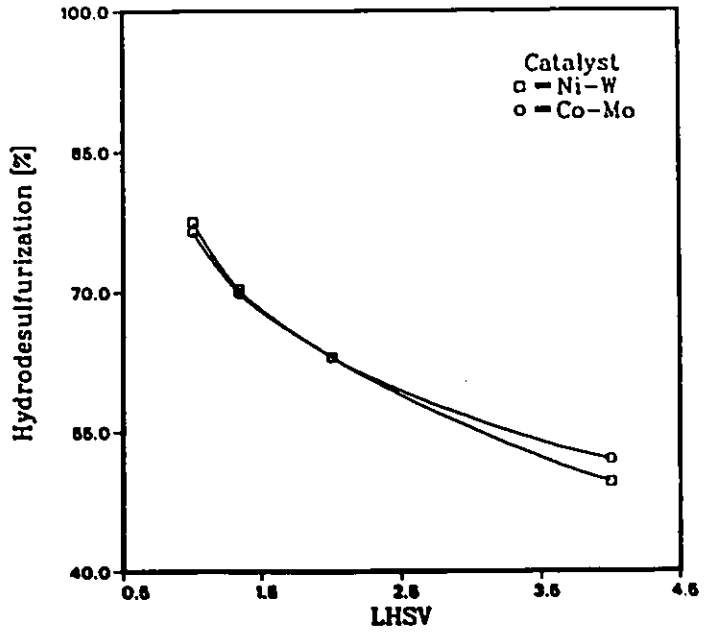

Figure 53: Effect of LHSV on Hydrodesulfurization. T = 350°C

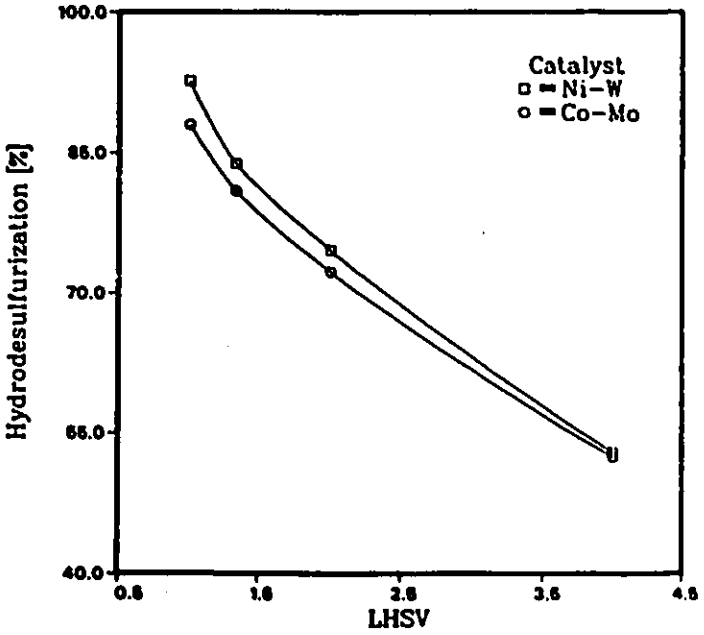

Figure 54: Effect of LHSV on Hydrodesulfurization. T = 375°C

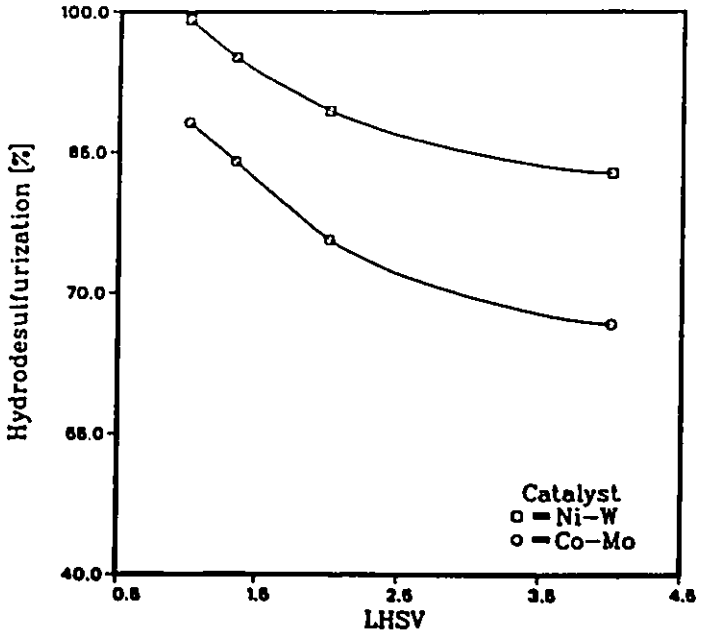

Figure 55: Effect of LHSV on Hydrodesulfurization. T = 400°C

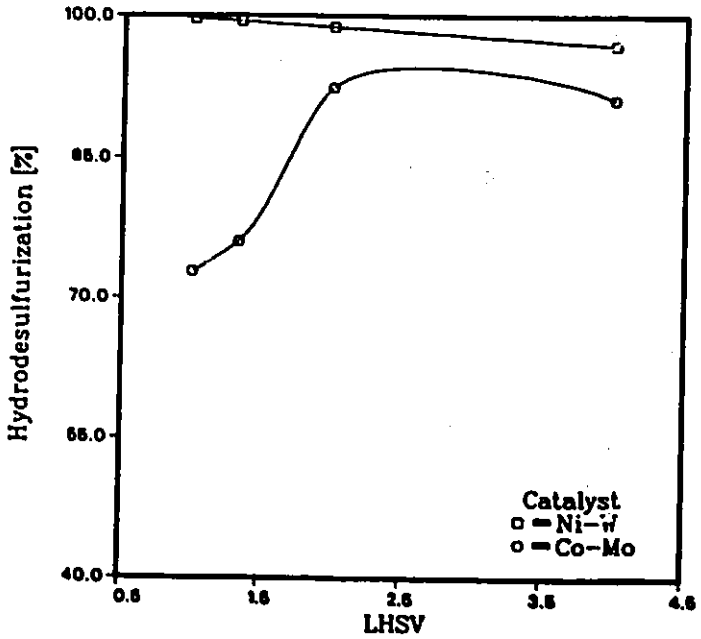

Figure 56: Effect of LHSV on Hydrodesulfurization. T = 425°C

The operating conditions were changed to the standard operating conditions in the beginning and at the end as well as in between various temperatures.

It can be observed in Tables 13 and 14 for the Co-Mo runs and Tables 15 and 16 for the Ni-W runs (all of them in appendix B) there were no appreciable changes in the catalysts activity . Nevertheless, it can be seen that in many cases the last replicate (i.e. the one taken after the system was operated at 425°C) showed a value farther from the mean if compared with the other replicates.

4.2.4 Kinetic Model

The data for the sulfur and nitrogen concentrations in the oil samples taken out at various temperatures and flow rates were fitted into the pseudo power-law rate equation of the type shown below:

$$r = \frac{dC}{dt} = -k_m [C]^m \tag{13}$$

where C is the concentration of nitrogen or sulfur in wt. %, and m is the order of the rate equation. Using the ideal plug-flow model (Equation 10) from section 2.4.1 and combining the rate constant with the effectiveness factor, the equation can be integrated for a first order reaction. The result is

$$\ln \frac{C_i}{C_o} = \frac{k_1}{(LHSV)} \tag{14}$$

where k_1 is the first order rate constant, and subscripts i and o indicate the inlet and outlet concentration of the sulfur or nitrogen.

However, this model does not consider the thermal effects that can initially affect the reaction rate. The importance of oil processing has been reported by Miki and co-workers [44]. They studied the hydrocracking of atmospheric residue without using any catalyst in an autoclave type of reactor. They observed some HDS and HDN on the final products. The proportion of HDS and HDN occuring without catalyst is dependent upon the type of feed and operating conditions, especially temperature.

Thus the model can be modified by adding a constant depending only on temperature, as given in Equation 15:

$$\ln \frac{C_i}{C_o} = \frac{k_1}{(LHSV)} + \mathcal{I} \tag{15}$$

If temperature effects are negligible, $\mathcal{I}$ will tend to zero. In this case Equation 15 will be equivalent to Equation 14. The value of $\mathcal{I}$ will increase with temperature.

If the left-hand side of Equation 15 is plotted against the factor (1/LHSV), then a straight line should result if the equation holds true. Speight [58, page 68] and Frost [18] have reported that HDS with commercial catalysts follows a pseudo-first order rate equation. Frost also reports the same findings for HDN reactions. This has already been verified by Sambi [50, page 34–35] and by Mann and Díaz [37,36]. Further justification for the use of this model is given on page 40 and in section 2.4.1.

A least-square regression technique was used to fit the linear model into the given set of data points. In this case the fitting was the best possible straight line passing through all the data points. All analysis of regression must include some way of verifying the quality of fit of a given model to the given data. In this case the coefficient of determination (COD) was calculated. This is the ratio of the model's sum of squares to the total sum of squares. The closer the COD value is to one the better is the fit.

For better understanding Equation 15 will be specified for each case, i.e. changing C for S in the case of sulfur and N in the case of nitrogen. It follows, then

$$\ln \frac{S_f}{S_p} = \frac{k_S}{(LHSV)} + \mathcal{I}_S \qquad \text{for} \quad \text{HDS} \tag{16}$$

and

$$\ln \frac{N_f}{N_p} = \frac{k_N}{(LHSV)} + \mathcal{I}_N \qquad \text{for} \quad \text{HDN} \tag{17}$$

Table 5: Rate Constants for HDN

Pressure = 6.9 MPa
Gas Flow Rate = 890 m^3/m^3

Ni-W Catalyst Temperature (°C)	HDN Pseudo-first order Rate Constant (h^{-1})	Intercept $\mathcal{I}$ (h^{-1})	COD
350	0.614	0.3627	0.9878
375	0.525	0.5803	0.9780
400	1.689	0.3439	0.9862
425	1.543	0.8014	0.9799

Co-Mo Catalyst Temperature (°C)	HDN Pseudo-first order Rate Constant (h^{-1})	Intercept $\mathcal{I}$ (h^{-1})	COD
350	0.707	0.4365	0.9951
375	0.871	0.3936	0.9812
400	1.214	0.8400	0.9924
425	1.276	0.9050	——

where k_S and k_N are rate constants for pseudo–first order HDS and HDN rate equations respectively, and S_f, N_f and N_p, N_p are sulfur and nitrogen concentrations in feed and product oils respectively, and $\mathcal{I}_S$ and $\mathcal{I}_N$ are intercepts that represent only the effect of temperature on hydrotreating.

In Figure 57 data, for HDS using the Co-Mo catalyst are plotted. Figure 58 shows data for HDN for the same catalyst. Figures 59 and 60 give plots of HDS and HDN data respectively, using the Ni-W catalyst.

The individual k-values from the slopes were evaluated and are given in Table 5 for HDN and in Table 6 for HDS. Although it was not possible to find comparative values in the literature for all the k's, some values have been reported by Frost [18], Speight [58] and Sambi [50, page 93]. Sambi reported values for k_N and k_S at the following conditions: temperature 375°C, pressure 6.9 MPa, LHSV of 1.0 to 4.0 and gas flow rate of 890 m^3/m^3. Table 7 shows a comparison between the values obtained in both

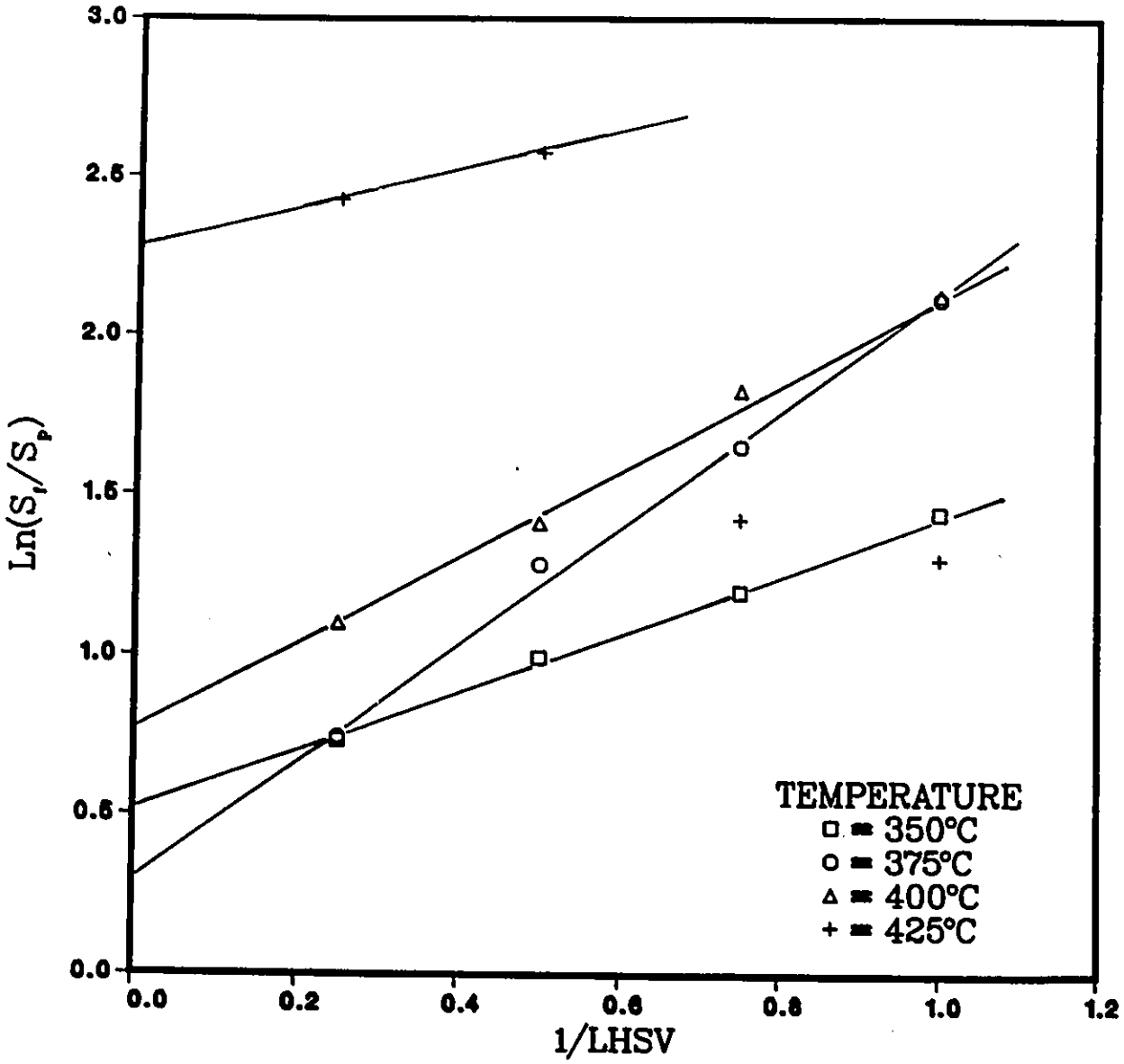

Figure 57: $Ln(S_f/S_p)$ vs 1/LHSV for the Co-Mo Catalyst

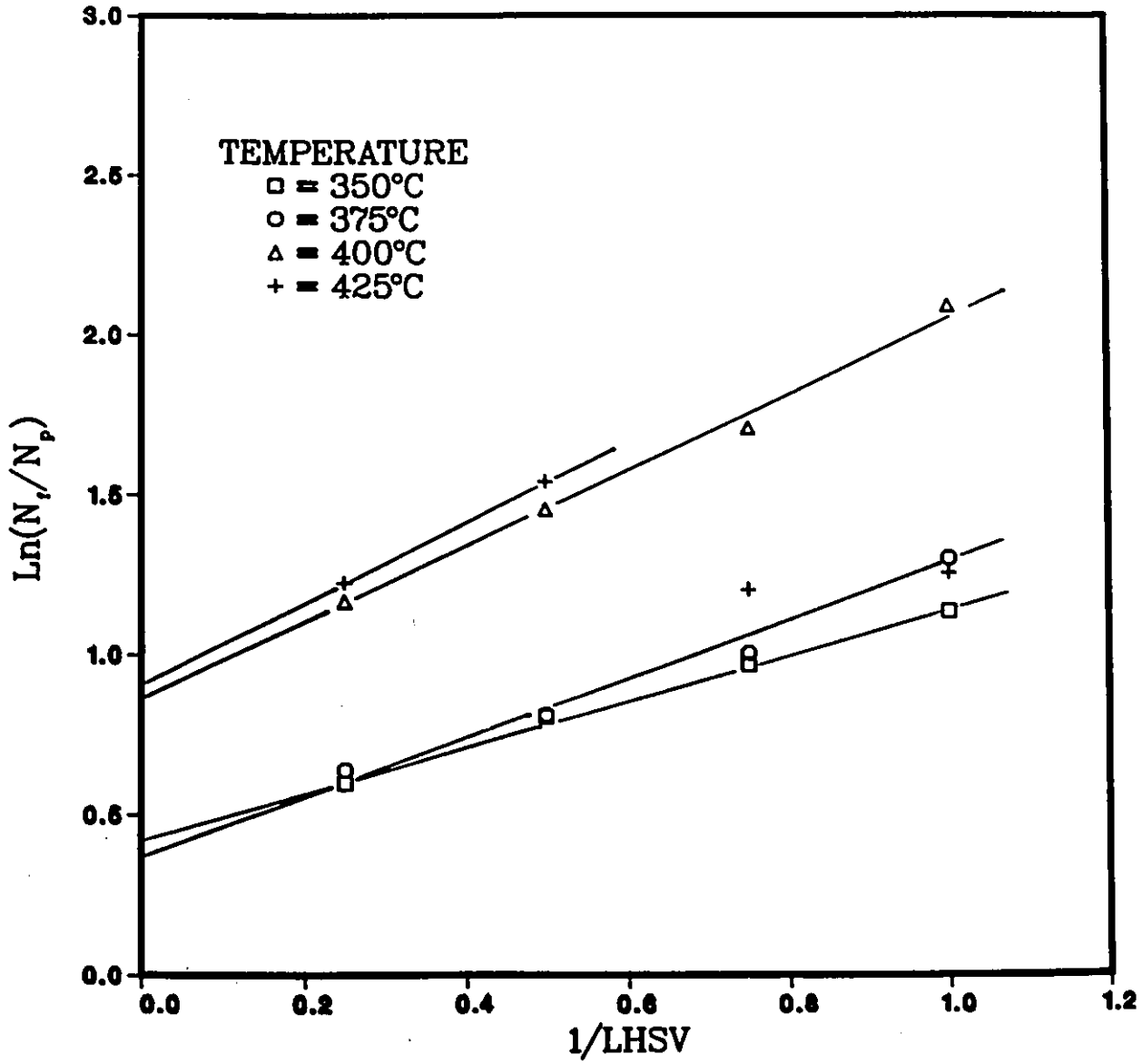

Figure 58: $Ln(N_f/N_p)$ vs 1/LHSV for the Co-Mo Catalyst

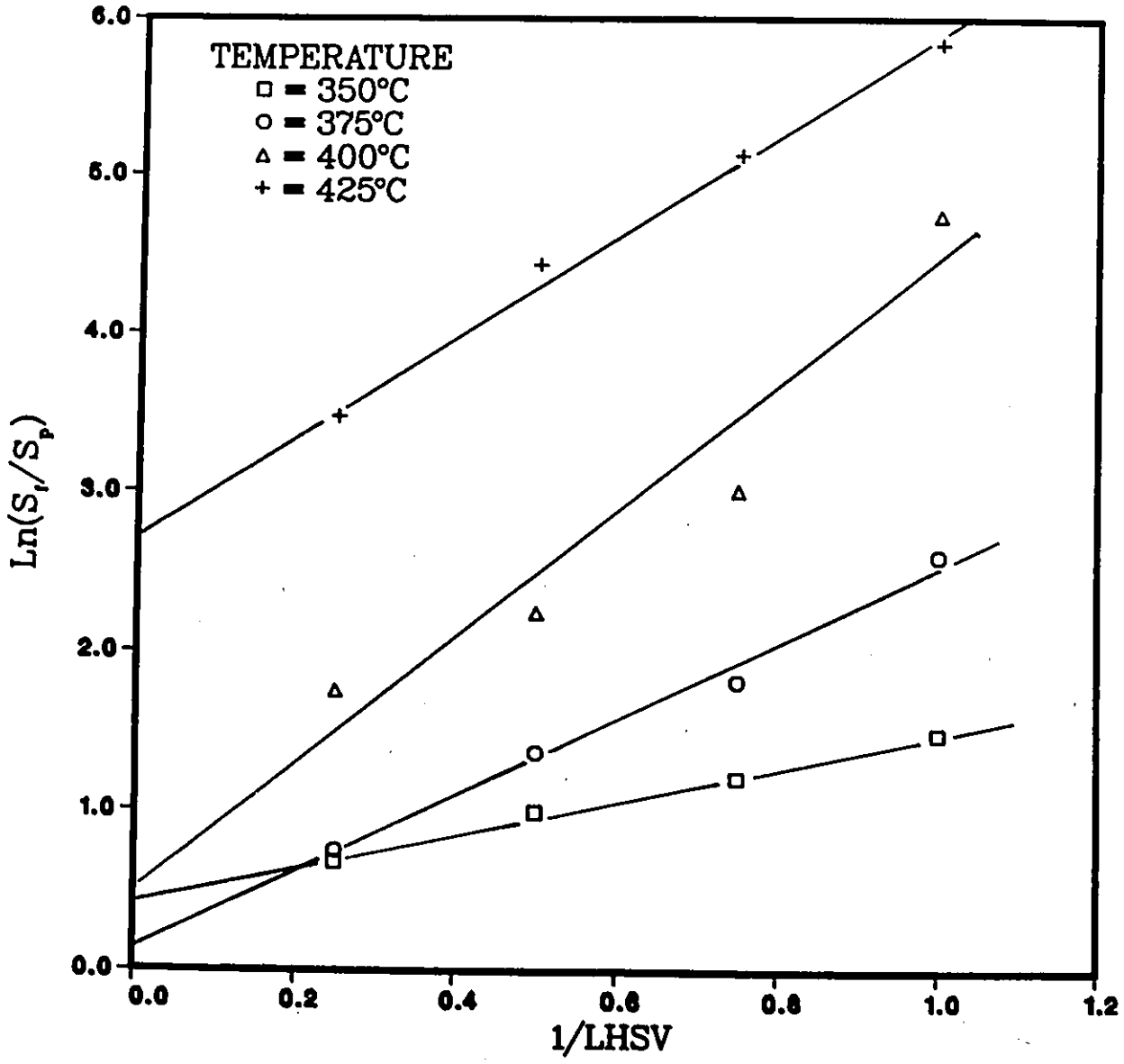

Figure 59: $Ln(S_f/S_p)$ vs 1/LHSV for the Ni-W Catalyst

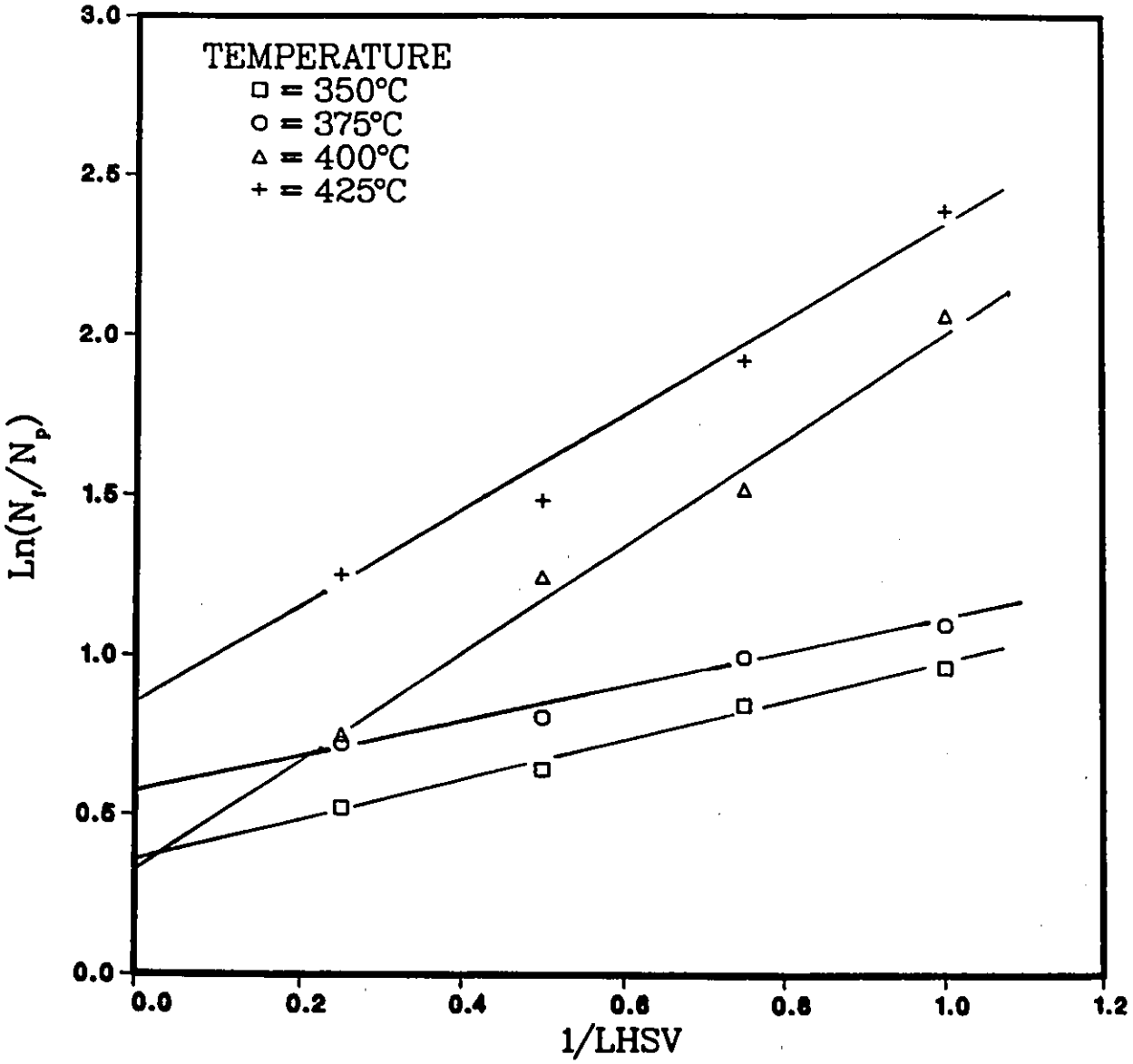

Figure 60: $Ln(N_f/N_p)$ vs 1/LHSV for the Ni-W Catalyst

Table 6: Rate Constants for HDS

Pressure = 6.9 MPa
Gas Flow Rate = 890 m^3/m^3

Ni-W Catalyst Temperature (°C)	HDS Pseudo–first order Rate Constant (h^{-1})	Intercept $\mathcal{I}$ (h^{-1})	COD
350	1.058	0.4340	0.9960
375	2.410	0.1300	0.9890
400	3.900	0.5060	0.9211
425	3.100	2.7830	0.9926

Co-Mo Catalyst Temperature (°C)	HDS Pseudo-first order Rate Constant (h^{-1})	Intercept $\mathcal{I}$ (h^{-1})	COD
350	0.936	0.5050	0.9984
375	1.804	0.3200	0.9950
400	1.404	0.7400	0.9952
425	0.544	2.2860	——

Table 7: Comparative Values of HDN and HDS Rate Constants

Catalyst	Sambi's Study		Present Study	
	k_S (h^{-1})	k_N (h^{-1})	k_S (h^{-1})	k_N (h^{-1})
Co-Mo	2.08	0.86	1.804	0.871
Ni-W	3.00	0.50	2.410	0.525

studies. It can be observed that the constants for HDN are practically the same in both cases, whereas for HDS the difference is about 20 %. As this is a very steep slope, a small experimental error may suffice to change the slope significantly. Nonetheless the values obtained are considered to be in good agreement with those previously reported.

The intercepts are constants depending only on temperature, in general terms it is shown that as the temperature increases so does the intercept.

A Standard Arrhenius type of correlation was used for evaluating the respective activation energies. The values of ln(k) were plotted against (1000/T°K). A linear least-square technique was used to obtain the best fit. The Arrhenius equation is defined as follows:

$$k = A\exp(-E/RT) \tag{18}$$

where k is the rate constant, A is the coefficient, E is the activation energy, T is the absolute temperature and R is the gas constant.

The corresponding values of the activation energies (E = -slope ×1000× R) and the coefficient A (A = exp(intercept)), obtained for both catalysts for both nitrogen and sulfur data, are listed in Table 8.

Table 8: Activation Energies for HDN and HDS

Catalysts	Ni-W HDN	Co-Mo HDN
E(Kcal/gmol)	16.56	8.97
$A(h^{-1})$	3.18×10^5	974
	HDS	HDS
E(Kcal/gmol)	21.67	21.05
$A(hr^{-1})$	4.43×10^7	2.27×10^7

4.2.5 Reactor Performance

The basic assumption in this study was that the reactor operation was essentially isothermal and in the plug-flow regime. For better understanding of these subjects the studies of several researchers were considered as well : Charpentier [11], Charpentier and Favier [10], van Klinken and van Dongen [62], Morsi et al. [48,49], Rao and Drinkenburg [47], and Herskowitz and Smith [26,27]. Causes for deviation from the ideal plug-flow regime have been discussed in chapter 2. These fundamentals were applied to the present reactor system to verify its performance.

Effective Catalyst Utilization

The effective utilization of the catalyst could be adversely affected by inefficient catalyst wetting or by channelling of the liquid in the packed bed. As indicated in Chapter 2 sections 2.4.1 and 2.4.1 for a tube diameter to particle size ratio (d_t/d_p) greater that 20, channelling of liquid in a trickle-bed reactor is negligible. In the present case the tube inside diameter was 5.2 mm and the particle size was about 0.2 mm, giving a d_t/d_p ratio of $\sim$ 26. Therefore no adverse channelling effects were expected.

Although wetting efficiencies in laboratory trickle-bed reactors are generally low, this factor did not present a problem. By diluting the catalyst bed with equal volume of an inert material (α-alumina), as recommended in section 2.4.1, the wetting efficiency

increased to a point where complete catalyst wetting could be assumed. van Klinken and van Dongen [62] present a comprehensive study about catalyst bed dilution in case of laboratory scale reactors. Their system was very similar to the one used in this study, which gives a more sound basis for prediction of the reactor performance.

Axial Dispersion

This is one of the factors which can make the reactor performance deviate from the ideal plug-flow regime. This criterion is described in section 2.4.1. As previously mentioned, for the axial dispersion effect to be less than 5 %, the reactor length to particle diameter ratio (L/d_p) should be more than 350. In the actual case, a 100 cm long reactor and a particle size of about 0.2 mm were used. This gives a L/d_p ratio of 5000. From this, it can be concluded that as per this criterion, there was no possibility of backmixing or axial dispersion effects, and the initial assumption of ideal plug flow was fully valid.

4.2.6 Effectiveness Factor and Mass Transfer Effects

Smith [56] describes in detail the steps that a heterogeneous reaction should follow in order to occur. Hydrotreating reactions, being carried out in a heterogeneous system, follow these steps. These ones occur on active catalyst sites, therefore the reactants must reach thoses site if the reaction is to occur. These sites are mostly inside the catalyst pores.

In previous sections, the possible problems that might be encountered in reactants reaching the catalyst surface have been discused. In such a case, the steps to follow are:

(a) Diffusion of reactants into the pores of the catalyst.

(b) Adsorption of the species on the active sites.

(c) Chemical reaction on the active site.

(d) Desorption of the products from the catalyst site.

(e) Diffusion of products out of the catalyst pores.

The slowest of the above mentioned steps will determine the overall rate of reaction. If the chemical reaction is to be the controlling step, it is necessary to have the experimental set-up designed in such a way that all the other steps have a faster rate. In order to attain this goal in studies like hydrotreatment, the particle size of the catalyst is reduced enough to achieve an effectiveness factor of close to one.

From the available information [38] on the effectiveness factor of the catalyst used in similar studies, a particle size of 0.2 mm would give an effectiveness factor very close to one. Usually smaller particle size would have ensured a closer-to-one effectiveness factor but it would have also increased the pressure drop throughout the reactor system. The efficiency of this particle size was verified by Sambi [51, page 153], giving very positive results. Therefore it can be concluded that for all practical reasons, the effectiveness factor of the catalysts used in this study was considered as one.

4.2.7 Heat Transfer Effects

During the entire study it was assumed that trickle-bed operation was isothermal. Non-isothermal conditions may occur due to two main factors:

(a) excessive heat effects involving the chemical reactions that occur in the process, and/or,

(b) defective temperature control around the reactor.

In hydrotreatment, the heats of reaction are generally very low ($\sim$ 25 to $\sim$ 30 Kcal/gmol). The catalyst is always wetted by the liquid oil (see section 2.4.1). This helps both the inter-particle and the intra-particle heat transfer. As the reactor inside diameter was only 0.52 cm, no significant temperature gradient was expected in the radial direction of the catalyst bed.

In the present study, the temperature control around the reactor was considered very efficient. As described on page 50, a sand bath was used to maintain the reactor at a contant temperature. The temperature inside the sand bath was checked several times at several points inside it and the agreement was always found to be within 2°C of the specified temperature. Also, the temperature was verified along the reactor with three thermocouples at all operating conditions. The agreement as stated before was

about ± 1°C, which strengthens the validity of the original assumption of isothermal operation.

Chapter 5

Conclusions and Recommendations

5.1 Conclusions

Most of the conclusions are given at the end of the discussions on each part of the present study. However, some of the important conclusions are summarized as follows:

(a) The catalyst preparation and testing scheme demonstrated good reproducibility.

(b) In general, for all cases density and viscosity decreased with increase in temperature. The same behaviour was observed with decrease in LHSV.

(c) The C/H ratio of the product samples showed a good hydrogenation capability of the catalysts studied.

(d) As expected, the Ni-W catalyst showed better HDS capability than the Co-Mo catalyst. The Ni-W catalyst was able to remove up to 99 % of the sulfur whereas the Co-Mo catalyst removed a maximum of 92 %.

(e) The Co-Mo catalyst showed better HDN capability than the Ni-W catalyst. The Co-Mo catalyst removed more nitrogen at most temperatures and flow rates (an average of 6 % more nitrogen removed) than the Ni-W catalyst.

(f) The kinetic study of both catalysts showed a good fit, for both nitrogen and sulfur removal, using a pseudo-first order model.

(g) The analysis of the characteristics of the replicates showed that the activity of the catalysts did not decrease substantially throughout the sampling period (most of the values fell within the 95 % confidence interval).

(h) Reactor performance was close to isothermal plug-flow conditions.

5.2 Recommendations

(a) Hundreds of different compounds can be found in heavy oil. During hydrotreatment they react following different pathways. It is not possible to identify all these reactions, due to the complexity of the system, with the available facilities. Therefore it is recommended to pursue studies using single compounds as feedstock. A more detailed kinetic study could be thus performed which may be more indicative of the mechanism.

(b) In the actual system, the amount of deposited coke on the catalyst at a given time could not be considered. Further studies should be carried out to evaluate the effects that coke deposits have on similar catalysts.

Bibliography

[1] S. Andrew. Heterogeneous catalyst preparation : The fabrication of microstructures. In B. Delmon, P. A. Jacobs, and G. Poncelet, editors, *Preparation of Catalysts : Scientific Bases for the Preparation of Heterogeneous Catalysts*, pages 429–448, Division de Catalyse, Société Chimique de Belgique, Elsevier Scientific Publishing Co., Amsterdam, 1976.

[2] D. Bacon. *Collection and Interpretation of Industrial Data.* Department of Chemical Engineering, Queen's University, Kingston, Ontario, 1983.

[3] D. Barthomeuf. Acidic catalysis with zeolites. In F. Ribeiro, A. Rodrigues, L. Deane, and C. Naccache, editors, *Zeolites : Science and Technology*, pages 317–345, NATO Advanced Study Institute on Zeolite–Science and Technology, Martinus Nijhoff Publishers, The Hague, 1984.

[4] H. A. Benesi, R. U. Bonnar, and C. F. Lee. Determination of pore volume of solid catalysts. *Analytical Chemistry*, 27:1963–1965, 1955.

[5] A. P. Bolton. Molecular sieve zeolites. In R. B. Anderson, editor, *Experimental Methods in Catalytic Research*, page 33, Academic Press, New York, 1976.

[6] G. K. Bores. Scientific basis for catalyst preparation. In B. Delmons, P. A. Jacobs, and G. Poncelet, editors, *Preparation of Catalysts : Scientific Bases for the Preparation of Heterogeneous Catalysts*, pages 223–250, Division de Catalyse, Société Chimique de Belgique, Elsevier Scientific Publishing Co., Amsterdam, 1976.

[7] S. Brunauer, P. H. Emmett, and E. Teller. Adsorption of gases in multimolecular layers. *Journal of the American Chemical Society*, 60:309, 1938.

[8] J. J. Carberry. *Chemical and Catalytical Reaction Engineering.* McGraw Hill Book Co., New York, 1976.

[9] H. J. Chang and B. L. Crynes. Effect of catalyst pore and pelet sizes on deactivation in SRC oil hydrotreatment. *AIChE Journal*, 32(2):224–232, February 1986.

[10] J. Charpentier and M. Favier. Some liquid holdup experimental data in trickle-bed reactors for foaming and non-foaming hydrocarbons. *AIChE Journal*, 21(6):1213–1218, 1975.

[11] J. C. Charpentier. Recent progress in two phase gas-liquid mass transfer in packed beds. *The Chemical Engineering Journal*, 11:161–181, 1976.

[12] D. B. Dadyburjor. Selectivity over unifunctional multicomponent catalyst with nonuniform distribution of components. *Industrial & Engineering Chemistry. Fundamentals*, 24(1):16–27, 1985.

[13] T. R. Davis and H. F. Rase. Characteristics of a nickel–contaminated cracking catalyst: Differences in the reaction and sintering characteristics of each catalyst component. *Industrial & Engineering Chemistry. Fundamentals*, 25(4):581–588, 1986.

[14] V. de Beer and G. Schuit. CoO–MoO_3–γ–Al_2O_3 catalyst. Influence of the support. A review. In B. Delmons, P. A. Jacobs, and G. Poncelet, editors, *Preparation of Catalysts : Scientific Bases for the Preparation of Heterogeneous Catalysts*, pages 343–370, Division de Catalyse, Société Chimique de Belgique, Elsevier Scientific Publishing Co., Amsterdam, 1976.

[15] H. de Lasa. Engineering aspects of catalytic cracking. In F. Ribeiro, A. Rodrigues, L. Deane, and C. Naccache, editors, *Zeolites : Science and Technology*, pages 491–513, NATO Advanced Study Institute on Zeolite–Science and Technology, Martinus Nijhoff Publishers, The Hague, 1984.

[16] D. Decroocq, R. Bulle, S. Chatila, J. P. Franck, and Y. Jacquin. *Le Craquage Catalytique de Coupes Lourdes. Publications de L'Institut Français du Pétrole*, Société des Éditions Technip, Paris, 1978.

[17] P. A. Faeth and C. B. Willingham. *The Assembly, Calibration and Operation of a Gas Adsorption Apparatus for Measurement of Surface Area, Pore Volume Distribution and Density of Finely Divided Solids.* Department of Physical Chemistry, Mellon Institute of Industrial Research, Pittsbourgh, September 1953.

[18] C. M. Frost and P. L. Cottingham. *Technical Report RI 7557.* Technical Report, U.S. Dept. of Interior, Bureau of Mines, 1975.

[19] H. J. Gary and G. E. Handwerk. *Petroleum Refining : Technology and Economics.* Marcel Dekker, Inc., New York, 2nd edition, 1984.

[20] M. Goddard and D. M. Ruthven. Adsorption of C_8 aromatics on NaY zeolite. In D. Olson and A. Bisio, editors, *Proceedings of The Sixth International Zeolite Conference*, pages 268–275, Butterworths & Co. Ltd., Surrey, 1984.

[21] G. Gottardi and E. Galli. *Natural Zeolites.* Volume 18 of *Minerals and Rocks*, Sringer-Verlag, Berlin, 1985.

[22] W. A. Gruse and D. R. Stevens. *Chemical Technology of Petroleum.* McGraw Hill Book Co., New York, 3rd edition, 1960.

[23] 1970 Refining Processes Handbook. Hydrotreating. *Hydrocarbon Processing*, 204–232, September 1970.

[24] H. W. Haynes, Jr. , J. F. Parcher, and N. E. Helmer. Hydrocracking polycyclic hydrocarbons over dual–functional zeolite (faujasite)–based catalyst. *Ind. Eng. Chem. Process Des. Dev.*, 22(3):401–409, 1983.

[25] M. Herskowitz and S. Mosseri. Global rates of reactions in tricle–bed reactors : Effects of gas and liquid flow rates. *Industrial & Engineering Chemistry. Fundamentals*, 22(1), 1983.

[26] M. Herskowitz and J. M. Smith. Liquid distribution in trickle–bed reactors. Part I : Flow measurements. *AIChE Journal*, 24(3):439–450, 1978.

[27] M. Herskowitz and J. M. Smith. Liquid distribution in trickle–bed reactors. Part II : Tracer studies. *AIChE Journal*, 24(3):450–454, 1978.

[28] P. A. Jacobs. *Carbonogenic Activity of Zeolites.* Elsevier Scientific Publishing Co., Amsterdam, 1977.

[29] D. Kallo, G. Onyestyak, and J. Paap Jr. Hydrosulfurization of C=C bond and Me^{2+} zeolite. In D. Olson and A. Bisio, editors, *Proceedings of The Sixth International Zeolite Conference*, pages 444–453, Butterworths & Co. Ltd., Surrey, 1984.

[30] T. F. Kellet, C. A. Trevino, and A. F. Sartor. Decision tree helps selecting hydrotreating catalyst. *Oil & Gas Journal*, 78(18):244–251, May 1980.

[31] K. J. Klingman and H. H. Lee. Catalyst deactivation by multilayer coking : A kinetic model. *AIChE Journal*, 32(2):309–312, February 1986.

[32] Y. Kotera, K. Ogawa, M. Oba, K. Shimonura, M. Yonemura, A. Veno, and N. Todo. Preparation of MoO_3–CoMo–Al_2O_3 catalyst and its characteristics. In B. Delmon, P. A. Jacobs, and G. Poncelet, editors, *Preparation of Catalysts : Scientific Bases for the Preparation of Heterogeneous Catalysts*, pages 371–380, Division de Catalyse, Société Chimique de Belgique, Elsevier Scientific Publishing Co., Amsterdam, 1976.

[33] D. M. Little. *Catalytic Reforming.* PennWell Publishing Co., Tulsa, Oklahoma, 1985.

[34] M. Lo Jacono and M. Schiavello. The influence of preparation methods on structural and catalytical properties of transition metal ions supported on alumina. In B. Delmon, P. A. Jacobs, and G. Poncelet, editors, *Preparation of Catalysts : Scientific Bases for the Preparation of Heterogeneous Catalysts*, pages 473–488, Division de Catalyse, Société Chimique de Belgique, Elsevier Scientific Publishing Co., Amsterdam, 1976.

[35] R. López Lorenzo, F. A. Cossío de los Santos, and O. Bermúdez Mendizábal. New alternatives to processing heavy crude oils. *Journal of the Mexican Institute of Chemical Engineers (Revista IMIQ)*, 745, November–December 1985.

[36] R. Mann and R. Díaz Real. Hydrofining of athabasca derived heavy gas oil over Ni–W and Co–Mo catalysts. Presented at the American Institute of Chemical Engineers National Meeting, in Minneapolis MN, August 1987.

[37] R. Mann and R. Díaz Real. Hydrofining of heavy gas oil. In *Proceedings of the 1st Canadian Chemical Engineering Graduate Students Conference*, pages 238–245, Canadian Society for Chemical Engineering, Kingston, Ontario, October 1987.

[38] R. S. Mann, I. S. Sambi, and K. C. Khulbe. Personal communication.

[39] R. S. Mann, I. S. Sambi, and K. C. Khulbe. Catalytic hydrofining of heavy gas oil. *Industrial Engineering Chemistry Research*, 26:410–414, March 1987.

[40] R. S. Mann, I. S. Sambi, and K. C. Khulbe. Catalytic hydrotreatment of heavy gas oil. *Ind. Eng. Chem. Proc. Res. & Dev.*, 21(4):575, 1983.

[41] M. P. Manning, J. G. Garmirian, and R. C. Reid. Carbon deposition studies using nickel and cobalt catalysts. *Ind. Eng. Chem. Process Des. Dev.*, 21(3):404–409,

1982.

[42] D. E. Mears. The role of axial dispersion in trickle–flow laboratory reactors. *Chemical Engineering Science*, 26:1361–1366, 1971.

[43] R. A. Meyers, editor. *Handbook of Petroleum Refining Processes. Chemical Process Technology Handbook*, McGraw Hill Book Co., New York, 1986.

[44] Y. Miki, S. Yamadaya, M. Oba, and Y. Sugimoto. Role of catalyst in hydrocracking of heavy oil. *Journal of Catalysis*, 83:371–383, 1983.

[45] K. M. Ng. A model for flow regime transitions in cocurrent down–flow trickle–bed reactors. *AIChE Journal*, 32(1):115–122, January 1986.

[46] J. A. Paraskos, J. A. Frayer, and Y. T. Shah. Effect of holdup incomplete catalyst wetting and backmixing during hydroprocessing in trickle bed reactors. *Ind. Eng. Chem. Process Des. Dev.*, 14(3):315–322, 1975.

[47] V. G. Rao and A. A. Drinkenburg. Solid–liquid mass transfer in packed beds with cocurrent gas–liquid downflow. *AIChE Journal*, 31(7):1059–1068, July 1985.

[48] A. E. Sáez, R. G. Carbonell, and J. Levec. The hydrodynamics of trickling flow in packed beds . Part I : Conduit models. *AIChE Journal*, 32(3):353–368, March 1986.

[49] A. E. Sáez, R. G. Carbonell, and J. Levec. The hydrodynamics of trickling flow in packed beds . Part II : Experimental obsevations. *AIChE Journal*, 32(3):369–379, March 1986.

[50] I. S. Sambi. *Catalytic Hydrotreatment of Heavy Gas Oil.* Master's thesis, University of Ottawa, Ottawa, 1982.

[51] I. S. Sambi. *Hydrotreatment of Athabasca Bitumen Derived Heavy Gas Oil over Modified Zeolite Supported Catalyst.* PhD thesis, University of Ottawa, Ottawa, 1985.

[52] C. N. Satterfield. *Heterogeneous Catalysis in Practice.* McGraw Hill Book Co., New York, 1980.

[53] J. Scott, editor. *Zeolite Technology and Applications : Recent Advances.* Noyes Data Corp., New Jersey, 1980.

[54] E. I. Shaheen. *Catalytic Processing in Petroleum Refining.* PennWell Publishing Co., Tulsa, Oklahoma, 1983.

[55] J. H. Sinfelt. Influence of technology on catalytic science. *Industrial & Engineering Chemistry. Fundamentals*, 25(1):2–9, 1986.

[56] J. M. Smith. *Chemical Engineering Kinetics.* McGraw Hill Book Co., New York, 1981.

[57] J. G. Speight. *The Chemistry and Technology of Petroleum.* Volume 3 of *Chemical Industries*, Marcel Dekker, Inc., New York, 1980.

[58] J. G. Speight. *The Desulfurization of Heavy Oils and Residua.* Volume 4 of *Chemical Industries*, Marcel Dekker, Inc., New York, 1981.

[59] C. L. Thomas. Chemistry of cracking catalysts. *Industrial & Engineering Chemistry*, 41(11):2564–2573, November 1949.

[60] D. F. Tolen. Burst of advances enhance cat cracking. *Oil & Gas Journal*, 79(13):90–109, September 1981.

[61] H. Topsœ, B. Clausen, N. Topsœ, and E. Pedersen. Recent basic research in hydrodesulfurization catalysts. *Industrial & Engineering Chemistry. Fundamentals*, 25(1):25–36, 1986.

[62] J. van Klinken and R. H. van Dongen. Catalyst dilution for improved performance of laboratory trickle–flow reactors. *The Chemical Engineering Journal*, 35:59–66, 1980.

[63] P. B. Venuto and E. T. Habib, Jr. *Fluid Catalytic Cracking with Zeolite Catalysts.* Volume 1 of *Chemical Industries*, Marcel Dekker, Inc., New York, 1979.

Appendix A

Computer Programs

A.1 Programs for BET Surface Area.

A.1.1 Main Program : BET1 FORTRAN

```
C     THIS PROGRAM WILL CALCULATE THE VALUES IN THE WORK SHEET FOR
C     B.E.T. SURFACE AREA .FIRST FOUR VALUES OF DATA SHOULD BE FOR
C     EMPTY SPACE FACTOR CALCULATIONS. NEXT TWO VALUES   SHOULD BE
C     FOR CALCULATING THE NITROGEN TOTAL VOLUME.
C
C
C
      REAL P,PC,PO,TB,VT,VB,VS,VA,Y,X,FV,FS,FSM,RANGE,Y1,X1,
     1WT,S,XY,SX,SY,SXY,SXS,SYS,SLOPE,AINTER,RATIO
      INTEGER M,N,IER,SNUM,I,J
      DIMENSION P(15),PC(15),PO(15),TB(15),VT(15),VA(15),VB(15),VS(15),Y
     1(15),X(15),FV(6,5),FS(2),M(15),N(15),RANGE(4),Y1(15,1),X1(15)
C
C     DATA READ FROM A FILE DEFINED AS NO.5  PR8 DATA
C
      READ(5,1)SNUM,WT,L
1     FORMAT(///,15X,I6,/,15X,F6.4,/,15X,I2,//)
```

```
      DO 2 I=1,L
      READ(5,3)M(I),N(I),P(I),TB(I),PO(I)
3     FORMAT(10X,I1,1X,I1,1X,F5.1,1X,F4.1,1X,F5.1)
      M(I)=M(I)+1
      N(I)=N(I)+1
2     CONTINUE
C
C   READ THE NITROGEN BULB FACTORS FORM A FILE:  FB FORTRAN DEFINED AS
C   NUMBER 7.
C
      DO 50 I=1,6
      READ(7,53)FV(I,1),FV(I,2),FV(I,3),FV(I,4),FV(I,5)
53    FORMAT(5(F8.4,2X))
50    CONTINUE
C
C
C   CALCULATE EMPTY SPACE FACTOR
C
75    CONTINUE
      DO 5 I=1,L
      PC(I)=P(I)*(0.9955-  (TB(I)-25.0)*1.8E-4)
5     CONTINUE
      DO 6 I=1,2
      VT(I)=PC(I)*FV(M(I),N(I))/298.13
6     CONTINUE
      VT(3)=(VT(1)+VT(2))/2
      VT(4)=VT(3)
      DO 7 I=3,4
      VB(I)=PC(I)*FV(M(I),N(I))/298.13
      VS(I)=VT(I)-VB(I)
      FS(I-2)=VS(I)/PC(I)
 7    CONTINUE
      FSM=(FS(1)+FS(2))/2.
```

```
      DO 8 I=5,6
      VT(I)=PC(I)*FV(M(I),N(I))/298.13
8     CONTINUE
      DO 9 I=7,L
      VT(I)=(VT(5)+VT(6))/2.
      VB(I)=PC(I)*FV(M(I),N(I))/298.13
      VS(I)=PC(I)*FSM*(1.+PC(I)*6.65E-5)
      VA(I)=VT(I)-VB(I)-VS(I)
      Y(I)=1./(VA(I)*(PO(I)/P(I)-1.))
      Y1(I-6,1)=Y(I)
      X(I)=P(I)/PO(I)
      X1(I-6)=X(I)
9     CONTINUE
      WRITE(6,20)SNUM,WT
20    FORMAT(1H1,6X,'*',41X,'**',41X,'*',10X,'I',/,'
     1          ',/,30X,21('*'),/,30X,'*   SAMPLE NO:  ',I6,' *',/,30X,2
     111('*'),//,10X,'SAMPLE  WEIGHT = ',F8.4,/,'
     1            ',/,5X,'BU- PRES-  PC.  TEMP VAP.  VT(I)  VB(I)  VS(I)
     1  VA(I)   P/PO   Y',/,5X,'LBS SURE             PR.    CC     CC
     2  CC     CC ',//)
      DO 42 I=1,L
      M(I)=M(I)-1
      N(I)=N(I)-1
42    CONTINUE
      DO 21 I=1,2
      WRITE(6,22)M(I),N(I),P(I),PC(I),TB(I),VT(I)
22    FORMAT(5X,I1,'+',I1,1X,F5.1,1X,F5.1,1X,F4.1,7X,F6.3,/)
21    CONTINUE
      DO 23 I=3,4
      WRITE(6,24)M(I),N(I),P(I),PC(I),TB(I),VT(I),VB(I),VS(I),FS(I-2),FS
     1M
24    FORMAT(5X,I1,'+',I1,1X,F5.1,1X,F5.1,1X,F4.1,7X,F6.3,1X,F6.3,1X,F6.
     13,2X,'FS = ',F6.3,3X,'FSM = ',F6.3,/)
```

```
23    CONTINUE
      DO 25 I=5,6
      WRITE(6,26)M(I),N(I),P(I),PC(I),TB(I),VT(I)
26    FORMAT(5X,I1,'+',I1,1X,F5.1,1X,F5.1,1X,F4.1,7X,F6.3,/)
25    CONTINUE
      DO 27 I=7,L
      WRITE(6,28)M(I),N(I),P(I),PC(I),TB(I),PO(I),VT(I),VB(I),VS(I),VA(I
     1),X(I),Y(I)
28    FORMAT(5X,I1,'+',I1,1X,F5.1,1X,F5.1,1X,F4.1,1X,F5.1,1X,F6.3,1X,F6.
     13,1X,F6.3,1X,F6.3,1X,F6.4,1X,E11.5,/)
27    CONTINUE
      WRITE(6,41)
41    FORMAT(///,10X,'
     1',/,10X,'NO. OF      SLOPE        INTERCEPTPT       SURFACE
     2',/,10X,'POINTS        S              I              AREA',//)
      IK=L-6
      DO 11 I=3,IK
      DO 44 K=1,I
      DO 44 KK=1,3
44    CONTINUE
      SX=0.0
      SY=0.0
      SXY=0.0
      SXS=0.0
      SYS=0.0
      DO 12 J=1,I
      SX=SX+X1(J)
      SY=SY+Y1(J,1)
      SXY=SXY+X1(J)*Y1(J,1)
      SXS=SXS+X1(J)**2
      SYS=SYS+Y1(J,1)**2
12    CONTINUE
      SLOPE=(SXY-SX*SY/I)/(SXS-SX**2/I)
```

```
      AINTER=SY/I-SLOPE*SX/I
      RATIO=(SXY-SX*SY/I)**2/(SXS-SX**2/I)/(SYS-SY**2/I)
      S=4.38/((SLOPE+AINTER)*WT)
      WRITE(6,40)I,SLOPE,AINTER,S
40    FORMAT(12X,I2,2X,2(E13.6,4X),3X,F8.3,/)
      WRITE(6,71)RATIO
71    FORMAT(3X,'R**2= ',E11.5,//)
11    CONTINUE
      RANGE(1)=0.0
      RANGE(2)=0.6
      RANGE(3)=0.0
      RANGE(4)=0.08
      CALL USPLO(X1,Y1,1,(L-6),1,1,15HADSORPTION PLOT,15,4HP/PO,4,13HP/(
     1VA/(PO-P)),13,RANGE,1H*,0,IER)
      WRITE(6,30)IER
30    FORMAT(///,10X,'THE ERROR MESSAGE = ',I3)
      STOP
      END
```

A.1.2 Exec (Main Program) : EXBET EXEC

To execute type 'EXBET BET1'. Data will be taken from a file called PR8 DATA. The bulb factors will be read from file FB FORTRAN and results will be written in PR8 RESULT.

```
GLOBAL TXTLIB VLNKMLIB VFORTLIB CMSLIB IMSLDLIB PLOTLIB
FORTVS &1
FILE 5 DISK PR8 DATA(LRECL 80 BLKSIZE 80 RECFM F PERM
FILE 7 DISK FB FORTRAN(LRECL 80 BLKSIZE 80 RECFM F PERM
FILE 6 DISK PR8 RESULT A (PERM RECFM F LRECL 132
LOAD &1(CLEAR START
```

A.1.3 Data for Bulb Factors : FB FORTRAN

```
005.0909  006.9542  010.2767  019.0489  038.0320
006.4388  008.3022  011.6247  020.3968  039.3799
009.5122  011.3756  014.6981  023.4702  042.4533
017.1820  019.0454  022.3679  031.1400  050.1231
032.7967  034.6600  037.9825  046.7547  065.7378
082.3911  084.2545  087.5770  096.3491  115.3322
```

A.2 Programs for the Simulated Distillation ASTM-2887

A.2.1 Main Program : SIMDIS FORTRAN.

```
C    THIS PROGRAM ACCEPTS RAW DATA AS GENERATED BY THE GC INTEGRATOR
C
C    TO RUN : SIMDIS EXEC   TYPE "SIMDIS"
C
      INTEGER NS,NP,NT,NOFS,II
      REAL X,X1,X2,Y,Y1,SUM,MIDBP
      DIMENSION X(20),X1(20),X2(20),Y(20),Y1(20),NS(2)
C
C  GIVE THE VALUES OF TEMPERATURES CORRESSPONDING TO THE RETENTIONS
C  TIMES FOR EVERY 2.5 MINUTES INTERVAL TO Y1'S BELOW:-
C
C
      DO 9 I  =1,20
         Y1(I)=0.0
9            CONTINUE
      NT=9
      Y1(1)=101.44
      Y1(2)=155.92
      Y1(3)=205.04
```

```
      Y1(4)=257.60
      Y1(5)=317.00
      Y1(6)=371.76
      Y1(7)=425.76
      Y1(8)=475.36
      Y1(9)=535.28
C
C READ NUMBER OF SAMPLES AND THEN
C READ THE SAMPLE NO. AND THE VALUES OF THE AREAS FROM THE INTEGRATOR.
C
           READ(5,49)NOFS
49        FORMAT(14X,I3)
       WRITE(7,12)NOFS
12     FORMAT(I3)
       DO 48 J=1,NOFS
      READ(5,50)(NS(I),I=1,2)
50      FORMAT(13X,2A4)
      READ(5,53)NP
53      FORMAT(19X,I2)
         DO 6 I=1,NP
           READ(5,51)X(I)
51          FORMAT(E8.4)
6             CONTINUE
C
C  CUMMULATIVE AREA (X1(I)), AND % AREA (X2(I)) ARE CALULATED
C
      SUM=0.0
        DO 1 I=1,NP
          SUM=SUM+X(I)
            X1(I)=SUM
1             CONTINUE
      DO 2 I=1,NP
        X2(I)=(X1(I)/SUM)*100.0
```

```
          Y(I)=2.5*I
2             CONTINUE
C
C  CALCULATE THE MID-BOILING POINT BY USING A ST. LINE IN THE
C  IN-BETWEEN POINTS
C
      I=1
24        IF(X2(I+1).LT.50.0) GO TO 21
           GO TO 23
21          I=I+1
              GO TO 24
23              IF(X2(I+1).EQ.50.0) GO TO 22
       MIDBP=Y1(I+1)-(Y1(I+1)-Y1(I))*((X2(I+1)-50.0)/(X2(I+1)-X2(I)))
        GO TO 25
22        MIDBP=Y1(I+1)
C
C   WRITE THE GIVEN DATA IN AN OUT PUT FILE CALLED SD RESULT
C
25     WRITE(6,60)NS
60     FORMAT(1H1,///,15X,'SAMPLE  NUMBER :- ',2A4,/,15X,21('_'),////,17X
      1,'CUMULATIVE',2X,'RETENTION',3X,'PERCENT',2X,'TEMPERATURE',/,8X,'A
      1REA',8X,'AREA',7X,'TIME',7X,'AREA',7X,'DEG.C',/,5X,10('_'),2X,10('
      1_'),2X,9('_'),3X,7('_'),2X,11('_'),///)
       DO 3 I=1,NP
       WRITE(6,61)X(I),X1(I),Y(I),X2(I),Y1(I)
61     FORMAT(5X,E10.4,2X,F10.1,4X,F5.2,4X,F6.2,5X,F6.2,/)
3      CONTINUE
                  WRITE(6,62)MIDBP
62                   FORMAT(//,10X,'MID-BOILING-POINT = ',F6.2,' C')
C
C   WRITE VALUES IN A FILE CALLED GSD DATA FOR PLOTTING
C
       WRITE(7,38) NP,(NS(II),II=1,2)
```

```
38    FORMAT(I2,1X,2A4)
      DO 33 I=1,NP
        WRITE(7,34)X2(I),Y1(I)
34        FORMAT(F7.3,1X,F7.2)
33          CONTINUE
48             CONTINUE
                  STOP
                      END
```

A.2.2 Exec (Main Program) : SIMDIS EXEC

To execute type 'SIMDIS'. It automatically executes SIMDIS FORTRAN. Data will be taken from a file called SD DATA, and results will be written in two files SD RESULT, from where they can be printed, and GSD DATA from where they will be read by the plotting program.

```
&TRACE OFF
GLOBAL TXTLIB VLNKMLIB VFORTLIB CMSLIB IMSLDLIB PLOTLIB
FORTVS SIMDIS
FILE 5 DISK SD DATA (LRECL 80 BLKSIZE 80 RECFM F PERM
FILE 6 DISK SD RESULT A (PERM RECFM F LRECL 133
FILE 7 DISK GSD DATA A (PERM RECFM F LRECL 80
LOAD SIMDIS (CLEAR START
EXEC SENDFILE SD RESULT TO RDRPC AT UOTTAWA
EXEC SENDFILE GSD DATA TO RDRPC AT UOTTAWA
&EXIT
```

A.2.3 Data for the Plotting Program : GSD DATA

```
 2
 9 CM-221A
 14.830  101.44
 22.021  155.92
 24.908  205.04
```

```
 36.503  257.60
 56.168  317.00
 72.428  371.76
 80.436  425.76
 96.270  475.36
100.000  535.28
 9 CM-221B
 17.029  101.44
 25.896  155.92
 29.520  205.04
 44.279  257.60
 46.739  317.00
 66.841  371.76
 76.848  425.76
 96.105  475.36
100.000  535.28
```

A.2.4 Plotting Program : GRASDIS FORTRAN

```
C
C  TO EXECUTE USE THE GSDIS EXEC  BY TYPING "GSDIS GRASDIS"
C  DATA WILL BE TAKEN FROM  FILE  : GS DATA
C
C
      REAL XARRAY,YARRAY,X1,Y1,X2,Y2
      INTEGER NT,NOFS,NS,I,J,II
      DIMENSION XARRAY(21),YARRAY(21),NS(2)
      CALL PLOTS(075.0,27.5)
      CALL PLOT(3.0,2.0,-3)
      DO 7 I=1,21
      XARRAY(I)=0.0
      YARRAY(I)=0.0
 7    CONTINUE
```

```
      READ(5,12)NOFS
12    FORMAT(I3)
      DO 2 J=1,NOFS
      READ(5,50) NT,(NS(II),II=1,2)
50    FORMAT(I2,1X,2A4)
      DO 1 I=1,NT
      READ(5,51) XARRAY(I),YARRAY(I)
51    FORMAT(F7.3,1X,F7.3)
1     CONTINUE
      CALL SCALE(XARRAY(1),10.0,NT,1)
      CALL SCALE(YARRAY(1),16.0,NT,1)
      X1=XARRAY(NT+1)
      X2=XARRAY(NT+2)
      Y1=YARRAY(NT+1)
      Y2=YARRAY(NT+2)
      CALL AXIS(0.0,0.0,19HPERCENTAGE (%) AREA,-19,10.0,0.0,X1,X2)
      CALL AXIS(0.0,0.0,20HTEMPERATURE (DEG. C),20,16.0,90.0,Y1,Y2)
      CALL FLINE(XARRAY,YARRAY,NT,1,1,1)
      CALL SYMBOL(3.7,18.0,0.7,9HSIMULATED,0.0,9)
      CALL SYMBOL(2.0,16.3,0.7,12HDISTILLATION,0.0,12)
      CALL SYMBOL(2.0,15.0,0.42,11HSAMPLE NO: ,0.0,11)
      CALL SYMBOL(999.,999.,0.28,NS,0.0,8)
      CALL PLOT(30.0,0.0,3)
      CALL PLOT(30.0,-2.0,2)
      CALL PLOT(30.0,0.0,-3)
2     CONTINUE
      CALL PLOT(0.0,0.0,999)
      STOP
      END
```

A.2.5 Exec (Plotting Program) : GSDIS EXEC

To execute type 'GSDIS GRASDIS'. It takes the data from GSD DATA and plots the results.

```
GLOBAL TXTLIB  VLNKMLIB VFORTLIB CMSLIB PLOTLIB
FORTVS &1
FILE 5 DISK GSD DATA A1 (LRECL 80 BLKSIZE 80 RECFM F PERM
LOAD &1 (CLEAR START
```

Appendix B

Tables and Figures

In Tables 13 to 16 $\bar{Y}$ represents the mean of the sample, σ the standard deviation of the sample, σ^2 its variance and the symbol '$\pm$' the 95 % confidence interval. This interval was calculated using the following formula [2]:

$$\left[\bar{Y} - t_{\upsilon,\alpha/2}\frac{\sigma}{\sqrt{n}} \qquad to \qquad \bar{Y} + t_{\upsilon,\alpha/2}\frac{\sigma}{\sqrt{n}}\right] \tag{19}$$

where n is the number of replicates and α is the probability that this confidence interval does not contain the real mean. $t_{\upsilon,\alpha/2}$ is the t-probability density function with υ degrees of freedom at a specified value $\alpha/2$. υ is the number of degrees of freedom of the sample $(n-1)$. In this case σ^2 is an estimate of the real variance, because there are not enough data to justify it as the real variance.

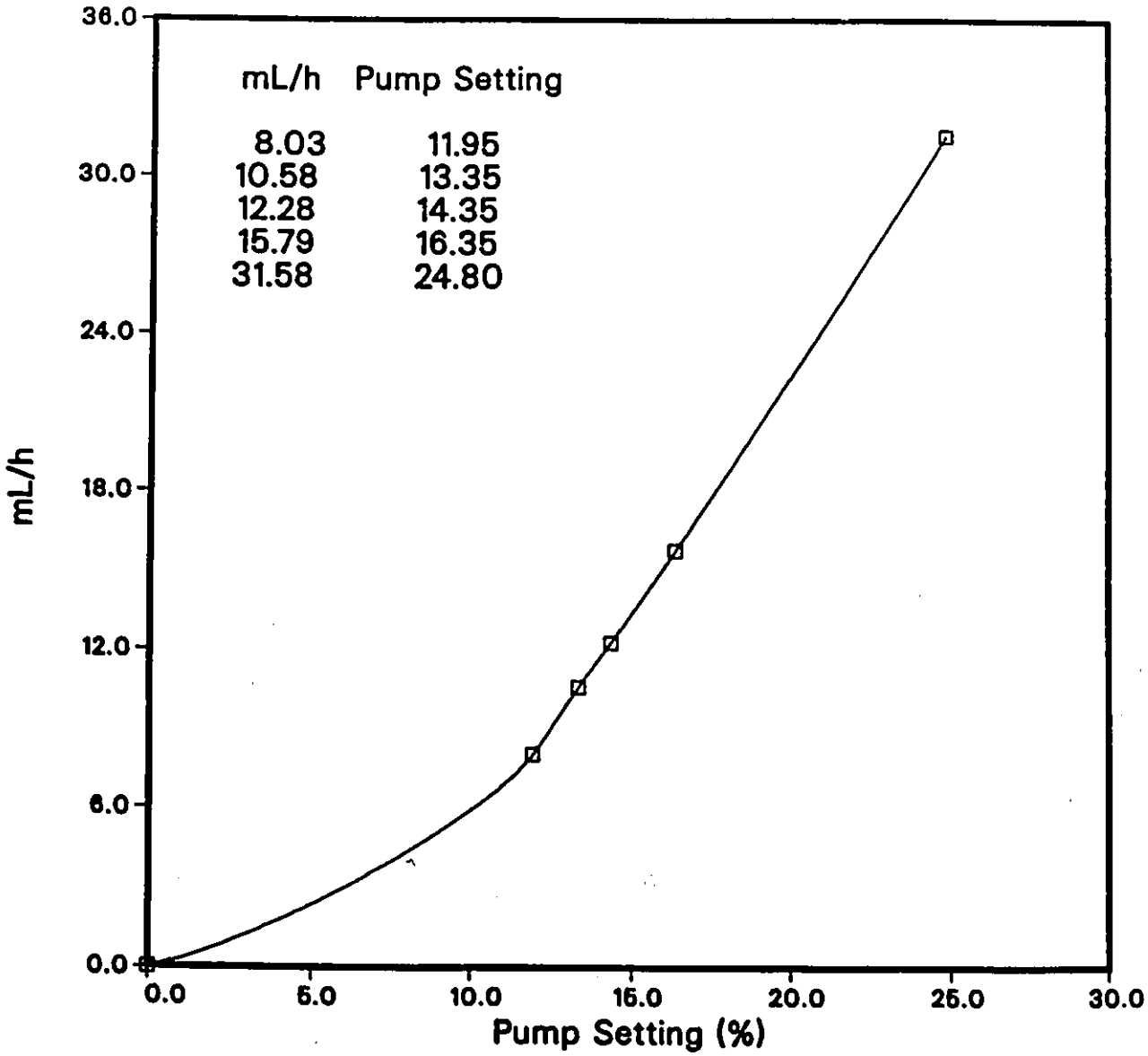

Figure 61: Pump Calibration Curve at 6.9 MPa

Table 9: Results of Kinetic Runs for the Ni-W Catalyst (I)

Pressure = 6.9 MPa
Gas Flow Rate = 890 m^3/m^3

Temperature (°C)	LHSV	Sulfur (wt. %)	Nitrogen ppm	C/H Ratio
Original Oil		4.081	4976	0.819
350	4.0	2.060	2947	0.592
350	2.0	1.512	2610	0.556
350	4/3	1.213	2127	0.579
350	1.0	0.917	1891	0.572
375	4.0	1.920	2408	0.494
375	2.0	1.036	2214	0.573
375	4/3	0.660	1832	0.589
375	1.0	0.301	1655	0.600
400	4.0	0.703	2341	0.711
400	2.0	0.432	1426	0.746
400	4/3	0.199	1082	0.708
400	1.0	0.035	628	0.709
425	4.0	0.126	1419	0.697
425	2.0	0.048	1124	0.653
425	4/3	0.024	724	0.767
425	1.0	0.012	454	0.695

Table 10: Results of Kinetic Run for the Ni-W Catalyst (II)

Pressure = 6.9 MPa
Gas Flow Rate = 890 m^3/m^3

Temperature (°C)	LHSV	Density (g/cm^3)	Viscosity mPa·s	Aniline Point (°C)	Mid. B-Pt. (° C)
Original Oil		0.9884	246.5	47.8	321.16
350	4.0	0.9896	126.4	49.1	293.28
350	2.0	0.9705	111.5	50.7	288.79
350	4/3	0.9679	102.4	51.0	284.14
350	1.0	0.9538	87.8	51.5	281.03
375	4.0	0.9676	102.2	51.3	281.98
375	2.0	0.9521	80.9	52.6	266.06
375	4/3	0.9510	66.0	52.5	264.19
375	1.0	0.9507	63.1	52.5	259.54
400	4.0	0.9557	62.2	52.3	292.89
400	2.0	0.9501	57.1	51.6	287.84
400	4/3	0.9451	47.2	52.5	283.88
400	1.0	0.9418	40.4	52.2	273.49
425	4.0	0.9548	57.2	50.0	269.62
425	2.0	0.9484	33.7	49.4	286.96
425	4/3	0.9441	22.0	48.0	333.18
425	1.0	0.9321	15.4	46.8	346.50

Table 11: Results of Kinetic Runs for the Co-Mo Catalyst (I)

Pressure = 6.9 MPa
Gas Flow Rate = 890 m^3/m^3

Temperature (°C)	LHSV	Sulfur (wt. %)	Nitrogen ppm	C/H Ratio
Original Oil		4.081	4976	0.819
350	4.0	1.960	2730	0.606
350	2.0	1.510	2222	0.628
350	4/3	1.231	1886	0.626
350	1.0	0.964	1600	0.611
375	4.0	1.942	2620	0.605
375	2.0	1.133	2211	0.653
375	4/3	0.781	1820	0.632
375	1.0	0.490	1354	0.630
400	4.0	1.358	1549	0.685
400	2.0	0.992	1160	0.640
400	4/3	0.654	899	0.636
400	1.0	0.484	613	0.666
425	4.0	0.360	1462	0.585
425	2.0	0.310	1063	0.588
425	4/3	0.980	1493	0.587
425	1.0	1.111	1419	0.623

Table 12: Results of Kinetic Run for the Co-Mo Catalyst (II)

Pressure = 6.9 MPa
Gas Flow Rate = 890 m^3/m^3

Temperature (°C)	LHSV	Density (g/cm^3)	Viscosity mPa·s	Aniline Point (°C)	Mid. B-Pt. (° C)
Original Oil		0.9884	246.5	47.8	321.16
350	4.0	0.9733	136.9	49.4	324.97
350	2.0	0.9649	97.6	51.4	306.28
350	4/3	0.9627	92.4	50.2	262.38
350	1.0	0.9598	90.9	50.4	301.23
375	4.0	0.9634	101.0	51.3	318.98
375	2.0	0.9573	80.8	52.8	310.74
375	4/3	0.9539	67.5	50.5	302.50
375	1.0	0.9502	61.3	51.5	303.10
400	4.0	0.9588	71.3	50.7	242.07
400	2.0	0.9512	54.7	51.5	257.30
400	4/3	0.9410	34.1	53.0	282.82
400	1.0	0.9386	37.2	52.6	339.75
425	4.0	0.9452	40.0	49.2	323.08
425	2.0	0.9377	23.3	49.9	248.18
425	4/3	0.9439	46.5	49.0	318.05
425	1.0	0.9410	33.3	49.4	294.27

Table 13: Replicate Runs for the Co-Mo Catalyst (I)

	Density g/cm^3	Viscosity mPa·s	A. Point (°C)	M.B.P. (°C)
	0.9670	89.65	51.53	277.32
	0.9626	97.52	50.13	302.32
	0.9603	100.49	51.46	267.14
	0.9618	100.47	50.50	314.74
	0.9662	110.24	50.80	312.13
$\bar{Y}$	0.9636	99.673	50.88	294.73
σ	2.892×10^{-3}	7.3833	0.6006	21.36
σ^2	8.362×10^{-6}	54.513	0.3679	456.249
$\pm$	3.590×10^{-3}	9.1661	0.7531	26.5177

Table 14: Replicate Runs for the Co-Mo Catalyst (II)

	N ppm	S wt. %	C/H
	1992	1.82	0.606
	1882	1.80	0.622
	1983	1.69	0.616
	2272	1.74	0.613
	2444	1.71	0.569
$\bar{Y}$	2100.6	1.7512	0.6052
σ	245.36	0.05511	0.021
σ^2	60201.53	0.003037	4.41×10^{-4}
$\pm$	304.606	0.0684	0.02607

Table 15: Replicate Runs for the Ni-W Catalyst (I)

	Density g/cm^3	Viscosity mPa·s	A. Point (°C)	M.B.P. (°C)
	0.9640	107.85	50.23	286.68
	0.9694	104.66	50.06	284.23
	0.9676	115.51	50.73	287.08
	0.9635	109.72	50.80	295.84
	0.9686	106.89	49.96	281.39
$\bar{Y}$	0.9666	108.93	50.35	287.12
σ	2.702×10^{-3}	4.1047	0.3864	5.296
σ^2	7.302×10^{-6}	16.849	0.1439	28.048
$\pm$	3.355×10^{-3}	5.0959	0.4797	6.5748

Table 16: Replicate Runs for the Ni-W Catalyst (II)

	N ppm	S wt. %	C/H
	1999	1.305	0.697
	2001	1.413	0.580
	2367	1.351	0.731
	1840	1.351	0.720
	1762	1.282	0.775
$\bar{Y}$	1993.8	1.3404	0.7006
σ	232.77	0.05039	0.0731
σ^2	54185.73	0.002539	5.35×10^{-4}
$\pm$	288.986	0.06256	0.0908

Appendix C

Impregnation Solution Calculations

The water soluble salts of nickel and tungsten were nickel(ous) nitrate [$Ni(NO_3)_2 \cdot 6H_2O$ (Formula weight 290.81)] and ammonium metatungstate [$(NH_4)_6H_2W_{12}O_{40}$ (Formula weight 2956.450)]. For cobalt and molybdenum the salts were cobaltous nitrate [$Co(NO_3)_2 \cdot 6H_2O$ (Formula weight 291.05)] and ammonium molybdate [$(NH_4)_6Mo_7O_{24} \cdot 4H_2O$ (Formula weight 1235.86)].

The impregnation solutions were preparated keeping the Ni/WO_3 (CoO/MoO_3) ratio of 0.3 and a concentration sufficient to give a total of 5 % loading of both active metal oxides combined. The formula weight of NiO is 74.71 and that of WO_3 is 231.85. And those of CoO and MoO_3 are 74.93 and 143.94 respectively.

The mounts of the salts required for a given support of known pore volume were calculated as follows:

- Total volume of the solution = 100 mL
- Pore volume of the support = v mL/g

Amount of nickel nitrate required

$$\frac{(0.05) \cdot 1}{v} \times 100 \times \frac{0.3}{1.3} \times \frac{\frac{290.81}{1}}{74.71} = \frac{4.4914}{v} g$$

Amount of ammonium metatungtate required

$$\frac{(0.05)\cdot 1}{v} \times 100 \times \frac{1.0}{1.3} \times \frac{\frac{2956.45}{12}}{231.85} = \frac{4.0871}{v} g$$

Amount of cobaltous nitrate required

$$\frac{(0.05)\cdot 1}{v} \times 100 \times \frac{0.3}{1.3} \times \frac{\frac{291.05}{1}}{74.93} = \frac{4.4817}{v} g$$

Amount of ammonium molybdate required

$$\frac{(0.05)\cdot 1}{v} \times 100 \times \frac{1.0}{1.3} \times \frac{\frac{1235.86}{7}}{143.94} = \frac{4.7176}{v} g$$

Appendix D

Material Balance

The material balance was done on the oil feed and the exit stream, for both catalysts. The inlet flow was measured by volume and then, converted into weight. The steady state out-flow of oil was determined by weighing the product oil collected in a known period of time. The amount of hydrocarbons going out in the gas stream could not be calculated due to a failure in the column detection system as explained in section 3.2.2.

Coke formation can cause serious problems in catalytic processes, as indicated in section 2.2.3. The amount of total coke formation on the catalysts was determined by removing the catalyst from the reactor and weighing it. It was then calcined at 700°C for 12 h to oxidize all the deposits on the catalyst. The difference in weight was the measure of the weight of coke deposited on the catalyst. For the Co-Mo catalyst the coke deposition was of 2.9462 g after the whole run was completed. And for the Ni-W catalyst, it was 2.2969 g in the same circumstances.

The coke formation rate is a function of the operating conditions as well as the age of the catalyst. To know exactly how much coke was found on the catalyst within a given period of time would have required a different set-up of the experiment. Thus, it was excluded from this analysis.

Tables 17 and 18 show the results of the material balance for the sixteen kinetic runs for both catalysts, Ni-W and Co-Mo respectively. The results are listed at 350°C first, followed by the other temperatures in increasing order; and within each temperture range from the highest to the lowest LHSV. The period taken as basis for all calculations is one hour. The first column gives the mass feed ratio of oil based on

the pump calibration curve. The second column gives the mass of hydrogen additioned to the oil. Column three and four give the loss of mass due to sulfur and nitrogen removal, and column five gives the weight of oil sample callected in one hour. The last column is the net material balance.

It must be noticed that neither the coke formed on the catalysts nor were the hydrocarbons that went out with the gas stream accounted for in this material balance. The amount of gaseous hydrocarbons could amount up to 0.5 g (see Sambi [51, page 146]). Also the pump valve did not have the desired precision, although care was taken to set the liquid flows according to the previous calibration (see Pump Calibration Curve on page 125). Nonetheless from the data obtained we can infer that at higher LHSV the gas formation is higher than at low LHSV. Also some of the oil is most likely used up in the coke formation. In general most of the liquid feed as well as the product oil could be accounted for.

Table 17: Material Balance for the Ni-W Catalyst Runs

Basis : One hour. All Units in grams

Oil in	$+H_2$	-S	-N	Oil out	Balance
31.2136	1.0726	0.6389	0.0641	29.8710	1.7122
15.6068	0.6924	0.4061	0.0369	15.2556	0.6006
10.4572	0.4123	0.3022	0.0298	10.1425	0.3950
7.9368	0.3171	0.2501	0.0245	7.6255	0.3538
31.2136	1.6645	0.6742	0.0802	29.6818	2.4419
15.6068	0.6585	0.4751	0.0431	15.3133	0.4338
10.4572	0.3817	0.3576	0.0329	10.1094	0.3390
7.9368	0.2778	0.3000	0.0264	7.5747	0.3135
31.2136	0.5144	1.0541	0.0822	29.1881	1.4006
15.6068	0.2346	0.5696	0.0554	14.9784	0.2380
10.4572	0.1860	0.4058	0.0407	9.8208	0.3759
7.9368	0.1342	0.3210	0.0345	7.4271	0.2884
31.2136	0.6026	1.2342	0.1110	29.3391	1.1319
15.6068	0.3864	0.6293	0.0601	14.5898	0.7140
10.4572	0.1366	0.4241	0.0445	10.0966	0.0286
7.9368	0.1292	0.3229	0.0359	7.2377	0.4695

Table 18: Material Balance for the Co-Mo Catalyst Runs

Basis : One hour. All Units in grams

Oil in	$+H_2$	-S	-N	Oil out	Balance
31.2136	1.0006	0.6617	0.0701	29.8019	1.6805
15.6068	0.4903	0.4011	0.0430	15.2158	0.4372
10.4572	0.2829	0.2980	0.0323	9.7973	0.6186
7.9368	0.2340	0.2476	0.0268	7.3824	0.5140
31.2136	1.3638	0.6680	0.0735	32.8364	-1.0005
15.6068	0.4486	0.4604	0.0432	15.3320	0.2198
10.4572	0.4005	0.3451	0.0330	10.7972	-0.3176
7.9368	0.2307	0.2849	0.0287	7.5124	0.3415
31.2136	0.8266	0.8496	0.1070	31.3635	-0.2799
15.6068	0.5971	0.4819	0.0535	16.3080	-0.6395
10.4572	0.3479	0.3583	0.0426	10.3734	0.0308
7.9368	0.1402	0.2854	0.0346	7.0699	0.0308
31.2136	1.0514	1.1611	0.1097	28.8136	2.1806
15.6068	0.4601	0.5884	0.0611	13.9224	1.4950
10.4572	0.2975	0.3242	0.0364	9.2957	1.0984
7.9368	0.1674	0.2357	0.0282	6.9424	0.8979

Appendix E

Hydrogen Consumption

As the inlet flow of hydrogen could not be measured, the material balance on hydrogen was not carried out. Hydrogen is consumed for conversion of S to H_2S and N to NH_3, and for hydrogenation of unsaturated and cracked hydrocarbons. The hydrogen used for hydrogenation was calculated from the hydrogen analysis of the feed and the product oil. Consumption of hydrogen for S and N conversions was determined from the amount of S and N removed.

Some of the hydrogen used for hydrogenation was consumed in products that went out with the gas stream, hence it could not be considered in this calculation. This amount is expected to be small compared with the total consumption figures, and thus it would not have changed them significatively.

Observing Tables 19 and 20 there is no clear correlation between hydrogen consumption and operating conditions. It is belived that some inaccuracy during the sampling process and/or error in the analyses of oil samples might have affected these results. But as the experiment was not designed especially for this purpose there is no conclusive proof on this respect.

Table 19: Hydrogen Consumption for the Ni-W Catalyst Runs

Pressure = 6.9 MPa
Gas Flow Rate = 890 m^3/m^3

Temperature (°C)	LHSV	Hydrogen Consumption m^3/m^3
350	4.0	394.83
350	2.0	509.13
350	4/3	457.33
350	1.0	465.22
375	4.0	604.94
375	2.0	488.75
375	4/3	429.16
375	1.0	415.36
400	4.0	206.83
400	2.0	194.93
400	4/3	227.25
400	1.0	219.26
425	4.0	244.08
425	2.0	308.19
425	4/3	176.90
425	1.0	212.70

Table 20: Hydrogen Consumption for the Co-Mo Catalyst Runs

Pressure = 6.9 MPa
Gas Flow Rate = 890 m^3/m^3

Temperature (°C)	LHSV	Hydrogen Consumption m^3/m^3
350	4.0	370.18
350	2.0	366.83
350	4/3	327.58
350	1.0	350.11
375	4.0	498.52
375	2.0	340.08
375	4/3	448.13
375	1.0	349.07
400	4.0	314.36
400	2.0	446.55
400	4/3	394.73
400	1.0	224.61
425	4.0	400.66
425	2.0	355.23
425	4/3	338.72
425	1.0	256.92

UNIVERSITÉ D'OTTAWA
UNIVERSITY OF OTTAWA